

# 1 White Paper of the ICFA-ICUIL Joint Task Force – High Power Laser Technology for Accelerators

Wim Leemans, LBNL  
Chair of the ICFA-ICUIL Joint Task Force and Editor of the White Paper  
Mail to: [wpleemans@lbl.gov](mailto:wpleemans@lbl.gov)

## Executive Summary

Particle accelerators and lasers have made fundamental contributions to science and society, and are poised to continue making great strides in the 21st century. Lasers are essential to modern high performance accelerator facilities that support fundamental science and applications, and to the development of advanced accelerators. In accelerator and radiation science, which aims at developing advanced acceleration and radiation source concepts, lasers provide the power for laser plasma accelerators or dielectric-structure-based direct-laser accelerators. For present-day light sources they are used to drive photocathodes in high-brightness electron guns; to control and measure beam properties; and to seed the amplification process in the latest generation of light sources that rely on electron-beam-based free-electron lasers. (At the user beamlines of light sources, they are also widely used in pump-probe experiments.) Lasers are also used in radiation sources, such as those producing high harmonics in gases, or those producing intense gamma-ray beams via inverse Compton or Thomson scattering against relativistic electron beams. Medical applications are emerging that rely on laser produced particle and radiation beams that offer the potential to be compact and cost effective.

The demand for high average laser power even in near-future accelerator applications is already outpacing the state of the art in lasers. A class of more-futuristic accelerators for particle physics, driven entirely by lasers, would require average laser power far exceeding today's state of the art. The performance of lasers has grown in dramatic ways, thanks to inventions such as chirped pulse amplification. Today, lasers can achieve petawatt-level peak power operating at 1 Hz; lower-energy systems (10 mJ) can operate at tens of kHz. These performance improvements have enabled a vast range of scientific opportunities, including proof-of-principle experiments on the most advanced accelerator concepts. As these laser-based techniques mature, the need for higher average power has come to the fore. Higher average power enables laboratory-tested concepts to be turned into facilities: light sources that serve a broad range of users; industrial and medical applications; or the most demanding of all, particle colliders.

Developing high average power (tens to hundreds of kilowatts), high peak power (petawatt) lasers is an extremely challenging task that will take several decades of aggressive R&D and, most likely, revolutionary new concepts and ideas.

To ensure that the laser and accelerator communities understand each other's needs and to assist them in enabling vigorous progress, a standing Joint Task Force, was established by ICFA and ICUIL. The JTF has held two international workshops thus

far.<sup>1</sup> Four general areas in future accelerator science and technology were considered that will either be driven by lasers or have a need for laser technology beyond today's state of the art : colliders for high-energy physics based on lasers; laser stripping for H<sup>-</sup> sources; light sources (such as X-ray free electron lasers), and medical ion therapy accelerators.

The goals of the workshops were to:

- Establish a comprehensive survey of requirements for colliders, light sources and medical applications, with emphasis on sources that require lasers beyond the state of the art or at least the state of current use. Emphasis was placed on the fact that the workshops were not intended to carry out a down-selection of specific designs or technology choices, but instead, were meant to take an inclusive approach that represents a community consensus.
- Identify future laser system requirements and key technological bottlenecks.
- From projected system requirements, provide visions for technology paths forward to reach the survey goals and outline the laser-technology R&D steps that must be undertaken.

Requirements for laser performance in each of the four areas were established and laser technologies that could meet these requirements were assessed, as detailed in this whitepaper. The following general conclusions for laser development were established:

- *Power.* Improvements in average and peak power are needed for all of the application areas under consideration, especially colliders for high-energy physics. Advances in these parameters made on behalf of the accelerator community will have spinoff benefits for other uses. In turn, accelerators should benefit from laser advancements made for other purposes, though unique requirements indicate that the accelerator community would benefit from a dedicated and tailored R&D effort.
- *Efficiency.* To deploy and continue to advance accelerators and radiation sources, the accelerator field will need not only high average power and high peak power lasers, but also high “wall-plug” efficiency.
- *High Power Optics.* Laser components and optics that can withstand high-average-power operation will be crucial to these advances.
- *Multi-way, interactive R&D cooperation.* Engagement of the national labs, universities and industry will be essential for comprehensive R&D of new materials and new architectures for lasers, as well as for novel concepts in acceleration and radiation generation.
- *Graduate and postdoctoral education.* Innovation in accelerator and laser science and technology can be strengthened by expanding opportunities for students and postdocs. In some areas, better funding will be needed to bring in competition and foster stronger ties with other disciplines. Operating user facilities at national laboratories, with support for university researchers, are excellent for this.

---

<sup>1</sup> The First and Second Workshops of the Joint ICFA-ICUIL Taskforce on High Average Power Lasers for Future Accelerators were held at GSI (Darmstadt, Germany), from April 8-10, 2010, and at LBNL (Berkeley, USA), from September 20-22, 2011, respectively.

The JTF has identified several promising candidate technologies that could provide a path to the laser parameters required by future accelerator applications. A vigorous R&D program on these technology candidates is needed in the near future. The research should be guided in part by the laboratories that will require these new developments. The collaboration between ICFA and ICUIL could play a crucial role, with the accelerator scientists providing guidance on what is needed, and the laser scientists on what is possible.

The average power and efficiency requirements of HEP applications may be met by some of the identified technologies after a period of development effort. Thus it is important to start a vigorous research program to start and incubate some of these technologies. Considering the size of the gap and the timing of the users' needs, it would be a long-range R&D program, perhaps five to ten years. To assess its potential, we recommend that exploratory-level research on a modest scale be started immediately.

Other applications are less demanding than colliders, but still need high average power and efficiency from their lasers. Their goals might be reached *en route* to the ultimate goal of lasers suitable for colliders, and at a much earlier date. A large scale real-world use of these interim results could provide leverage, scalability, and new technologies that are helpful in achieving the final goal.

This whitepaper is organized by application. Discussed first are lasers for high-energy and high-intensity accelerators, then a discussion of laser stripping for H<sup>-</sup> generation in ion sources. The next section covers lasers for light sources: photocathodes, FELs, etc., including Compton and Thomson scattering against an electron beam, and high-harmonic generation in gases. Laser applications in medical accelerators for proton and heavy-ion therapy are covered next. Finally a draft roadmap for laser development in support of these areas is presented, showing our vision of a long-term R&D program joining the user perspective of the accelerator community with the expertise of laser laboratories. This roadmap will be further developed in upcoming workshops.

## **Acknowledgements**

I would like to thank the many colleagues who took the time to help us survey this intersection of complex, fast-moving fields and chart a course toward future progress. Section 1.1, "*Laser Applications for Future High-Energy and High-Intensity Accelerators*," led by Weiren Chou, had among its authors Ralph Assmann, Andy Bayramian, Joel England, Eric Esarey, Cameron Geddes, Dino Jaroszynski, Thomas Kuehl, Wim Leemans, Yun Liu, Bob Noble, Carl Schroeder, Tor Raubenheimer, Mike Seidel, Toshiki Tajima, Valery Telnov and Kaoru Yokoya. Section 1.2, "*Laser Applications for Light Sources*," under Bruce Carlsten, incorporated the work of Thomas Kuehl, Siegfried Schreiber, Carl Schroeder, Rahul Shah, Franz Tavella, Bill White, Russell Wilcox, and Arik Willner. For Section 1.3, "*Laser Applications for Medical Particle Beam Therapy*," Ingo Hofmann, current section chair and Mitsuru Uesaka, the 2010 section chair, would like to thank Jose Alonso, Marcus Babzien, Stepan Bulanov, Charlie Ma, Viktor Malka, Dave Robin, Markus Roth, and Andrew Sessler; and are indebted to Paul Bolton, M. Borghesi, Victor Malka, Ulrich Schramm, and Joerg Schreiber for their contributions and comments. Regarding Section 1.4, "*Laser Technology Development Roadmaps*," editor and OPCPA-subsection author Almantas Galvanauskas would like to thank Jay Dawson for the subsection on fiber

lasers (with feedback/review by J. Limpert and J. Nillson); Darren Rand and T.Y. Fan on solid-state lasers; M. Babzien regarding CO<sub>2</sub> lasers; and A. Bayramian and Jay Dawson on facility-class lasers.

Joe Chew provided editorial support for both the present effort and the earlier Joint Task Force whitepaper.

## 1.1 Laser Applications for Future High-Energy and High-Intensity Accelerators

### 1.1.1 Introduction

The consensus in the world high-energy physics community is that the next large collider after the LHC will be a TeV-scale lepton collider. Options currently under study include the ILC (0.5-1 TeV), CLIC (up to 3 TeV) and the muon collider (up to 4 TeV), all using RF technology. On the other hand, the very high gradients ( $\sim 10$  GeV/m) possible with laser acceleration open up new avenues to reach even higher energy and more compact machines. At this workshop participants discussed and set forth a set of beam and laser parameters for a 1-10 TeV  $e^+e^-$  collider based on two different technologies – laser plasma acceleration (LPA) and direct laser acceleration (DLA). Because the effectiveness of a collider is judged by its luminosity, and the cross section for a process creating a large mass  $M$  varies as  $1/M^2$ , a high energy machine must also have high luminosity. The luminosity goal for a 10 TeV collider is  $10^{36}$  cm<sup>-2</sup>s<sup>-1</sup>, a factor of 100 higher than for a 1 TeV machine. To reach this goal, the laser system must have high average power ( $\sim 100$  MW) and high repetition rate (kHz to MHz).

Moreover, the laser-based collider must have high wall-plug efficiency in order to keep power consumption at a reasonable level. To set this efficiency goal, the workshop compared the efficiency of a number of large accelerators, either in operation or in a design phase. The results are listed in Table 1. Our goal is 10% for an LPA.

**Table 1:** Comparison of wall-plug efficiency of various accelerators.

<i>Accelerator</i>	<i>Beam</i>	<i>Beam energy (GeV)</i>	<i>Beam power (MW)</i>	<i>Efficiency AC to beam</i>	<i>Note on AC power</i>
PSI Cyclotron	H <sup>+</sup>	0.59	1.3	0.18	RF + magnets
SNS Linac	H <sup>-</sup>	0.92	1.0	0.07	RF + cryo + cooling
TESLA (23.4 MV/m)	$e^+/e^-$	$250 \times 2$	23	0.24	RF + cryo + cooling
ILC (31.5 MV/m)	$e^+/e^-$	$250 \times 2$	21	0.16	RF + cryo + cooling
CLIC	$e^+/e^-$	$1500 \times 2$	29.4	0.09	RF + cooling
LPA	$e^+/e^-$	$500 \times 2$	8.4	0.10	Laser + plasma

It is difficult to set a reasonable goal for cost. Ideally, the cost of a collider based on laser technology should be significantly lower than colliders based on conventional RF technology in order to make this new technology attractive. Take the 0.5 TeV ILC as an example. The total estimated cost is about \$8B, of which about 1/3 is the RF cost. This

gives roughly \$5M per GeV for RF. The laser cost of a LPA or DLA collider should be significantly lower in order to be competitive.

The workshop also studied the laser requirements for a  $\gamma\gamma$  collider. This idea, originated at BINP, is based on the consideration that the cross section for Higgs production in a  $\gamma\gamma$  collider is significantly larger than in an  $e^+e^-$  collider of the same energy. In 2008, it was proposed to the ICFA to build a 100-200 GeV  $\gamma\gamma$  collider as the first stage of a full scale ILC in order to lower the construction cost and realize a more rapid start for the project. This proposal went unapproved for a number of reasons: physics potential, cost saving potential, and need for additional laser R&D. This workshop concluded that, as a matter of fact, the required laser systems for an ILC  $\gamma\gamma$  collider may already be within reach of today's technology, whereas for a CLIC or LPA based  $\gamma\gamma$  collider the required laser technology could piggyback on the inertial fusion project LIFE at LLNL or the high power laser project ELI in Europe (see Sec. 1.1.4).

In addition to high-energy colliders, lasers also find application at another frontier – high-intensity accelerators. Lasers have been used in beam diagnostics for some time now, including beam profile monitor (“laser wire”) and beam polarization measurement. These require only low power lasers. A challenge, however, is to use a laser for stripping  $H^-$  particles during injection into a high-intensity proton machine, such as the SNS, J-PARC or Project X. In these MW-scale machines, the thin foils made of carbon or diamond that have been used for stripping would experience a severe heating problem and have limited lifetime. Experiments have demonstrated that a laser beam interacting with  $H^-$  particles can convert them to protons. However, to replace foils in real machine operation, the laser must have high average power (kW) and high repetition rate (hundreds of MHz). This workshop investigated the required laser parameters for the SNS and Project X.

### **1.1.2 One- to Ten-TeV $e^+e^-$ Colliders Based on Laser Plasma Acceleration**

Advanced acceleration techniques are actively being pursued to expand the energy frontier of future colliders. Although the minimum energy of interest for the next lepton collider will be determined by high-energy physics experiments presently underway, it is anticipated that  $\geq 1$  TeV center-of-mass energy will be required. The laser-plasma accelerator (LPA) is one promising technique for reducing the size and cost of future colliders—if the needed laser technology is developed. LPAs are of great interest because of their ability to sustain extremely large acceleration gradients, resulting in compact accelerating structures [1-3].

#### **1.1.2.1 Principles of the LPA**

Laser-plasma acceleration is realized by using a short-pulse, high-intensity laser to ponderomotively drive a large electron plasma wave (or wakefield) in an underdense plasma (see Figure 1). The electron plasma wave has relativistic phase velocity – approximately the group velocity of the laser – and can support large electric fields in the direction of propagation of the laser.

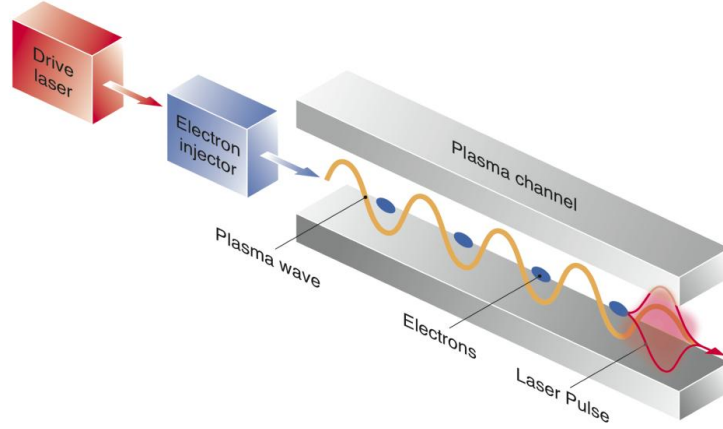


**Figure 1:** Laser-plasma acceleration: An intense laser pulse drives a plasma wave (wake) in a plasma channel, which also guides the laser pulse and prevents diffraction. Plasma background electrons injected with the proper phase can be accelerated and focused by the wake [1].

When the laser pulse is approximately resonant (duration on the order of the plasma period), and the laser intensity is relativistic (with normalized laser vector potential  $a_0 = eA/m_e c^2 \sim 1$ ), the magnitude of the accelerating field is on the order of  $E_0[\text{V/m}] = 96(n_0[\text{cm}^{-3}])^{1/2}$ , and the wavelength of the accelerating field is on the order of the plasma wavelength  $\lambda_p[\text{mm}] = 3.3 \times 10^{10}(n_0[\text{cm}^{-3}])^{-1/2}$ , where  $n_0$  is the ambient electron number density. For example,  $E_0 \approx 30 \text{ GeV/m}$  (approximately three orders of magnitude beyond conventional RF technology) and  $l_p \approx 100 \text{ mm}$  for  $n_0 = 10^{17} \text{ cm}^{-3}$ .

Rapid progress in laser-plasma accelerator research, and in particular the demonstration of high-quality GeV electron beams over cm-scale plasmas in 2006 at Lawrence Berkeley National Laboratory [4], has increased interest in laser-plasma acceleration as a path toward a compact TeV-class linear collider [5]. A conceptual diagram of an LPA-based collider [1] is shown in Figure 2.

In the standard laser wakefield acceleration configuration, the electron plasma wave is driven by a nearly resonant laser (pulse duration on the order of the plasma period) propagating in a neutral, underdense ( $\lambda_p \gg l$ , where  $l$  is the laser wavelength) plasma. There are several regimes of plasma acceleration that can be accessed with a laser driver. Two regimes that have attracted attention for collider applications are the quasi-linear regime [3] and the bubble [6] (or blow-out [7]) regime.

The quasi-linear regime is accessible for parameters such that  $\pi^2 r_L^2 / \lambda_p^2 \gg a_0^2 / 2\gamma_L$ , where  $a_0^2$  can be written as a function of the laser intensity  $I_0$ :  $a_0^2 = 7.3 \times 10^{-19} (l[\text{mm}])^2 I_0[\text{W/cm}^2]$  (linear polarization),  $\gamma_L = (1 + a_0^2 / 2)^{1/2}$ , and  $r_L$  is the laser spot size. The amplitude of the accelerating field of the plasma wave in the quasi-linear regime is  $E_z \approx 0.76(a_0^2 / 2\gamma_L)E_0$ . This regime is characterized by regular plasma wave buckets and nearly-symmetric regions of acceleration-deceleration and focusing-defocusing (see Fig. 3). In the quasi-linear regime, the accelerating and focusing phase regions for electrons and positrons are symmetric, since the wakefield is approximately sinusoidal.

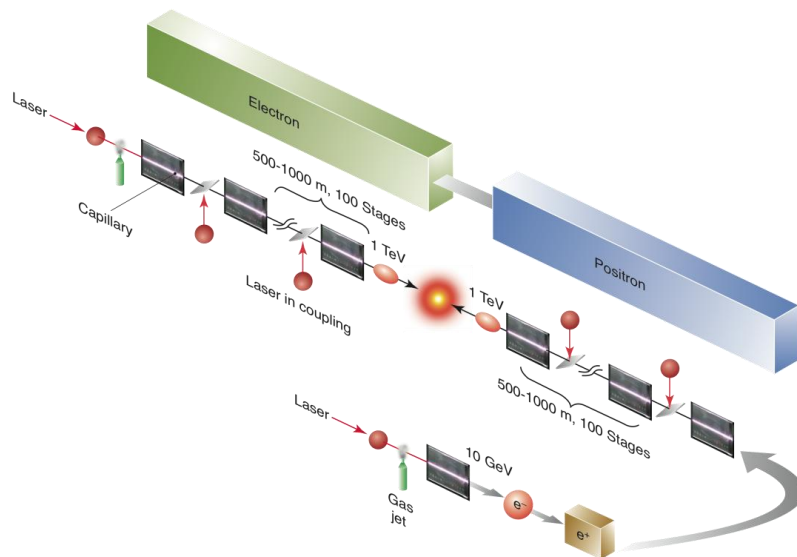


**Figure 2:** Concept for an LPA-based electron-positron collider. Both the electron and positron arms start with a plasma-based injection-acceleration module where controlled injection techniques are applied to produce a high quality  $\sim 10$  GeV electron beam. Electrons are then accelerated to 1 TeV using 100 laser-plasma modules, each consisting of a 1-m long preformed plasma channel ( $10^{17} \text{ cm}^{-3}$ ) driven by a 30 J laser pulse giving a 10 GeV energy gain. A fresh laser pulse is injected into each module. Similarly, positrons are produced from a 10 GeV electron beam through pair creation and then trapped and accelerated in a LPA module to  $\sim 10$  GeV. Subsequent LPA modules would accelerate positrons to 1 TeV. A luminosity of  $10^{34} \text{ cm}^{-2} \text{ s}^{-1}$  requires  $4 \times 10^9$  particles/bunch at a 13 kHz repetition rate [1].

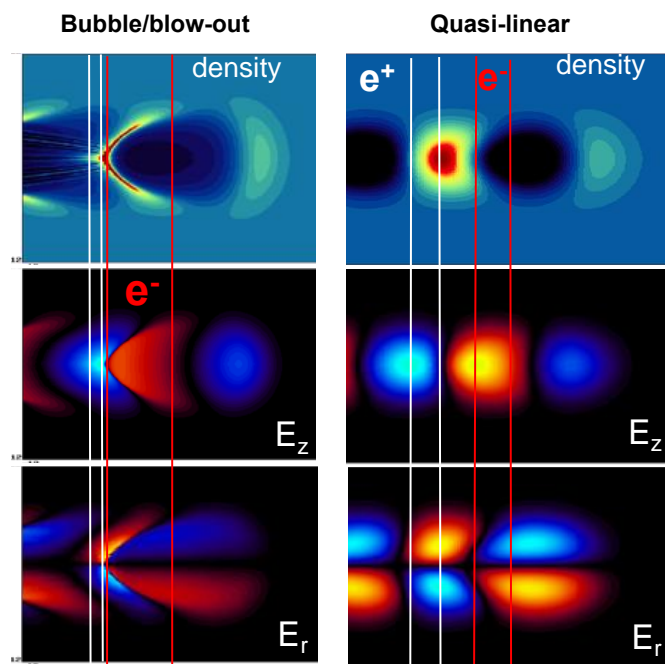


**Figure 3:** Wakes generated in the bubble (*left column*) and quasi-linear (*right column*) regimes by a laser pulse with  $a_0=4$  (*left*) and  $a_0=1$  (*right*). Top figures are axial electric field, central figures are density, and bottom figures are transverse electric fields. The black boxes indicate the accelerating/focusing regions for electrons, and the green boxes are for positrons (Courtesy of C. Benedetti *et al.*, LBNL).

The bubble regime of LPA occurs for laser-plasma parameters such that  $\pi^2 \Gamma_L^2 / \lambda_p^2 \ll a_0^2 / 2\gamma_L$ . This regime is characterized by complete removal of plasma electrons and creation of an ion cavity (see Fig. 3, *left*). The bubble regime has several attractive features for acceleration of electron beams. Inside the moving ion cavity, the focusing forces for electrons are linear (and attractive) and uniform for all phases and the accelerating field is independent of transverse position with respect to the cavity axis. The major drawback of accessing the highly-nonlinear bubble regime is that acceleration of positrons is problematic because the entire ion cavity is defocusing for positrons, and a positron beam will be scattered transversely. There does exist a small phase region immediately behind the bubble where positrons could be accelerated and focused; however, here some of the attractive properties of the bubble regime (e.g., uniform accelerating and constant linear focusing) are lost.

The amount of charge that can be accelerated in a plasma wave is determined by the plasma density and the size of the accelerating field. The maximum charge that can be loaded is given by the number of charged particles required to cancel the laser excited wake (beam loading limit). A collider will operate with asymmetric shaped particle bunches such that bunches can be loaded with charge near the beam loading limit without a large wake-induced energy spread. The maximum number of loaded charged particles into a small ( $\ll \lambda_p = 2\pi/k_p$ ) segment is approximately  $N \sim n_0 k_p^{-3} (E_z/E_0)$ .

In general, the energy gain in a single laser-plasma accelerator stage may be limited by laser diffraction effects, dephasing of the electrons with respect to the accelerating field phase velocity (approximately the laser driver group velocity), and laser energy depletion into the plasma wave. Laser diffraction effects can be mitigated by use of a plasma channel (transverse plasma density tailoring), guiding the laser over many Rayleigh ranges. Dephasing can be mitigated by plasma density tapering (longitudinal plasma density tailoring), which can maintain the position of the electron beam at a given phase of the plasma wave. Ultimately, the single-stage energy gain is determined by laser energy depletion. The energy depletion length scales as  $L_d \sim \lambda_p^3 / \lambda^2 \propto n_0^{-3/2}$ , and the energy gain in a single stage scales with plasma density as  $W_{\text{stage}} \approx E_z L_d \propto n_0^{-1}$ .

After a single laser-plasma accelerating stage, the laser energy is depleted and a new laser pulse must be coupled into the plasma for further acceleration. This coupling distance is critical to determining the overall accelerator length (set by the average, or geometric, gradient of the main linac) and the optimal plasma density at which to operate. One major advantage of laser plasma acceleration over beam-driven plasma acceleration is the potential for a short coupling distance between stages, and, therefore, the possibility of a high average (geometric) accelerating gradient and a relatively short main linac length. (Reducing the main linac length requires the coupling length between stages to be on the order of the length of a single plasma acceleration stage.) Although conventional laser optics might require meters of space to focus intense lasers into subsequent LPA stages, plasma mirrors show great promise for use as optics to direct high-intensity laser pulses, requiring only tens of cm to couple a drive laser into a plasma accelerator stage. A plasma mirror uses overdense plasma creation by the intense laser on a renewable surface (e.g., metallic tape or liquid jet) to reflect the laser beam.

### 1.1.2.2 *Experimental Progress on Laser-Plasma Accelerators*

Rapid progress in laser-plasma accelerator research has been made over the past decade (see [3] for a review). In particular, the production of high-quality GeV electron beams over cm-scale plasmas was demonstrated in 2006 at Lawrence Berkeley National Laboratory [4]. Since that time, LPA research at many facilities worldwide has demonstrated GeV-level energies. This has been enabled by guiding of the laser pulse over cm distances (tens of times the natural diffraction range of the laser) using tailored plasma density channels, which act like optical fibers and which perform self-focusing. The beams have percent level energy spread and estimates of normalized emittance are at the mm-mrad level. To further improve performance, particle injection into the micron-scale accelerator structure is being controlled via several mechanisms including wake phase velocity control using plasma density tailoring, the beat between colliding laser pulses, and ionization of high-Z species to produce electrons near the peak of the laser intensity. This has recently produced beams which are both stable and can be tuned in energy. Continued injector and accelerator structure (guiding, laser mode, etc.) control work is in progress to further reduce energy spread and emittance. A critical technology for a LPA based collider will be staging of several modules in series. Experiments are expected to begin addressing this issue in the coming year, including the use of plasma mirrors or other techniques to minimize distance between stages and maintain geometric gradient. Also in progress are experiments to extend LPAs to 10 GeV using PW laser drivers in meter-scale plasmas.

### 1.1.2.3 *Design Considerations for Laser-Plasma Colliders*

The beam-beam interaction at the interaction point (IP) of a collider produces radiation (beamstrahlung) that generates background for the detectors and increases the beam energy spread, resulting in loss of measurement precision. The beam-beam interaction is characterized by the Lorentz-invariant beamstrahlung parameter  $\Upsilon$  (mean field strength in the beam rest frame normalized to the Schwinger critical field). The current generation of linear collider designs based on conventional technology operate in the classical beamstrahlung regime  $\Upsilon \ll 1$ . Next generation linear colliders ( $\geq 1$  TeV) will most likely operate in the quantum beamstrahlung regime with  $\Upsilon \gg 1$ .

In the quantum beamstrahlung regime, the average number of emitted photons per electron scales as  $n_\gamma \propto \Upsilon^{2/3}$  and the relative energy spread induced scales as  $\delta_E \propto \Upsilon^{2/3}$ . Assuming that the center of mass energy, luminosity, beam power, and beam sizes are fixed,  $n_\gamma \propto \delta_E \propto N^{2/3} \sigma_z^{1/3}$ , where  $\sigma_z$  is the particle bunch length [5]. In this regime, beamstrahlung is reduced by using shorter bunches and smaller charge per bunch. Laser-plasma accelerators are intrinsically sources of short (fs) electron bunches, due to shortness of the plasma wavelength  $\lambda_p$ .

Of particular interest is how the various laser and electron beam parameters characterizing a LPA-based collider scale with respect to plasma density and laser wavelength. These scaling laws, originally derived in Ref. [5], are summarized in Table 2.

**Table 2:** Basic plasma density and laser wavelength scalings [5].

<b>Parameter</b>	<b>Scaling</b>
accelerating gradient	$n^{1/2}$
LPA stage length	$n^{-3/2}\lambda^{-2}$
LPA stage energy gain	$n^{-1}\lambda^{-2}$
Number of stages	$n\lambda^2$
Total length	$n^{-1/2}$
Number of e/bunch	$n^{-1/2}$
Laser pulse duration	$n^{-1/2}$
Laser spot size	$n^{-1/2}$
Laser peak power	$n^{-1}\lambda^{-2}$
Laser pulse energy	$n^{-3/2}\lambda^{-2}$
Laser rep. rate	$n$
Beam power	$n^{1/2}$
Laser average power	$n^{-1/2}\lambda^{-2}$
Wall plug power	$n^{1/2}$

Using the scaling laws presented in Table 2, the baseline example of a LPA collider presented in Ref. [5] can be scaled to different plasma densities and laser wavelengths. Tables 1-3 and 1-4 show estimates of parameters for electron-positron colliders for four cases: a 1 TeV center-of-mass (CoM) collider with a plasma density of  $n_0 = 10^{17} \text{ cm}^{-3}$ , a 1 TeV CoM collider using a single-LPA stage with a plasma density of  $n_0 = 2 \times 10^{15} \text{ cm}^{-3}$ , a 10 TeV CoM collider with a plasma density of  $n_0 = 10^{17} \text{ cm}^{-3}$ , and a 10 TeV CoM collider with a plasma density of  $n_0 = 2 \times 10^{15} \text{ cm}^{-3}$ . In all these cases a laser wavelength of  $\lambda = 1 \text{ }\mu\text{m}$  and a laser intensity of  $3 \times 10^{18} \text{ W/cm}^2$  ( $a_0 = 1.5$ ) are assumed. The laser-plasma accelerator parameters are based on scaling laws for the quasi-linear regime obtained from simulation codes. A mild plasma density taper is assumed. The length of one linac is of order of 0.1 km for the 1 TeV CoM,  $n_0 = 10^{17} \text{ cm}^{-3}$  case, and of order 1 km for the 10 TeV CoM,  $n_0 = 10^{17} \text{ cm}^{-3}$  case. Using a lower plasma density with a lower accelerating gradient requires a one-linac length of 0.5 km for a 1 TeV CoM collider and 5 km for a 10 TeV CoM collider.

**Table 3:** Beam parameters of 1 TeV and 10 TeV  $e^+e^-$  colliders based on LPA technology.

Case: CoM Energy (Plasma density)	1 TeV ( $10^{17} \text{ cm}^{-3}$ )	1 TeV ( $2 \times 10^{15} \text{ cm}^{-3}$ )	10 TeV ( $10^{17} \text{ cm}^{-3}$ )	10 TeV ( $2 \times 10^{15} \text{ cm}^{-3}$ )
Energy per beam (TeV)	0.5	0.5	5	5
Luminosity ( $10^{34} \text{ cm}^{-2} \text{ s}^{-1}$ )	2	2	200	200
Electrons per bunch ( $\times 10^{10}$ )	0.4	2.8	0.4	2.8
Bunch repetition rate (kHz)	15	0.3	15	0.3
Horizontal emittance $\gamma\epsilon_x$ (nm-rad)	100	100	50	50
Vertical emittance $\gamma\epsilon_y$ (nm-rad)	100	100	50	50
$\beta^*$ (mm)	1	1	0.2	0.2
Horizontal beam size at IP $\sigma_x^*$ (nm)	10	10	1	1
Vertical beam size at IP $\sigma_y^*$ (nm)	10	10	1	1
Disruption parameter	0.12	5.6	1.2	56
Bunch length $\sigma_z$ ( $\mu\text{m}$ )	1	7	1	7
Beamstrahlung parameter $\Upsilon$	180	180	18,000	18,000
Beamstrahlung photons per e, $n_\gamma$	1.4	10	3.2	22
Beamstrahlung energy loss $\delta_E$ (%)	42	100	95	100
Accelerating gradient (GV/m)	10	1.4	10	1.4
Average beam power (MW)	5	0.7	50	7
Wall plug to beam efficiency (%)	6	6	10	10
One linac length (km)	0.1	0.5	1.0	5

The conversion efficiencies assumed are 50% for laser to plasma wave and 40% for plasma wave to beam (laser to beam efficiency is 20%). A high laser wall plug efficiency of 50% is also assumed, giving an overall efficiency, wall plug to beam, of 10%. Notice that the laser energy per stage per bunch is on the order of tens of J (for  $n_0 = 10^{17} \text{ cm}^{-3}$ ) and the required rep rates are of the order of tens of kHz (for  $n_0 = 10^{17} \text{ cm}^{-3}$ ), clearly indicating the need for the development of laser systems with high average power (hundreds of kW) and high peak power (hundreds of TW). Another set of LPA collider parameters, using a different baseline example, can be found in Ref. [8].

As the plasma density scalings shown in Table 2 indicate, operating at lower density reduces the required wall plug power for fixed luminosity. This is achieved by using more charge/bunch at a lower repetition rate. As discussed in Ref. [5], operating at higher charge/bunch implies more severe beam-beam effects at the IP. Table 3 shows that at  $n_0 = 2 \times 10^{15} \text{ cm}^{-3}$  the beamstrahlung induced energy loss is prohibitively high. Here the beamstrahlung induced fractional energy loss is estimated from  $\delta_E \approx 1.24(\alpha^2 \sigma_z / r_e \gamma) Y^2 [1 + (3Y/2)^{2/3}]^2$ , and “100%” indicates that this formula predicts energy loss greater than the incoming particle energy, i.e., that the energy loss is so severe that the particle orbit is strongly perturbed during the passage through the counterpropagating bunch.

A process that extracts the energy of the remaining wakefields in the plasma as well as in the bunches has been suggested [9]. Inserting circuitry in the plasma as a passive feedback system extracts the wakefield energy, converts this energy into electricity, and feeds it into an external circuit. The conversion efficiency is on the order of unity. Thus, it would enhance the coupling efficiency of the laser pulse to the wakefield

energy by at least a factor of 2 (or even more). Other energy extraction methods may be envisioned, such as using a trailing anti-resonant laser pulse (or a low energy e-beam) to gain energy from the remaining plasma wave and to transport that energy out of the plasma [5].

**Table 4:** Laser and plasma parameters of 1-10 TeV  $e^+e^-$  colliders based on LPA technology.

Case: CoM Energy (Plasma density)	1 TeV ( $10^{17} \text{ cm}^{-3}$ )	1 TeV ( $2 \times 10^{15} \text{ cm}^{-3}$ )	10 TeV ( $10^{17} \text{ cm}^{-3}$ )	10 TeV ( $2 \times 10^{15} \text{ cm}^{-3}$ )
Wavelength ( $\mu\text{m}$ )	1	1	1	1
Pulse energy/stage (kJ)	0.032	11	0.032	11
Pulse length (ps)	0.056	0.4	0.056	0.4
Repetition rate (kHz)	15	0.3	15	0.3
Peak power (PW)	0.24	12	0.24	12
Average laser power/stage (MW)	0.48	3.4	0.48	3.4
Energy gain/stage (GeV)	10	500	10	500
Stage length [LPA + in-coupling] (m)	2	500	2	500
Number of stages (one linac)	50	1	500	10
Total laser power (MW)	48	3.4	480	34
Total wall power (MW)	160	23	960	138
Laser to beam efficiency (%) [laser to wake 50% + wake to beam 40%]	20	20	20	20
Wall plug to laser efficiency (%)	30	30	50	50
Laser spot rms radius ( $\mu\text{m}$ )	69	490	69	490
Laser intensity ( $\text{W}/\text{cm}^2$ )	$3 \times 10^{18}$	$3 \times 10^{18}$	$3 \times 10^{18}$	$3 \times 10^{18}$
Laser strength parameter $a_0$	1.5	1.5	1.5	1.5
Plasma density ( $\text{cm}^{-3}$ ), with tapering	$10^{17}$	$2 \times 10^{15}$	$10^{17}$	$2 \times 10^{15}$
Plasma wavelength (mm)	0.1	0.75	0.1	0.75

Table 5 shows the present readiness of the laser systems, plasma and beam generation and other required accelerator components for a laser-plasma linear collider.

#### 1.1.2.4 *Post-BELLA Laser-Plasma Accelerator Applications*

In 2006, a cm-scale laser-plasma accelerator (LPA) was first demonstrated at LBNL that produced 1 GeV electron beams with a time integrated energy spread of about 2.5%, containing 30 pC of charge, using a 40 TW laser pulse (2 J/pulse) [4]. Presently PW peak power, short-pulse (<100 fs) laser systems are under construction at several laboratories, and it is anticipated that such systems will enable 10 GeV LPA electron beams produced in 1 m of plasma, operating at plasma densities of  $10^{17} \text{ cm}^{-3}$ . A compact source of 10 GeV LPA beams would potentially have many applications. For example, such beams could be used to power a free-electron laser (FEL), producing femtosecond X-rays for basic science applications (a later section of this whitepaper discusses laser requirements for LPA-driven FELs). A compact source of 1-10 GeV LPA beams also could be used as a beam test facility for beam dynamics studies and high-energy physics detector testing.

**Table 5:** Laser-plasma accelerator technology readiness:  $\checkmark$  means presently achievable;  $—$  means within one order of magnitude of the required value (or expectation of being there in the near to medium term); X means not presently achievable (requires significant long term R&D).

<b>Laser Properties</b>	
Peak intensity: $\sim 10^{18}$ W/cm <sup>2</sup>	$\checkmark$
Peak Power: $\sim 0.1$ PW @ $n \sim 10^{17}$ cm <sup>-3</sup> $\sim 10$ PW @ $n \sim 10^{15}$ cm <sup>-3</sup>	$\checkmark$ $—$
Pulse duration: $> 50$ fs	$\checkmark$
Pluse energy: $\sim 10$ J @ $n \sim 10^{17}$ cm <sup>-3</sup> $\sim 10$ kJ @ $n \sim 10^{15}$ cm <sup>-3</sup>	$\checkmark$ X
Pulse shaping	$—$
Average Power: $\sim$ MW	X
Rep. rate: $\sim 1 - 10$ kHz	X
Efficiency (wall-to-laser): $> 10\%$	X
<b>Plasma and Beam Properties</b>	
Plasma channel length: $\sim 1$ m @ $n \sim 10^{17}$ cm <sup>-3</sup> $\sim 300$ m @ $n \sim 10^{15}$ cm <sup>-3</sup>	$—$ X
Plasma channel tapering: $\sim 1$ m @ $n \sim 10^{17}$ cm <sup>-3</sup> $\sim 300$ m @ $n \sim 10^{15}$ cm <sup>-3</sup>	$—$ X
Stability (pointing for IP)	X
Shaped bunches	X
Transverse emittnace ( $< 0.1$ mm mrad)	$—$
Longitudinal emittance ( $< \%$ )	$—$
Charge ( $\sim 10^9$ )	$—$
<b>Accelerator Components</b>	
LPA staging	$—$
Laser-plasma coupling (plasma mirrors)	$—$
LPA-compatible injector	$—$
Compact beam cooling	X
Compact final focus (plasma lens)	X

Current PW, short-pulse laser systems under construction (e.g., the BELLA Facility at LBNL, or the ELI-Beamlines in Prague) would operate at low repetition rate (1-10 Hz) and would be low average-power laser systems. Although, for example, a compact, low-repetition rate LPA-driven FEL could provide high-peak brightness light for user experiments, the applicability of this technology for large-scale user facilities requiring high-average brightness would require repetition rates that are beyond today's state of the art in high-peak-power lasers. Table 6 shows an example of a 10 GeV accelerator in a single LPA stage operating at  $10^{17}$  cm<sup>-3</sup>. Development of kHz, high peak power laser systems would enable a compact source of multi-kW, ultra-short ( $< 10$  fs), 10 GeV electron beams for user applications. The single-stage LPA example shown in Table 6 could be staged, using multiple laser systems, to higher electron beam energy.

**Table 6:** 10 GeV laser-plasma accelerator with laser driver at 1 Hz to 1 kHz.

<b>Parameter</b>	
Plasma density	$10^{17} \text{ cm}^{-3}$
Electrons/bunch	$4 \times 10^9$
Repetition rate	1 Hz – 1 kHz
Laser wavelength	1 $\mu\text{m}$
Laser pulse duration	0.1 ps
Beam energy gain/stage	10 GeV
Stage length	1 m
Average laser power/stage	32 W – 32 kW
Beam power (single stage)	6.4 W – 6.4 kW

### 1.1.3 Linear Colliders Based on Dielectric Laser Acceleration

#### 1.1.3.1 Dielectric Laser Acceleration: Linear Collider Parameters

Dielectric laser acceleration (DLA) refers to the use of micron-scale dielectric structures driven by lasers operating in the optical to near infrared regime [10-12]. The use of a laser as the drive source for the accelerating field offers several benefits, including the high repetition rates ( $> 10 \text{ MHz}$ ) and strong electric fields ( $> 0.5 \text{ GV/m}$ ) that modern lasers can provide, combined with improved commercial availability and cost when compared with microwave sources. The use of dielectric structures circumvents the problem of power loss in metallic cavities at optical frequencies; it also allows for an order of magnitude higher accelerating gradients due to the higher breakdown thresholds (1-5 GV/m) of dielectric materials.

Charged particles are accelerated inside a central channel inside a dielectric photonic crystal material. The channel acts as both the vacuum pipe for the beam and as a confining mechanism for an electromagnetic mode. Assuming that the guiding channel's transverse dimensions are of the order of the drive laser wavelength (1 to 10 microns) the power coupling efficiency to the particle bunches can in principle be as high as 40%, with optimal efficiency at bunch charges at the fC level [13]. In order for successive bunches to sit in the accelerating phase of the wave, the requisite bunch durations are on the attosecond scale with intra-bunch spacing equal to the laser wavelength (or an integer multiple thereof). As a result of the various technical requirements just mentioned, the beam parameters for an accelerator based on this technology would be quite different from both traditional machines and other advanced schemes.

DLA offers several compelling potential advantages over traditional microwave cavity accelerators. Accelerating gradient is limited by the breakdown threshold for damage of the confining structure in the presence of intense electromagnetic fields. In the DLA scheme operating at typical laser pulse lengths of 0.1 to 1 ps, the laser damage fluences for dielectric materials such as silicon and glass correspond to peak surface

electric fields of 400 to 2000 MV/m (compared to the breakdown limits of 40 to 100 MV/m for metal cavities). The corresponding gradient enhancement represents a reduction in active length of the accelerator between 1 and 2 orders of magnitude. Power sources for DLA-based accelerators (lasers) are cheaper than microwave sources (klystrons) for equivalent average power levels due to the wider availability of, and private sector investment in, commercial laser sources. The high laser-to-particle coupling efficiency makes required pulse energies are consistent with tabletop microjoule class lasers. Fabrication techniques for constructing three-dimensional dielectric structures with nanometer-level precision are well established in the semiconductor industry and the capillary fiber industry. Once a suitable fabrication recipe is developed, on-chip DLA devices with multiple stages of acceleration and waveguides for coupling power to and from the structure could be manufactured at low per-unit cost on silicon wafers.

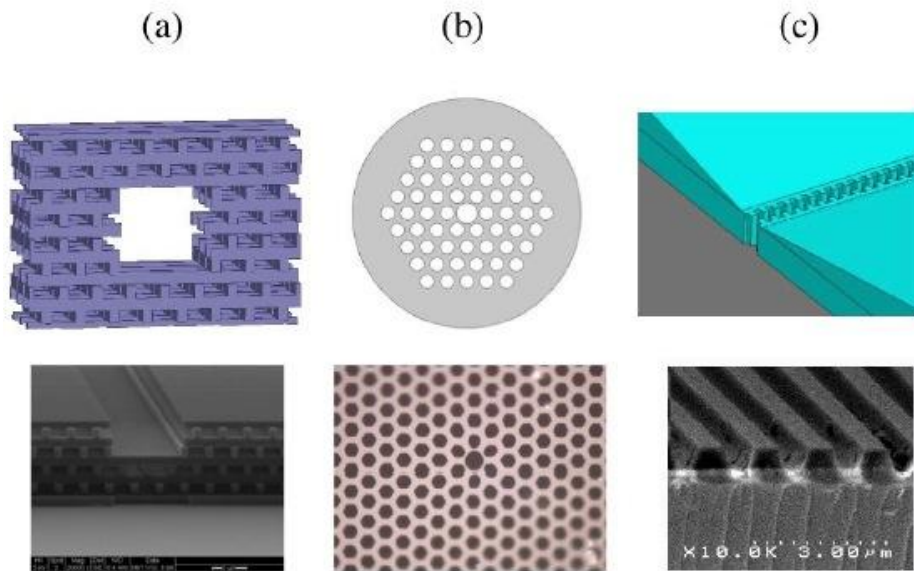


**Figure 4:** Three dielectric laser accelerator topologies: (a) a 3D silicon photonic crystal structure, (b) a hollow-core photonic bandgap fiber, and (c) a dual-grating structure, showing conceptual illustration (top) and recently fabricated structures (bottom).

Several DLA topologies are under investigation as part of the SLAC E-163 program, as seen in Fig. 4: (a) a silicon “woodpile” photonic crystal waveguide, (b) a glass photonic bandgap (PBG) hollow-core optical fiber, and (c) a structure where the beam is accelerated by a transversely incident laser beam in the gap between two gratings. Significant progress has been made in the fabrication of partial or full prototypes of these structures with geometries optimized for accelerator use, as seen in the bottom images. Steps required to make these into working prototypes include alignment and bonding of two of the 9-layer half woodpile structures seen in (a), reducing the fiber dimensions in (b) from an operating wavelength of 7 to 2 microns (where lasers and detectors are more readily available), replacing borosilicate with the more radiation-hard silica, and aligning and bonding two of the gratings shown in (c), which are designed for 800-nm laser operation.

To reach 10 TeV center-of-mass energies, a next generation lepton collider based on

traditional RF microwave technology would need to be over 100 km in length and would likely cost tens of billions of dollars to build. Due to the inverse scaling of the interaction cross section with energy, the required luminosity for such a machine would be as much as 100× higher than proposed 1-3 TeV machines (ILC and CLIC), producing a luminosity goal of order  $10^{36} \text{ cm}^{-2} \text{ s}^{-1}$ . In attempting to meet these requirements in a smaller cost/size footprint using advanced acceleration schemes, the increased beam energy spread from radiative loss during beam-beam interaction (beamstrahlung) at the interaction point becomes a pressing concern. Since the beamstrahlung parameter is proportional to bunch charge, a straightforward approach to reducing it is to use small bunch charges, with the resulting quadratic decrease in luminosity compensated by higher repetition rates. This is the natural operating regime of the DLA scheme, with the requisite average laser power (>100 MW) and high (>10 MHz) repetition rates to be provided by modern fiber lasers.

**Table 7:** Strawman Parameters for 3 DLA Topologies

<b>Parameter</b>	<b>Units</b>	<b>"ILC"</b>	<b>Woodpile</b>	<b>Fiber</b>	<b>Grating</b>
E_cms	GeV	10000	10000	10000	10000
Bunch Charge	e	3.0E+10	1.8E+04	3.8E+04	1.0E+04
# bunches/train	#	2820	136	159	375
train repetition rate	MHz	5.0E-06	25	5	10
macro bunch length	psec	1.00	1.00	0.50	0.33
design wavelength	micron	230609.58	1.55	1.89	0.80
Invariant Emittances	micron	10/0.04	1e-04/1e-04	1e-04/1e-04	1e-04/1e-04
I. P. Spot Size	nm	158/1	0.06/0.06	0.06/0.06	0.06/0.06
Beamstrahlung E-loss	%	16.3	2.4	5.4	3.8
<b>Enhanced Luminosity</b>	<b>/cm<sup>2</sup>/s</b>	<b>1.23E+36</b>	<b>2.04E+36</b>	<b>4.09E+36</b>	<b>2.82E+36</b>
Beam Power	MW	338.8	49.0	24.2	30.0
Wall-Plug Power	MW	1040.0	490.2	242.0	300.4
Gradient	MeV/m	30	197	400	830
Total Linac Length	km	333.3	50.8	25.0	12.0

**Table 8:** Laser Parameter Requirements from DLA 2011 Workshop

<b>Requirement</b>	<b>Woodpile</b>	<b>Fiber</b>	<b>Grating</b>	<b>Resonant Structure</b>
Pulse Energy	200 nJ	1 μJ	10 μJ	1-10 μJ
Average Power	200W	1 kW	10kW	1kW
Wavelength	>2μm	>1μm	>1μm	>1μm
Pulse Widths	1 ps	1 ps	0.1-0.2 ps	1.8-10ps
CEP Locking	< 1°	< 1°	< 1°	< 1°
Repetition Rate (MHz)	100-1000	100-1000	100-1000	100-1000
Wallplug Efficiency	30-40%	30-40%	30-40%	30-40%

Numbers for a 10 TeV collider scenario are shown in Table 7. For comparison, we have extrapolated a corresponding case for traditional RF technology by scaling the parameters for the proposed International Linear Collider (ILC) to 10 TeV. In these examples, DLA meets the desired luminosity, and with a significantly smaller beamstrahlung energy loss. Other advanced collider schemes such as beam-driven plasma and terahertz also rely upon a traditional pulse format for the electron/positron

beam and would therefore compare similarly to laser plasma acceleration in this regard. Although the numbers in Table 7 are merely projections used for illustrative purposes, they highlight the unique operating regime that has DLA poised as a promising technology for future collider applications.

Corresponding laser requirements are summarized in Table 8, which is derived from results of the DLA 2011 ICFA Mini-Workshop at SLAC [14]. The parameters reflect the unusual pulse format of the electron beam: namely very high rep rates with low per-pulse energy but high average power. In addition, because each laser pulse can drive an entire bunch train in the DLA scenario, sub-picosecond pulse lengths are not required. Fiber lasers at 1 micron wavelengths and hundreds of watts of average power have already been demonstrated to be capable of meeting most of these parameter requirements and higher power (>1 kW) mode-locked systems at longer wavelengths (e.g., 2 micron thulium-doped lasers) are expected to be commercially available in the near future.

### 1.1.3.2 *Challenges and Opportunities*

Although DLA is a promising concept for future accelerators, it is a relatively new field of study, and the demanding requirements of a linear collider pose a variety of challenges. We discuss some of these challenges below to help set the direction and priorities for future research.

#### *Demonstration of Gradient*

Achievable gradient in DLA structures is limited by the damage threshold of the dielectric material at infrared wavelengths and picosecond pulse durations. Recent progress has been made to characterize a variety of common and exotic materials (quartz, silicon, and oxides of aluminum, hafnium, and zirconium) in both bulk and post-fabrication topologies [15]. Experiments for beam-on demonstrations of the prototypes in Fig. 4 are currently in progress at Stanford and SLAC National Accelerator Laboratory, the initial goals of which are to demonstrate acceleration and measure achievable gradient [16]. The first prototype to be tested will be the dual-grating structure of Fig. 4(c).

#### *Detector Resetting at High Repetition Rates*

The repetition rates proposed in Table 7 for a future DLA collider are of the same order of magnitude as those currently in use at the ATLAS detector at LHC, which has a maximum crossing rate of 40 MHz. Since the DLA luminosities in Table 7 have been scaled to match that for traditional RF technology at the same center-of-mass energy, but with lower charge per bunch, the total number of events per second has merely been redistributed over a larger number of crossings. At ATLAS, only 200 crossings are recorded per second, using a sophisticated trigger system that selectively filters them [17]. Techniques for filtering and processing large numbers of crossings will continue to improve, and constitute a challenge for HEP generally that is not limited to the DLA concept.

### *Transverse Wakes and Beam Breakup*

Preliminary estimates of emittance growth due to transverse wakefields and beam-breakup (BBU) instability were performed by Eric Colby for the Report of the 2011 ICFA Mini-Workshop on Dielectric Laser Acceleration [14]. The train of bunches was represented by macroparticles propagating through a simplified BBU model [18] using estimates of the transverse wakes corresponding to a vacuum channel in bulk dielectric. The results indicated approximately 2 nm of emittance growth with 500 GeV of acceleration over 1 km, with tolerances of 30 nm on the transverse co-alignment of the quadrupole and accelerator elements. However, simulation of the transverse wakes for particular structures and more sophisticated modeling of the BBU will be needed to better understand the tolerances required to mitigate these effects.

### *Efficient Coupling and Dissipation of Power*

Proper handling of kilowatts of average laser power in micron-scale structures requires the development of integrated couplers with high (near 100%) efficiency. Significant progress has been made recently in simulating such couplers for the woodpile structure using silicon-on-insulator (SOI) waveguides [19]. The power distribution scheme is then envisioned as a fiber-to-SOI coupler that brings a pulse from an external fiber laser onto the integrated chip, distributes it between multiple structures via SOI power splitters, and then recombines the spent laser pulse and extracts it from the chip via a mirror-image SOI-to-fiber output coupler [20], after which the power is either dumped or, for optimal efficiency, recycled [21].

### *Compatible Electron and Positron Sources*

As seen in Table 7, the bunch charges for optimal laser-to-beam coupling efficiency are in the range of 1-20 fC. In order for successive bunches to sit in the accelerating phase of the wave, the requisite bunch durations are on the attosecond scale, with intrabunch spacing equal to the laser wavelength. A technique for generating the requisite optically microbunched attosecond scale beams was recently demonstrated at SLAC [22], and recent work in field emission needle-tip emitters demonstrates that electron beams with the requisite charge and emittance requirements are within reach [23]. Development of compatible positron sources remains an important unsolved problem.

#### **1.1.4 $\gamma\gamma$ Colliders**

An electron-electron linear collider can be converted to a photon-photon collider by converting the electron beams into photon beams by irradiating laser beams just before the collision point as shown in Figure 5.

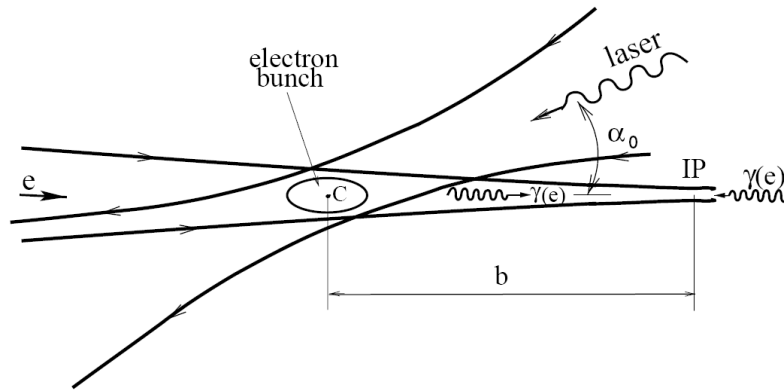


**Figure 5:** Illustration of the principle of a  $\gamma\gamma$  collider.

This scheme opens the possibility for investigating different physics from the collider than when it is operating with charged particle beams. The wave length  $\lambda_L$  of the laser should be as short as possible for creating high energy photons from a given electron energy. However, it must satisfy

$$\lambda_L [\mu\text{m}] > \sim 4 E_e [\text{TeV}]$$

where  $E_e$  is the electron energy, because, otherwise, the created high-energy photons would be lost by electron-positron pair creation in the same laser beam. To obtain a narrow photon energy spectrum the laser beam should be circularly polarized (and electrons longitudinally polarized). Linear polarization may sometimes be needed depending on the physics processes being studied.

Since the transverse electron beam size at the conversion point is much smaller than the laser spot size, the probability of conversion is almost entirely determined by the laser parameters and is independent of the electron parameters as long as the electrons go through the entire length of the laser pulse. For almost all the electrons to be converted into photons, the required flash energy of the laser pulse is approximately given by

$$A = \omega_L * \sigma_C / S_L$$

where  $\omega_L$  is the laser photon energy,  $\sigma_C$  the cross section of Compton scattering, and  $S_L$  the effective cross section of the laser beam.  $S_L$  cannot be too small due to the Rayleigh length requirement. Thus, in any case  $A$  is a few Joules. On the other hand, the required pulse structure of the laser beam, which must match the electron beam, strongly depends on the collider design. In particular, a superconducting collider (e.g. ILC), a normal-conducting collider (e.g., CLIC) or a laser plasma accelerator (LPA) demand very different pulse structures. The pulse structure can be characterized by a few parameters:  $n_b$  the number of bunches in a train,  $t_b$  the interval between bunches,  $n_b * t_b$  the train length, and  $f_{\text{rep}}$  the repetition frequency of the trains. The train length is  $O(\text{ms})$  for superconducting colliders but is  $O(\mu\text{s})$  or less for a normal-conducting collider.

Table 9 shows examples of the required laser parameters for low-energy (Low-mass Higgs region)  $\gamma\gamma$  colliders based on the ILC, CLIC and LPA parameters. The parameters for the ILC is based on those given by V. Telnov [24] slightly modified according to the

present ILC parameters [25]. The parameters for CLIC are based on the proposal CLICHÉ [26] with the updated parameters of CLIC [27]. V. Telnov made important correction to some of the CLIC parameters as well as provided the laser parameters. [28] (For the ILC a possible use of FEL is proposed [29] but this is irrelevant in the present context.) The parameters for LPAs are scaled versions of those in Section 1.1.2 and [5].

All of these parameters are subject to change depending on the project evolution as well as on the optimization of the interaction region. Owing to the long bunch train (980  $\mu$ s) and large bunch spacing (370 ns) for the ILC it is possible to use an optical cavity for accumulating the laser power (the multiplication factor  $Q$  in the table) so that the requirements for the laser are greatly relaxed at the cost of very high precision optical system [30]. This type of optical cavities is similar to that currently under construction for a Compton X-ray source at KEK [31].

For the CLIC it would be difficult to employ an optical cavity because the bunch train is short (177 ns) and the bunch spacing small (0.5 ns). However, the required laser system is similar to a single laser beam line of the Laser Inertial Fusion Energy (LIFE) project at LLNL in the US and can be readily adapted from the existing proposal for the LIFE laser beam.

Figure 6 shows the beam structure of a CLIC-based  $\gamma\gamma$  collider. The laser pulse train for the collider consists of a burst of 354 five-joule, one-picosecond pulses separated by 0.5 ns for a total of 1770 J/burst. These bursts occur at 50 Hz, yielding an average power of 88.5 kW of 1-micron light. The LIFE laser on the other hand is designed to produce over 130 kW of average power with pulse energies of 8.1 kJ at 16 Hz. To make the change to the new pulse format, several changes to the architecture would be required. First, the front end of the laser system would need to be modified to generate the pulse bursts, which is well within current technology capabilities. Due to the low energy of each pulse, only a minimal stretch is needed for the pulses:  $\sim 10\times$ , to 10 ps. This can be accomplished with a very simple stretcher / compressor pair. The diode arrays will need to be triggered at the higher 50 Hz repetition rate. Likewise the Pockels cell in the beam line cavity will have to be modified to enable 50 Hz operation. Since the extracted energy in a burst will only be 1770 J, there is ample margin in the LIFE energetics and extraction design for the laser to perform at this level. Finally, at the output of the laser, the stretched pulses will need to be compressed. Since the energy is low, the beam can be readily expanded to lower the fluence onto moderate aperture gratings and minimize average power effects. After compression, the pulses can be focused by an off-axis parabola onto the intended collider target.

Technology similar to this has also been proposed for the Extreme Light Infrastructure (ELI) project in Europe [32].

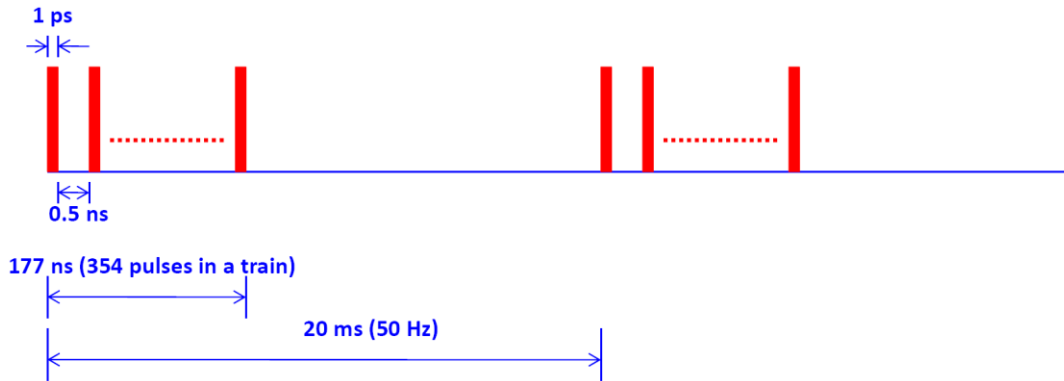


**Figure 6:** CLIC-based  $\gamma\gamma$  collider beam structure.

For an LPA-based  $\gamma\gamma$  collider or low-energy  $e^+e^-$  collider, the same accelerator systems tradeoffs apply for efficiency and gradient as in the 0.5 TeV and higher energy LPA cases considered in section 1.1.2. Since luminosity requirements are a modestly less than those for a 1 TeV  $e^+e^-$  collider, similar accelerator parameters are appropriate to the 1 TeV column in Table 3, with reduced repetition rate of 4 kHz. While the system tradeoffs remain the same, due to the lower beam energy and repetition rate required wall plug power requirements are several-fold lower. The linac length will also be shorter which makes geometric gradient less critical. Hence while parameters similar to those of section 1.1.2 are suitable for a lower energy machine (by using fewer stages), operation can also be considered at higher plasma density where per-pulse laser energy and electron bunch charge is lower and repetition rate is higher. This may be advantageous for laser development purposes as an intermediate step between present facilities and a TeV-scale machine. For example, operating at density of  $10^{18}/\text{cc}$  instead of  $10^{17}/\text{cc}$  would increase repetition rate from 4 kHz to 40 kHz, and reduce laser energy per stage from 32 to 1 J. The price for this: the pulse length also falls from 56 fs to 18 fs, which may require special techniques for some laser systems. As for the higher energy options, 2  $\mu\text{m}$  lasers can be used in place of 1  $\mu\text{m}$ , requiring one-fourth the laser energy per stage and four times as many stages, with other parameters remaining constant.

A key difference from CLIC and ILC based options is that LPAs are expected to produce single bunches rather than bunch trains. Hence the scattering laser should have a repetition rate matched to the accelerator driver, and duration in the range of a few picoseconds. To minimize the required accelerator energy, the laser wavelength should be set by  $\lambda_L [\mu\text{m}] \sim 4 E_e [\text{TeV}]$ , which yields a 0.3  $\mu\text{m}$  laser with a 75 GeV beam to produce the required 120 GeV center of mass. Again, laser alternatives exist, and a 1  $\mu\text{m}$  laser can be used with a 100 GeV electron beam. Table 9 shows the 1  $\mu\text{m}$  laser paired with the LPA operating at  $10^{18}/\text{cc}$  and the 0.3  $\mu\text{m}$  laser with the LPA at  $10^{17}/\text{cc}$ , but these options are interchangeable.

**Table 9:** Beam and laser parameters of  $\gamma\gamma$  colliders.

<b>Electron Beam Parameters</b>	<b>ILC</b>	<b>CLIC</b>	<b>LPA</b> $n_e=10^{17}/\text{cc}$	<b>LPA</b> $n_e=10^{18}/\text{cc}$
Energy per electron beam (GeV)	100	100	75	100
Max energy of photons (GeV)	60 (75)	60	60	60
$\gamma\gamma$ luminosity at the high energy peak ( $10^{34} \text{ cm}^{-2} \text{ s}^{-1}$ )	0.13	0.19	0.3	0.3
Electrons per bunch ( $\times 10^{10}$ )	2	0.68	0.4	0.13
Number of bunches in a train ( $n_b$ )	2640	354	1	1
Distance between bunches ( $t_b$ , ns)	370	0.5	n/a	n/a
Length of the train ( $n_b * t_b$ , $\mu\text{s}$ )	980	0.177	n/a	n/a
Repetition frequency ( $f_{\text{rep}}$ , Hz)	5	50	4	40
Electron bunch length $\sigma_z$ ( $\mu\text{m}$ )	300	44	1	0.3
Normalized emittance $\varepsilon_{x/y}$ (mm-mrad)	10/0.035	1.4/0.050	0.1	0.1
Beta-function at IP $\beta_{x/y}$ (mm)	4/0.3	2/0.02	0.15	0.2
Beam size $\sigma_{x/y}$ (nm)	450/7.3	120/2.3	10	10
Distance between conversion point and IP (mm)	$\sim 1.5$	$\sim 0.5$	$< 75$	$< 350$
Crossing angle (mrad)	25	25	$< 50$	$< 50$
<b>Laser Parameters</b>				
Wavelength ( $\mu\text{m}$ )	1 (0.5)	1	0.3	1
Rayleigh range (mm), $f\#$	$\sim 0.5, 20$	$\sim 0.4, 18$	0.3	1
Laser pulse energy (J)	$\sim 10/Q$	5	2	6
Pulse length (r.m.s., ps)	$\sim 1.5$	$\sim 1$	2	7
Peak power (TW)	$\sim 2.5/Q$	2	1	1
Average power (kW)	150/Q	90	8	240
Laser power in a train (MW)	25/Q	10000	n/a	n/a
Cavity enhancement factor	$Q \sim 300$	1	1	1

Notes on the ILC and CLIC columns of Table 9:

- 1) Distance between the Compton conversion point (CP) and the interaction point (IP) is  $b = \gamma\sigma_y$ .
- 2) Thickness of the laser target is equal to 1.2 collision lengths.
- 3) Luminosity in the high energy peak means  $L_{\gamma\gamma}(W > 0.8W_{\text{max}})$
- 4) For the ILC, the numbers are given for  $\lambda = 1 \mu\text{m}$ . Those in ( ) are for  $\lambda = 0.5 \mu\text{m}$ .
- 5) For the ILC,  $\lambda = 1 \mu\text{m}$  is OK and  $\lambda = 0.5 \mu\text{m}$  may be possible. But for CLIC only  $\lambda = 1 \mu\text{m}$  is allowed because the disruption angle is 1.5 times larger. [The disruption angle is proportional to  $(N/\sigma_z)^{1/2}$ .]
- 6) ‘‘Undulator’’ parameter  $\xi^2 = 0.15$  (0.2) was used for  $\lambda = 1$  (0.5)  $\mu\text{m}$ , corresponding to reduction of  $W_{\text{max}}$  by 5%.

Notes on the LPA columns of Table 9:

- 1) Parameters for LPA example at  $10^{17}/\text{cc}$  and  $10^{18}/\text{cc}$  are drawn from Section 1.1.2 and Ref. [5].
- 2) Laser parameters for LPA example refer to scattering laser. For drive laser parameters, see Table 3.

## 1.1.5 Plasma Accelerators as Injectors with the Example of LHeC

### 1.1.5.1 Introduction

Plasma-based linear accelerators carry the promise to allow feasibility of compact and therefore less expensive linear colliders for high energy physics (HEP). The path to a laser plasma accelerator (LPA) is described elsewhere and parameter tables for linear colliders based on this technology have been worked out. It will still require a significant time until a TeV-class LPA can be constructed. In the meantime it would be important to use laser plasma acceleration with applications for lower beam energies.

One possible use case is a laser-plasma linac as injector for other accelerators. Such an application would allow gaining experience with this technology and developing it into full maturity. As an example we describe an idea for the application of a laser-plasma accelerator to LHeC.

### 1.1.5.2 Example: The Large Hadron Electron Collider (LHeC)

The LHeC is a concept for extending the LHC [33] physics program with collisions of 7 TeV protons and 60 GeV electrons in the interaction region “IR2” of LHC. Its conceptual design is described in [34]. The options of a ring-ring (RR) or linac-ring (LR) layout are presently being considered. In the RR scheme, a second ring accelerator is installed into the LHC tunnel and used for the storage and acceleration of the 60 GeV electron beam. In the LR scheme an energy recovery linac is used to accelerate electrons to 60 GeV and to bring them into collision with the stored LHC beam. The LR requires a new tunnel for the linac, aiming at IR2 of the LHC. The design parameters for LHeC are listed in Table 10.

#### 1.1.5.2.1 Electron Beam Requirement for LHeC (RR)

The ring-ring option of the LHeC requires that electron bunches are generated, sufficiently pre-accelerated and injected into the LHeC electron ring. The target beam parameters for injection are as follows:

- |                                     |  |
|-------------------------------------|--|
| 1) Beam energy:                     | 10 GeV   |
| 2) Bunch population:                | $20 \times 10^9 e^-$<br>( $14 \times 10^9 e^-$ for nom. performance) |
| 3) Normalized transverse emittance: | 0.29 mm-rad  |
| 4) Pulses for injection:            | $\sim 5$ Hz  |

This beam would allow filling the required 2808 bunches of the LHC within about 10 minutes. The bunch length is not critical, as long as the transverse-mode coupling instability can be kept under control. Single bunch injection is preferred but accumulation (as was done in LEP) can be envisaged if required. Accumulation is the repeated injection into the same RF bucket of the ring. Several methods exist for this.

**Table 10:** The main parameters for the LHeC, for electron (left) and proton (right) beams. Both the ring-ring (RR) and linac-ring (LR) options are listed. This table was copied from the LHeC conceptual design report [34].

electron beam	RR	LR	LR <sup>*)</sup>	proton beam	RR	LR
e- energy at IP[GeV]	60	60	140	bunch pop. [ $10^{11}$ ]	1.7	1.7
luminosity [ $10^{32} \text{ cm}^{-2}\text{s}^{-1}$ ]	13	10	0.4	tr.emit. $\gamma\epsilon_{x,y}$ [ $\mu\text{m}$ ]	3.75	3.75
polarization [%]	40	90	90	spot size $\sigma_{x,y}$ [ $\mu\text{m}$ ]	30, 16	7
bunch population [ $10^9$ ]	20	1.0	1.5	$\beta^*_{x,y}$ [m]	1.8,0.5	0.1
e- bunch length [mm]	10	0.3	0.3	bunch spacing [ns]	25	25
bunch interval [ns]	25	25	50			
transv. emit. $\gamma\epsilon_{x,y}$ [mm]	0.58, 0.29	0.05	0.1			
rms IP beam size $\sigma_{x,y}$ [ $\mu\text{m}$ ]	30, 16	7	7			
e- IP beta funct. $\beta^*_{x,y}$ [m]	0.18, 0.10	0.12	0.14			
full crossing angle [mrad]	1	0	0			
geometric reduction $H_{hg}$	0.75	0.91	0.94			
repetition rate [Hz]	-	-	10			
beam pulse length [ms]	-	-	5			
ER efficiency	-	94%	-			
average current [mA]	131	6.4	0.27			
tot. wall plug power[MW]	100	100	100			



RR= Ring – Ring    LR =Linac –Ring

Ring: with 1° as baseline : L/2  
Linac: clearing gap: L\*2/3

\*) pulsed, but high energy ERL not impossible

#### 1.1.5.2.1 Electron Beam Requirement for LHeC (LR)

The linac-ring option of the LHeC requires generating and delivering to the LHC ring a different kind of electron beam:

- 1) Beam energy: 60 GeV
- 2) Normalized transverse emittance: 50  $\mu\text{m-rad}$
- 3) Bunch charge:  $2 \times 10^9$
- 4) Electron current: 6.4 mA
- 5) Electron flux:  $3.3 \times 10^{16}$  Hz
- 6) Bunch spacing: 50 ns
- 7) Mode: CW

The electron beam power at the IP is 384 MW. The concept of the LR LHeC foresees that most of this power is recouped in energy recovery linacs. Total required power for the electron beam should remain at or below 100 MW. The LR option foresees also a pulsed mode of the linacs for very high beam energies (above 140 GeV).

#### 1.1.5.3 Possibilities for a Laser-Plasma Linac and Issues

Laser plasma accelerators have seen tremendous advances over the recent years. The progress cannot be reviewed here in any detail, so we point to the published literature and the references therein. The EuroNNAc workshop in May 2011 provided an interesting overview and slides of the presentations can be accessed in [35]. The

electron beams achieved to date with laser plasma accelerators have the following typical properties:

- |                                     |                                 |
|-------------------------------------|---------------------------------|
| 1) Beam energy:                     | 0.1 – 1.0 GeV                   |
| 2) Normalized transverse emittance: | $\sim 10 \mu\text{m-rad}$       |
| 3) Bunch charge:                    | $\sim 1 \times 10^9$            |
| 4) Repetition rate:                 | 0.1 – 10 Hz                     |
| 5) RMS energy spread:               | $\sim 1\%$                      |
| 6) RMS bunch length:                | $\sim 0.5 \mu\text{m}$ (1.5 fs) |

The presently achieved electron beam parameters with laser plasma accelerators do not fit directly into the LHeC requirements. In particular, CW operation as foreseen for the LR option, is not feasible. A laser plasma accelerator for the LR option is also disfavored due to the absence of the energy recovery option, which is required for keeping the power needs of the electron machine below 100 MW.

The use of a laser plasma accelerator for the RR option of LHeC seems to have fewer feasibility challenges compared to the LR option, with the exception of the following issues for injection into the electron ring of the LHeC:

1. The **beam energy** of the electron beam must be increased by a factor of 10, to about 10 GeV. The ongoing BELLA project [36] at LBNL is targeted to demonstrate the generation of 10 GeV electron beams from a laser plasma accelerator. Its goal should be achieved within the next 2 years.
2. The **bunch population** should be increased by a factor of 10-20 beyond present achievements. Alternatively, accumulation of 10 injections per RF bucket would be required, resulting in a  $10\times$  increase in the required repetition rate. Lasers can be operated at high repetition rates.
3. The **bunch length** of the generated bunches is much shorter than required. This is, *a priori*, no problem, as the electron beam will approach its equilibrium distribution once stored. However, fast instabilities must be controlled. In particular, the transverse mode coupled instability could be a problem, as it is worsened by short bunch length.

The first two items are expected to impose no fundamental feasibility issue for a possible use in the RR option of the LHeC. The third item is an interesting problem for further accelerator physics studies that explore the injection and control of ultra-short bunches in storage rings. There is no experimental experience with such bunches and theoretical studies would be required before assessing feasibility limits in this new regime.

#### 1.1.5.4 Conclusion

The electron beams generated today from laser plasma accelerators are approaching parameters that make their usage interesting for new applications. The use of advanced electron accelerators for linear colliders has been discussed in the literature. In this short report we have discussed the possible use of an advanced LPA as injector for the LHeC proposal. The application for the ring-ring option of the LHeC is indeed not fully

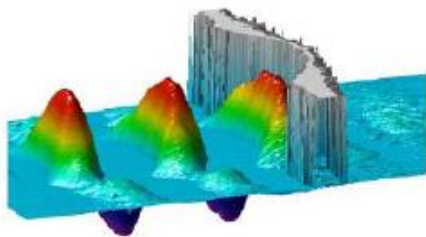
excluded and could be used to demonstrate gains in size and cost with the new technologies, while developing them to full maturity for linear collider applications. Required R&D studies would involve the study of injection with ultra-short bunches into a storage ring. This is an interesting topic and theoretical studies are required.

It is noted that only one example application has been considered in this short note, namely, the LHeC. However, other applications for high energy physics and photon science ring facilities can be envisaged—for example, top-up of electron storage rings during operation.

### 1.1.6 Perspectives on Laser Proton Acceleration to the TeV Range

Recently RPA acceleration has been demonstrated with laser intensities in the range just below  $10^{20}$  W/cm<sup>2</sup>. Proton and carbon bunches of about 1 MeV/u with relatively narrow bandwidth energy can be observed [40]. In a paper by Zheng *et al.* [37-38] perspectives are given on extending this to the TeV range. RPA acceleration requires an ultra-high intensity laser with circular polarization to interact with a very thin target. The requirement of well-defined beam quality is very demanding, and a pre-pulse level below  $10^{-10}$  is mandatory to allow for this process.

#### RPA(PSA): nm target



efficiency~10%, GeV

**Figure 7:** The process of RPA acceleration. The laser is impinging on the ultra-thin foil, building up a compressed layer of electrons, which in return transfers momentum to all the particles in the foil. [39-40]

The experimentally observed proton energy at  $\sim 5 \times 10^{19}$  W/cm<sup>2</sup> is approximately 1 MeV. The proton energy scales nearly linearly with the laser intensity, requiring about  $10^{23}$  W/cm<sup>2</sup> to produce 1 GeV proton beams. Starting from this energy level, further acceleration in a plasma wakefield would become possible. In the paper by Zheng *et al.* it is even proposed that this might be achieved by merely adding a region of gas behind the original RPA target.

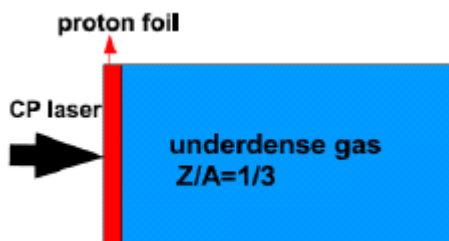


**Figure 8:** Combined RPA and wakefield acceleration as proposed by Zheng *et al.* [37-38]

The theoretical modelling of this is presently done by 1D calculation, which might not give a full description of the problem. Even if the process were not as favourable in this direct combination, the principle of injecting RPA accelerated protons into a stage using wakefield acceleration would seem applicable. The requirements on the laser driver are mainly driven by the RPA process, where laser intensity close to  $10^{23}$  W/cm<sup>2</sup> has to be reached. The present level reached with sufficient quality does not exceed  $10^{20}$  W/cm<sup>2</sup>. The wakefield acceleration requirement, by itself, will be similar to the case of electron acceleration.

## 1.1.7 Laser Stripping of H<sup>-</sup> Particles in High-Intensity Proton Accelerators

### 1.1.7.1 Laser Stripping of H<sup>-</sup> Particles for SNS

The Spallation Neutron Source (SNS) at the Oak Ridge National Laboratory (ORNL) is the world's most powerful short-pulsed, accelerator based neutron scattering facility for scientific research and industrial development. The SNS accelerator complex utilizes charge-exchange injection to “stack” a high-intensity proton beam in the accumulator ring for short-pulse neutron production. In this process, a 1 ms hydrogen ion (H<sup>-</sup>) beam pulse is transported to a carbon stripping foil located at the injection point of the ring. The electrons are stripped and the resulting proton is merged with the previously accumulated beam. This injection scheme is central to the operation of many accelerator facilities including the SNS, J-PARC, ISIS and PSR that use the H<sup>-</sup> beam. When the beam power is increased from the 1 MW to more than 3 MW as envisioned in the SNS Power Upgrade project, the stripping foils become radioactive and produce uncontrolled beam loss, which is one of the main factors limiting beam power in high intensity proton rings.

A “foil-less” charge exchange injection method was first proposed in the 1980s by using a field dissociation process. This scheme requires an impractically large laser power, which is indeed the central difficulty involved in ionizing neutral hydrogen. Danilov et al. proposed a three-step scheme for laser stripping. This scheme works as follows: First, H<sup>-</sup> ions are converted to H<sup>0</sup> by stripping off the first electron in a magnetic field; then H<sup>0</sup> atoms are excited from the ground state ( $n = 1$ ) to the upper levels ( $n \geq 3$ ) by a laser, and the excited states H<sup>0\*</sup> are converted to H<sup>+</sup> by stripping the second electron in a second magnetic field.

In a proof-of-principle experiment, a third harmonic beam from a Q-switched laser was used for stripping. The laser generates a 30 Hz, 6 ns pulses with a peak power of ~10 MW at 355 nm. The stripping efficiency reached 90%. A simple multiplication of 10 MW laser peak power and the duty factor of the SNS beam (6%) yields an average laser power of 0.6 MW at 355 nm to strip the entire H<sup>-</sup> beam. Similar numbers are obtained for other proton ring facilities. Obviously, this average power requirement is too large to make the device practical.

#### 1) Optimization of H<sup>-</sup> beam parameters

An appropriate dispersion derivative of the H<sup>-</sup> beam will be designed to eliminate the Doppler broadening of the absorption line width and therefore to reduce the required frequency sweep for the laser beam. The vertical size as well as the horizontal angular spread of the H<sup>-</sup> beam will be minimized. The

optimization of the  $H^-$  beam parameters will reduce required peak power of the laser to the 1 MW level. Reduction of the bunch length of the ion beam can further reduce the average laser power requirement.

## 2) Macropulse laser system

The laser parameters are determined by laser-hydrogen interaction physics and the linac operation condition at SNS. First, the energy gap between the ground and excited states in the hydrogen atom, beam energy and the interaction geometry at the accumulation ring requires a laser with UV emission. The peak power of micropulses needs to be  $\sim 1$  MW to achieve a sufficient stripping efficiency. The temporal structure of the laser system must match the bunch structure of the SNS accelerator which has a pulse width of  $\sim 50$  ps at a repetition rate of 402.5 MHz. The micropulses are further bunched into a macropulse with up to 1 ms duration at a repetition rate of 60 Hz. The ideal (minimum laser power requirement) condition would be that the laser beam has an identical temporal structure with the ion beam. A macropulse mode laser system has been designed by ORNL and Continuum, Inc. to meet the above requirements. A prototype laser has been fabricated by Continuum. The laser adopts a master oscillator power amplifier (MOPA) scheme contains an actively mode-locked fiber laser, three-stage Nd:YAG amplifiers, a wavelength conversion stage that converts the infrared radiation from the laser to the UV beam, and an electronic RF and control system that allows full remote-control of the laser. The macropulse duration of the present laser system is limited to 20  $\mu$ s due to the pumping scheme and the wavelength conversion efficiency. To achieve longer macro-pulse, diode pumping has to be used and the peak power has to be reduced.

## 3) Beam recycling optical resonator

In general, the photon-hydrogen interaction results in a negligible loss to the photon number due to tiny cross sections. Consider, for example, the case of the laser assisted  $H^-$  beam stripping scheme at SNS. According to the theoretical calculation, only  $10^{-5}$  of the photons are lost during a single photon-hydrogen interaction even for 100% stripping efficiency. It is therefore expected that the average laser power requirement can be significantly reduced by recycling the laser beam with a power build-up optical cavity and allocating the laser-particle beam interaction inside the cavity. Optical cavity technology has been well-developed for low-power, infrared, and often for continuous laser beams. However, in our case, the cavity needs to work on high intensity picosecond UV pulses operating at a macropulse mode with a very small duty factor, which imposes a technical challenge on the cavity stabilization and operation. A power enhancement factor of 50 – 100 will be needed for the final laser assisted stripping experiment. Since our UV beam source is a pulsed laser with a very low repetition rate and a very narrow macro pulse width, it is impossible for the feedback control system to respond and drive the piezo to the cavity resonant position at such a low duty factor. A dual color optical cavity is being developed at SNS to resolve the challenge. Since the UV beam is generated from the

infrared seed laser, we expect the cavity that is locked with the infrared beam will also be locked to the 10Hz UV beam.

Table 11 lists the parameters of the SNS H<sup>-</sup> beam, and Table 12 summarizes the required laser parameters with and without the beam recycling optical resonator.

**Table 11:** SNS H<sup>-</sup> beam parameters.

Beam energy (GeV)	1.0 (upgrade: 1.3)
Beam power (MW)	1.4 (upgrade: 3.0)
Beam macropulse length (ms)	1.0
Beam micropulse length (ps)	50
Peak macropulse H- current (mA)	38
Ring accumulation time (turn)	1060
Ring bunch intensity	$1.6 \times 10^{14}$
Vertical size (mm)	0.6
Vertical emittance (mm-mrad)	$0.225\pi$
Horizontal size (mm)	3
Vertical emittance (mm-mrad)	$0.225\pi$

**Table 12:** Required laser parameters for SNS laser stripping.

Method	Macropulse laser	Macropulse laser w/ 20x resonator
Laser wavelength (nm)	355	355
Micropulse length (ps)	50	50
Micropulse energy ( $\mu$ J)	50	2.5
Micropulse repetition rate (MHz)	402.5	402.5
Macropulse length (ms)	1	1
Macropulse energy (J)	20	1
Macropulse repetition rate (Hz)	60	60
Average power (W)	1200	60
Temporal profile	Flat	Flat
Contrast	N/A	N/A
Efficiency	Normal solid-state lasers	Normal solid-state lasers
Polarization	100/1	100/1
Cost	Multi \$M	Multi \$M
Laser beam quality	$M^2 < 1.2$	$M^2 < 1.2$
Pulse stability	1%	1%
Laser pointing stability ( $\mu$ rad)	1	1
Laser availability	24/7	24/7

### 1.1.7.2 Laser Stripping of $H^-$ Particles for Project X

Project X would convert  $H^-$  particles to protons at 8 GeV. This has the advantage of using a laser of longer wavelength because the photon energy would be increased by the relativistic  $\gamma$  factor ( $\gamma = 9.526$ ) due to the Doppler shift. The beam parameters are listed in Table 13 and the beam pulse structure is shown in Figure 9.

**Table 13:** Project X  $H^-$  beam parameters.

Kinetic energy (GeV)	8
Relativistic $\gamma$	9.526
Micropulse length (ps)	15 ps
Micropulse frequency (MHz)	325
Micropulse period (ns)	3.1
Macropulse length (ms)	1.25
Macropulse current (mA)	20
Macropulse frequency (Hz)	5
No. $H^-$ per micropulse	$4 \times 10^8$
No. micropulses per macropulse	$4 \times 10^5$
No. $H^-$ per macropulse	$1.6 \times 10^{14}$
No. $H^-$ per second	$8 \times 10^{14}$
Vertical beam size (mm)	1.5
Horizontal beam size (mm)	1.5
Beam power (MW)	1

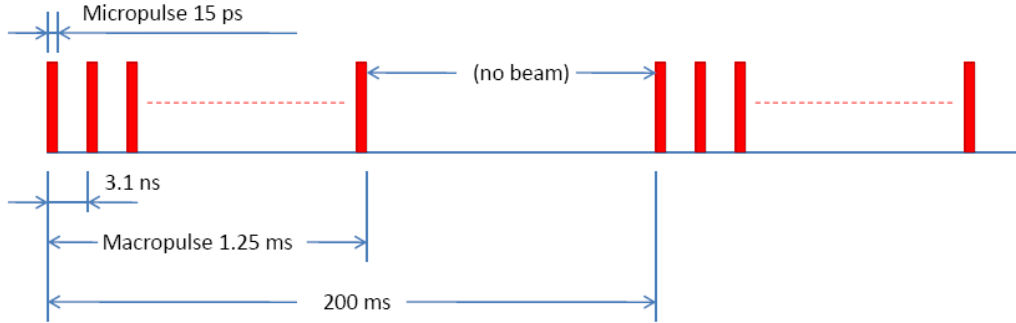


**Figure 9:**  $H^-$  pulse structure of Project X.

#### 1.1.7.2.1 Direct Laser Ionization

The photoionization of the ground state of the hydrogen atom  $H(1s)$  has been studied extensively in the past half century. For low intensity radiation there are exact expressions of this process in terms of the cross section obtained from the perturbation theory [41]. In this approximation, the incident photon flux density is much smaller than 1 atomic unit (a.u.) and the pulse duration is much longer than an optical cycle. However, this approximation is no longer valid when intense laser pulses are employed, since the peak electric fields can be comparable with or larger than 1 a.u. and the pulse may last only a few optical cycles or even a fraction of a cycle. Therefore, perturbative

methods are not applicable, and numerical methods for solving the time-dependent Schrödinger equation (TDSE) are required.

Ionization of hydrogen atoms by intense laser pulses is a complex subject that is still not fully understood [42-44]. Although many theoretical approaches have been proposed, they typically break down at high laser intensities or neglect important aspects of the laser-atom interaction such as long-range Coulomb interaction or realistic pulse shapes. On the other hand, numerical solutions of the TDSE provide accurate predictions, but are extremely computationally intensive and converge slowly at high intensities. Current results show that no simple relationship links ionization rate to pulse duration, frequency and intensity, due to competing ionization mechanisms, evolving energy levels, resonances and stabilization.

Calculations performed for 24.8 nm (50 eV), 2.5 fs (30 periods) pulses suggest that intensities beyond  $10^{17}$  W/cm<sup>2</sup> are required for efficient (> 90%) ionization of hydrogen atoms [45]. From an experimental standpoint, few absolute measurements of the ionization yield are available. An experiment performed with 600 fs, 248 nm laser pulses measured ~0.001% ionization for intensities of the order of  $10^{14}$  W/cm<sup>2</sup> [46].

#### 1.1.7.2.2 Three-Step Stripping

Electrons in hydrogen atoms exposed to intense laser radiation can be excited to higher states. For the Project X parameters, the  $n = 2$  transition can be triggered when the hydrogen beam interacts with a 1024 nm laser beam at an angle of ~96 degree. A laser peak power of ~3.5 MW is required for 90% stripping.

It may be possible to reduce the required laser energy by decreasing the incidence angle (Figure 10). However, this approach can only be investigated by performing detailed simulations of the response of hydrogen atoms to the laser field.

Counter-propagating geometry would require a laser at around 1.8  $\mu$ m, which could be achieved using an OPA. However, detailed calculations would be required to establish the power required, the role of Stark shifting, etc.

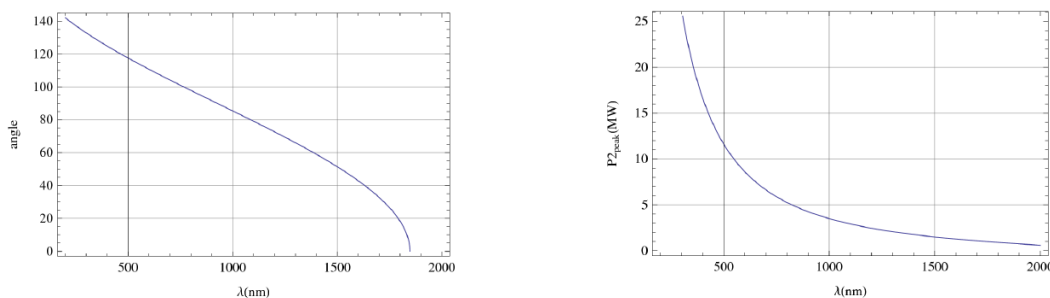


**Figure 10:** Wavelength vs. angle and power vs. wavelength required for ionization of hydrogen atoms.

## 1.2 Laser Applications for Light Sources

This section discusses the requirements on performance for lasers that are used in conjunction with RF accelerators; drivers for laser plasma accelerators that in turn power a free electron laser or other advanced radiation source; and for Thomson scattering based gamma-ray sources.

Lasers already play a significant role in existing light source facilities, but face new challenges with future light sources that aim at much higher repetition rates. Ultrafast (femtosecond) lasers reaching 1-10 kW levels will be required for seeding and user driven experiments. Lasers producing a few joules in 30-50 fs pulses at high repetition rate (100-1000 Hz) could be used to drive laser plasma accelerator. Thanks to their ability to produce GeV-class, ultra-short, high peak current electron bunches, these laser plasma accelerators could in turn drive compact free electron lasers operating in the soft X-ray regime. Higher energy per pulse lasers (~40 J) would be needed to drive multi-GeV electron bunches for hard X-ray FELs.

### 1.2.1 Lasers for RF Accelerator-Based Light Sources

Lasers are widely used in today's RF accelerator based light sources. Uses range from photocathode gun based linacs; to phase space manipulation (heating) or diagnosis of electron beams; seeding FELs with high harmonics from gases, liquids or solids; and user experiments on high-repetition-rate facilities.

#### 1.2.1.1 *Guns and Heaters*

The requirements for photocathode laser systems are different for various current and future light sources, mainly depending on the foreseen time structure of the electron beam and the foreseen photocathode material. The time structure parameters range from low-duty-cycle, single-shot schemes via microbunch trains (burst mode laser systems) to CW operation. The photocathode materials can be various metals or different types of semiconductors, and thus wavelength requirements can range from the UV (e.g., Cu and Cs<sub>2</sub>Te) to green (e.g., alkali antimonite) or IR (e.g., GaAs). The laser system has to be synchronized to the RF system with a precision of a small fraction of a degree of the specific RF phase, and almost all projects require temporal and spatial laser pulse shaping.

Besides the requirements for high power laser systems for burst mode and CW operation, two additional fields of research have been identified: 3D shaping of the laser pulses, and alternative cathode material developments.

A key parameter to extend the performance of short wavelength light sources is transverse emittance, which must be reduced. This quantity has a cathode dependent lower limit (thermal emittance). Space charge and RF curvature can cause further emittance growth. To minimize these other sources of emittance growth, 3D electron bunch shaping is promising: simulations for a 1 nC bunch showed a > 25% reduction of the projected emittance and >10% reduction of the central slice emittance in comparison to an optimized "beer can" laser pulse shape.

Smaller transverse emittance will extend the scientific reach of short wavelength FELs by, e.g., lasing at even shorter wavelengths; allowing saturation at lower beam energy or with shorter undulators; two-color lasing; and higher levels of transverse coherence at lower beam energies. In addition, the longitudinal phase space is very linear, enabling smoother bunch compression. At low bunch charges, very short electron bunches can be produced, allowing longitudinally coherent FEL laser pulses (single spike lasing). Additionally, this shaping will reduce the beam halo, reducing the radiation damage to undulator segments and diagnostics components.

Table 14 summarizes the laser requirements for photocathode systems.

**Table 14:** FEL photocathode laser systems requirements. Wavelength given is that applied to the cathode, often harmonics of the laser fundamental. If not otherwise indicated, powers listed assume a conservative quantum efficiency of the cathode of 1% and a factor of 10 for overhead associated with spatial and temporal shaping as well as transport losses. Pulse duration is FWHM. Yellow indicates that some further development is needed; red indicates a need for significant R&D.

	Wave-length	Pulse energy	Pulse duration	Rep rate	P <sub>peak</sub>	P <sub>ave</sub>	Comments
Nd:YLF	262 nm	10 $\mu$ J UV 100 $\mu$ J IR	15 ps	1 MHz burst of 0.8 ms with 10 Hz	700 kW UV 7 MW IR	0.1 W UV 1 W IR	FLASH (in operation, large overhead)
Yb fiber	515 nm	2 uJ green 5 $\mu$ J IR	10 ps	1 MHz	0.2 MW green 0.5 MW IR	2 W green 4 W IR	NGLS 1% QE green, 40 W IR if UV required
IR quadrupled	260 nm	10 $\mu$ J UV 100 $\mu$ J IR	20 ps	4.5 MHz burst of 0.65 ms with 10 Hz	500 kW UV 5 MW IR	50 W UV burst, 0.3 W overall 500 W IR burst, 3 W overall	European XFEL (large overhead)
IR doubled	~515 nm	200 nJ green 1.5 $\mu$ J IR	10 ps	1.3 GHz	40 kW green 20 kW IR	250 W green 500 W IR	ERL (BerlinPro type, sc gun)
IR 5 <sup>th</sup> harmonic	200 nm	5 $\mu$ J UV 50 $\mu$ J IR	10 ps	1.3 GHz	0.5 MW UV 5 MW IR	6.5 kW UV 65 kW IR	ERL (sc gun, low QE cathode 0.1%)

Another important field of research is the study of different cathode materials. Besides the usual aim of high quantum efficiency at manageable vacuum requirements, cathode development has goals that include:

- Lowering the power requirements and simplifying the photocathode laser system if high quantum efficiency photoemission at longer wavelength (green spectral range) can be used.
- Improving the usability of different cathode materials in superconducting RF cavities. Besides heat deposition by the photocathode laser beam, the RF joint with the cavity and the compatibility with high gradient SC cavities are issues.
- Reducing the thermal emittance. Since the solid state properties of the photocathode also determine the thermal emittance for given laser spot size, a proper choice of cathode material will have increasing proportional importance when the other sources of emittance are reduced further and further.

Laser heater systems are needed in many facilities for increasing the uncorrelated momentum spread of the electron beam from photocathode RF guns (Table 15). Usually, though, they can rely on the residual IR radiation from the photocathode drive laser system.

**Table 15:** Laser system requirements for the heater laser for an FEL.

	Wavelength	Pulse energy	Pulse duration	Rep rate	P <sub>peak</sub>	P <sub>ave</sub>	Comments
IR	800nm	~ 10 $\mu$ J	50 ps (FWHM)	1 MHz	200 kW	10 W	Residual IR from drive laser is typically suitable

### 1.2.1.2 FEL Seeding

Today's EUV, soft X-ray and hard X-ray free electron lasers are based on the self-amplified spontaneous emission (SASE) principle. While this is a very robust mode of operation, it makes it difficult to generate photon pulse properties tailored to scientific user needs in terms of defined pulse shape and length, longitudinal coherence, and timing stability. The drawbacks in FEL beam quality mainly stem from the SASE process starting up from the spontaneous undulator radiation (shot noise), which results in considerable spectral and energy fluctuations. Seeding the amplification process with external radiation rather than shot noise is a promising method to increase the spectral brilliance and to achieve pulses that are stable in frequency spectrum and in energy [47]. The output power of the seeded FEL is concentrated in a single line, which is many times narrower than the spectrum of the conventional SASE FEL (Fig. 11).

External seeding also makes it possible to synchronize the seeded FEL pulse with an additional pump-probe laser system to better than the pulse length, which is typically 10 fs or less. Synchronization to the fs level opens a wide field for revolutionary ultra-fast physics experiments. Such novel synchronization schemes are being developed at FLASH, Fermi@Elettra and other places [48]. These systems are based on compact ultra-stable fiber laser systems providing a timing reference. Synchronization systems are not yet mature and need considerable R&D.

There are two main classes of seeding: self-seeding [49, 50], where SASE radiation is filtered and used as a seed in a subsequent undulator, and external seeding. In external seeding, a laser co-propagates with the electron beam in a short undulator used as an energy modulator at some point before the final, radiating undulator. The energy modulation can be turned into a density modulation using a wide variety of beam optics and FEL interactions. At this point, there are three classes of externally seeding: direct seeding, where the modulation wavelength is the same as the radiated wavelength [51], compressed harmonic generation (CHG), where the modulation wavelength is directly compressed only with linear beam optics as the bunch length is compressed (like an accordion) [52], and harmonic generation (HG), where higher harmonics of the resulting density modulation are used to drive either an intermediate or the final undulator. This technique often includes multiplication techniques like high gain harmonic generation (HG) [53] or echo-enhanced harmonic generation (EEHG) [54].

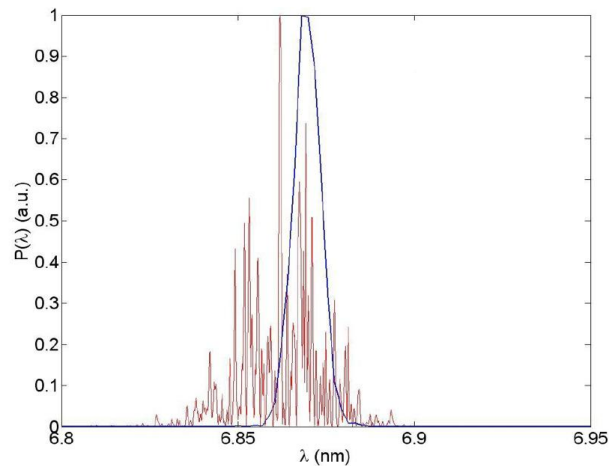


**Figure 11:** Typical wavelength spectral distribution of a single SASE FEL pulse. Red: calculated for a typical SASE process starting from shot noise. Blue: with external seeding.

The laser power requirement arises from needing significantly more power at the final undulator due to the pre-microbunched electron beam than from the beam's shot noise which drives the SASE amplification (a factor of 100 is typically required). For a wavelength  $\lambda$ , the power in the shot noise is given by  $P_{shot} \sim 1/(\lambda^{3/2})$  [55]. Also, phase and amplitude noise on the external laser seed (as well as nonlinearities in the beamline optics that generate the harmonic seed if any) lead to a broadening of the radiated X-ray spectrum. Analysis of this process is an active research area [56-59], but it is already clear that these harmonic generation processes lead to tighter requirements and additional power at the fundamental. Spectral bandwidth broadening may scale linearly with harmonic number for CHG processes and as the square root of harmonic number for HG processes [60]. In the following, requirements are established for direct seeding, to provide an overall basis.

Seeding of the amplification process by an external laser pulse has been considered for a long time and was demonstrated in a proof-of-principle experiment at SCSS/Japan [51]. Seeding improves the FEL beam properties considerably and thus extends the range of possible applications. A method of producing the seed radiation is the generation of higher harmonics (HHG) from near-infrared femtosecond laser pulses in rare gas media [62, 63]. Odd harmonics of the laser fundamental are created and used as seeding radiation pulses.

Beyond fundamental issues in the realization of seeding at VUV and X-ray wavelengths, it is particularly challenging to realize a femtosecond laser system for very short pulse lengths. The minimum pulse duration is determined by the bandwidth of the FEL gain process, resulting in a natural coherence time of approximately 4 fs at VUV wavelengths (at FLASH, for example) and below 1 fs at X-ray wavelengths. The seed pulse should be shorter than the electron bunch, thus increasing the impact of longitudinal slippage effects. As an example, simulations show that a seed energy of several nJ (or  $> 50$  kW peak power) with  $>1$  eV bandwidth is required at FLASH to seed a wavelength of 7 nm.

Due to the low conversion efficiency of the HHG process ( $\sim 10^{-6}$  to  $10^{-8}$ ) and transport losses, the energy of the external laser pulse has to be at least 5 mJ, which means close to 1 TW peak power. These power levels are particularly problematic at high repetition rates, where the resulting average power is hundreds to thousands of

watts. Methods for enhancement of the higher order harmonic generation process (i.e., quasi-phase matching) should also be considered as a possibility to reduce the energy requirements for the driver laser.

In Table 16, illustrative parameters for proposed future seeded fourth generation light sources in vastly different regimes are presented, to bracket currently anticipated needs. In Table 17 the respective seed laser parameters for more modest cw FELs and burst mode FELs are shown. As a specific example, a prototype beyond-state-of-the-art seed laser is being developed for FLASH. Presently, several tens of  $\mu\text{J}$ s at 7 fs are achieved with a repetition rate of 100 kHz [64]. In the near future, an upgrade to 1 to 3 mJ per pulse as required for the HHG seeding process is planned [65].

**Table 16:** Parameters for future FEL light sources

Type	High-rep rate seeded FEL facility (SCRF Linac)	Low-rep rate seeded FEL facility (NCRF Linac)
E (GeV)	2.5	12
I (mA)	1	$10^{-2}$
$\epsilon_x$ ( $\epsilon_y$ ) (mm-mrad)	< 0.8 (norm)	< 0.3 (norm)
Spectral peak (keV)	1	42
Peak brightness (ph/s/mm <sup>2</sup> /mrad <sup>2</sup> /0.1% BW @ spectral peak)	$10^{29}$ - $10^{33}$ (depends on FEL configuration)	$10^{27}$ - $10^{31}$ (depends on FEL configuration)
Average brightness (ph/s/mm <sup>2</sup> /mrad <sup>2</sup> /0.1% BW @ spectral peak)	$10^{18}$ - $10^{26}$ (depends on FEL configuration)	$10^{14}$ - $10^{22}$ (depends on FEL configuration)
Average flux (ph/s)	$10^{13}$ - $10^{17}$	$10^{10}$ - $10^{15}$
Average coherent flux (ph/s)	~ full coherence	~ full coherence
Photons/pulse	$10^8$ - $10^{12}$	$10^{10}$ - $10^{11}$
Charge/bunch (pC)	10-1000	100-250
Beam pulses per second	$10^6$	$10^4$
Beam pulse length (fs)	~ 100	~ 30
Machine size (m)	700	1000
Cost and Schedule	\$1B; 10-year construction	\$1B; 7-year construction
Comments	LBNL design concept	LANL design concept

Since it is not at all obvious which of the seeding options will be the most efficient and cost effective path forward, experiments are scheduled in order to investigate all methods. However, the answer may even vary from machine to machine.

For high average brilliance FELs like burst-mode FELs (FLASH and the European XFEL), cw FEL proposals (NGLS and NLS) or Energy Recovery Linacs (Cornell ERL, BerlinPro), the average laser power would have to be in the kW range. As an example, a repetition rate of 1 MHz requires a seed laser with an average power of 5 kW. Repetition rates beyond 1 MHz (e.g. 4.5 MHz for the European XFEL or 1 GHz for the ERL upgrade proposals) need considerable R&D, as they are beyond the reach of present technology. The main problems to be solved are similar in all high power lasers: the removal of heat together with the need for efficient pumping schemes (e.g., for

optical parametric chirped amplification). The requirements for a burst-mode amplifier are different than for continuous operation.

FLASH and XFEL run with a 10 Hz burst with and  $\sim 1\%$  duty-cycle. The average power is lower (reduced heat load for the laser amplifier) but the burst average power is higher due to MHz repetition rates. Possible laser approaches are:

- Burst-mode Laser amplifier systems
  - fiber front-end with an Innoslab or/and Thin-Disk booster
- Continuous Laser amplifiers 100 kHz
  - fiber front-end with an Innoslab or/and Thin-Disk booster
- Low repetition rate Joule-class Laser amplifiers
  - Ti:Sa, perhaps OPCPA, may be able to scale current laser amplifier designs

In the following, we consider seeding approaches for four different regimes:

- 1) 30 eV to 0.25 keV
- 2) 0.25 keV to 1.5 keV
- 3) 6 keV to 15 keV
- 4) 40 keV to 50 keV

### 30 eV to 0.25 keV

There are already active seeding efforts in this regime (e.g., the new FEL beamline FLASH2). An 10-40 nm HHG source is needed, with  $\sim 10$  nJ in single harmonic. This leads to a 0.1 mW HHG laser, with up to 100 nJ per pulse. Current HHG state-of-the-art technology should be satisfactory for HHG and EEHG harmonic generation. However, they are not yet feasible for direct seeding as can be seen in Figure 12 and Table 17.

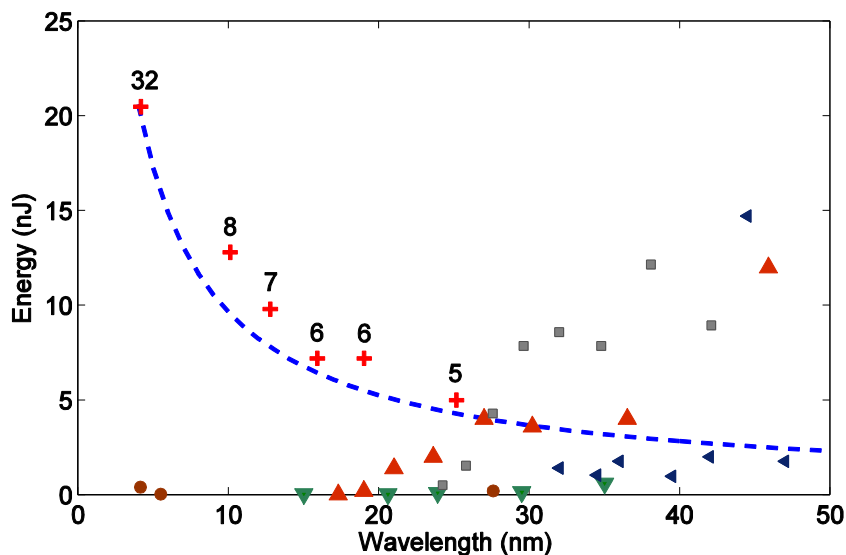


**Figure 12:** HHG state-of-the art, with the blue dashed line indicating 100 times the shot noise at that wavelength. The number by the crosses indicate the number of QPM jets needed. The triangles refer to HHG in Ar and Xe and the circles to QPM in capillaries. The squares are achieved with two-colour mixing.

**Table 17:** Laser requirements for seeding 30 eV to 0.25 keV FELs. Yellow indicates that some further development is needed; red indicates a need for significant R&D.

	<b>Laser</b>	<b>Seed</b>	<b>X-ray</b>	$\eta$	<b>Rep rate</b>	$P_{ave}$	<b>Comments</b>
EEHG	0.8 $\mu\text{m}$ 100 GW >10 fsec (mJ)	200 nm up to GW	2 nm	$>10^{-1}$ conv./ 10 losses	100 kHz and MHz burst	10s W 100s W for burst	~10s $\mu\text{J}$ UV and IR both required CEP (evt.)
HGHG	0.8 $\mu\text{m}$ 10 GW >10 fsec (100 $\mu\text{J}$ )	200 nm 100 MW	20 nm	$>10^{-1}$ conv./ 10 losses	100 kHz or MHz burst	10s W 100s W for burst	CEP stabilization required for ultrafast pulses
HHG	0.8 $\mu\text{m}$ 1 TW >10 fsec (10 mJ @<10nm)	<10 nm 1 MW >10 nm 100 kW	<10 nm (and > 10 nm)	$10^{-5}$ HHG/ 10 losses	100 kHz or MHz burst	kW 10s kW For burst	R&D CEP (evt.)

### *0.25 keV to 1.5 keV, 6 keV to 15 keV, and 40 keV to 50 keV*

These regimes lead to very challenging laser requirements. Seeding FELs at 0.25 keV to 1.5 keV requires laser sources capable of 100 kW at 1 nm ( $10^{-6}$  conversion efficiency limits the repetition rate). This will require significant R&D. Currently, a single line HHG source at ~keV has 1-10 fs duration, with  $10^{-8}$  conversion efficiency. With a net HHG efficiency of  $10^{-9}$  (which includes the 100 $\times$  shot noise requirement and an assumed 10 $\times$  transport loss) and shot noise equivalent power of 1 MW for a 10 fs pulse, a 10 J HHG drive laser is needed.

Seeding laser requirements for the two higher X-ray regimes are even more challenging and will likely require beam-based harmonic generation or self-seeding. 10 kW of SASE noise at 50 keV will require a 1 MW seed power. Laser power enhancement factors from using optical cavities will help [66], but they may not be a viable solution for >MHz repetition rates. Laser requirements for seeding these X-ray regimes are summarized in Table 18.

**Table 18.** Laser requirements for seeding 0.25 keV to 50 keV FELs. Yellow indicates that some further development is needed; red indicates a need for significant R&D.

	Laser	Seed	X-ray	$\eta$	Rep rate	$P_{ave}$	Comments
HHG+ HGHG or EEHG	0.4-4 $\mu\text{m}$ 100 GW 10 fsec (mJ)	20 nm 100 kW	1 nm	$10^{-5}$ HHG/ 10 losses	100 kHz and MHz (burst)	kW	Possible in future - with DPSS laser pumped OPCPA
Direct HHG	>4 $\mu\text{m}$ 1 PW 10 fsec (10 J)	1 nm 1 MW	1 nm	$10^{-5}$ HHG/ 100BW/ 10 losses (100 for narrower bandwidth)	120 Hz	kW	Scalability of current laser amplifiers to higher rep rate?
HHG+ HGHG	4 $\mu\text{m}$ 10 PW 10 fs (100 J)	4 nm 10 MW	0.1 nm	$10^{-5}$ HHG/ 100BW/ 10 losses	1 Hz	100 W	New laser amplifier technologies needed
HHG+ EEHG	4 $\mu\text{m}$ 10 PW 10 fs (100 J)	4 nm 10 MW	0.025 nm	$10^{-5}$ HHG/ 100BW/ 10 losses	1 Hz	100 W	New laser amplifier technologies needed

### 1.2.1.3 Lasers for Users

Users of light sources will typically require optical lasers in conjunction with the light source beam to either pump or probe matter (for example, the majority of LCLS experiments are pump-probe). Because many of these experiments will be investigating matter on time scales of the light source X-ray pulses, conventional lasers will need to provide short pulses at the rep-rate of the light source. These conventional pulses will need to be energetic enough to excite states in matter to be probed by the X-rays and will need to have flexibility in wavelength that allows pumping and probing of as many states as possible. Optical lasers can be used while wavelengths from 200 nm to 20  $\mu\text{m}$  will require harmonic generation and/or optical parametric amplifiers (OPAs). Also, experiments will be multi-color. In general, this implies tens of mJ of laser energy with pulse widths that range from <10 fs to picoseconds. Such a laser should also be compatible with harmonic conversion, as well as with pumping of OPAs. For example, current optical pump/probe lasers at LCLS supply 25 mJ of energy with pulse lengths of 35 fs at a 120 Hz rep rate. Scaling these requirements to 100 kHz rep rates will require kW-class short pulse lasers. Considerable R&D efforts will be required to handle the thermal loads for harmonics, OPAs, and even the transport optics.

Pumping and probing of matter with the X-ray source and a conventional laser implicitly requires a high degree of synchronicity between the light source and the optical laser. Pushing this synchronicity to levels to < 10 fs for future experiments will require non-conventional (most likely optical) timing distribution systems. Even with timing distribution systems capable of sub-picosecond drift and jitter, the inherent jitter in many of the light sources will require diagnostics that can measure the relative arrival times of the optical laser and the light source or electron bunch at the femtosecond level. In this case, the data can be post-processed with the temporal resolution of the measurement of the relative arrival times.

### 1.2.2 Lasers for Laser Plasma Accelerator Driven FELs

Laser-plasma accelerators (LPAs) produce ultra-high accelerating gradients (10-100 GV/m) enabling compact accelerators. In 2006, a cm-scale laser-plasma accelerator was first demonstrated at LBNL that produced 1 GeV electron beams with a time integrated energy spread of about 2.5%, containing 30 pC of charge, using a 40 TW laser pulse (2 J/pulse). Currently, experiments are underway at many institutions to demonstrate that such beams are capable of powering an FEL. Using a conventional undulator with cm-scale period, beams of a few hundreds of MeV would be sufficient to produce extreme ultra-violet radiation. Production of shorter wavelength radiation in the soft X-ray regime would require beams with energy on the order of a few GeV which could be produced from a single LPA by reducing the plasma density and using laser pulses with several J/pulse. Harder X-rays would require yet higher laser pulse energy (order 10 – 30 J) in 100 fs pulses, and plasma structures with length on the order of 1 m and plasma densities of order  $10^{17} \text{ cm}^{-3}$ .

In the following we consider the laser requirements for LPA generated electron beams suitable to drive an FEL. We consider FELs delivering light in the photon energy bands (i) 0.25 keV – 1.5 keV, (ii) 6 keV – 15 keV, and (iii) 40 keV – 50 keV. Assuming conventional undulator technology, delivering these photon energies requires electron beam energies of (i) 2 GeV, (ii) 10 GeV, and (iii) 20 GeV, respectively. To produce these beams, the accelerator may operate as a single LPA, or by staging several LPAs. Table 19 shows three possible configurations and the required laser parameters. For each LPA option the laser intensity is  $a=1.5$ , where  $a^2=7.3 \times 10^{-19} \lambda[\text{um}]^2 I[\text{W/cm}^2]$  is the normalized vector potential. The use of a parabolic plasma channel for guiding and linear plasma density tapering is also assumed.

Column (I) in Table 19 shows a high plasma density ( $10^{18} \text{ cm}^{-3}$ ) option, requiring 1 J of laser energy in 30 fs to produce 1 GeV electron beams (with  $10^9$  electrons/bunch). Such an LPA could be staged to reach the required 2 GeV for soft X-ray generation in an FEL.

Column (II) in Table 19 shows an LPA operating at a plasma density  $10^{17} \text{ cm}^{-3}$ , using an 8 J, 100 fs duration, 2 micron wavelength laser (e.g., fiber laser) to generate a 2.5 GeV electron beam for soft X-ray production. Such an LPA could be staged (4 stages) to reach 10 GeV for generation of 6 keV – 15 keV photons.

Column (III) shows a 10 GeV LPA operating at a plasma density of  $10^{17} \text{ cm}^{-3}$ , using a 1 micron wavelength, 32 J, 100 fs duration, laser pulse. The 10 GeV electron beam can be used for X-ray production in the energy range 6 keV – 15 keV. Two stages would extend the energy range to 20 GeV, enabling hard X-ray production in the energy range 40 keV – 50 keV.

Although a compact, low-repetition rate (1–10 Hz) LPA-driven FEL could provide high-peak brightness light for user experiments, the applicability of this technology for large-scale user facilities requiring high-average brightness would require repetition rates that are beyond the state-of-the-art of today's high-peak power lasers. Operating an FEL at kHz would require lasers with average power in the kW range for soft X-ray FELs and several tens of kW for hard X-ray FELs.

**Table 19.** Laser requirements for laser-plasma accelerator driven FELs. Significant laser R&D is required for high-average power operation.

Parameter	I	II	III
Plasma density ( $\text{cm}^{-3}$ )	$10^{18}$	$10^{17}$	$10^{17}$
Electrons/bunch	$10^9$	$4 \times 10^9$	$4 \times 10^9$
Repetition rate (kHz)	1 - 1000	10 - 1000	1 - 15
Laser wavelength ( $\mu\text{m}$ )	1	2	1
Laser pulse duration (ps)	0.03	0.1	0.1
Beam energy gain/stage (Gev)	1	2.5	10
Stage length (m)	0.03	0.25	1
Laser energy/stage (J)	1	8	32
Average laser power/stage (kW)	1 - 1000	80 - 8000	32 - 480

### 1.2.3 Thomson Scattering Sources for X-ray and Gamma-ray Production

Thomson scattering can provide quasi-monochromatic, tunable X-ray sources in a narrow divergence beam. Sources based on this principle will likely allow for a new dimension of ultrafast medical and material diagnostics, revolutionize remote material analysis (including homeland security applications), and provide the necessary photons for ultrahigh-resolution scattering microscopy. This concept has already been realized using conventional electron accelerators. As an example,  $\sim 10^8$  photons per shot at X-ray energies tunable between  $\sim 10$ -50 keV ( $\sim 10\%$  relative bandwidth) were achieved by a private company originating out of the Vanderbilt FEL. Available commercial short pulse laser systems would allow 10 Hz repetition rate. Proposed advances will augment average photon number by several orders of magnitude. Phenomenal miniaturization can be expected to occur as laser-based electron accelerators are incorporated. Beyond classical Thomson scattering in the incoherent regime, an envisioned scheme of generating a flying “relativistic electron mirror” holds the promise of coherent up-shift of laser light.

Current efforts in conventional accelerator based Thomson source are focused towards achieving a several order of magnitude increase in average photon flux by addressing the gross mismatch between laser and accelerator repetition. As the cross section for the scattering is extremely low, a negligible fraction of the laser light is scattered. Thus a natural solution for generating the high repetition rate and high intensity pulses is constructive addition of multiple pulses in a properly stabilized optical cavity.

Table 20 presents expected performance and required photon requirements specified at the 2011 workshop for both linac ( $< 5$  year timeline) and Energy Recovery Linac (ERL,  $> 5$  years). The laser source is based on a Yb laser with 1 ps, 100 nJ pulses operating at 100 MHz (10 W average power). This light is subsequently amplified with a cryo-cooled Yb multi-pass amplifier with  $100\times$  gain under development at MIT’s Lincoln Laboratory. The linac version requires development of the enhancement cavity, while the ERL based design will also demand increased laser repetition rate.

**Table 20:** Parameters and requirements of proposed Thomson sources from the MIT based group at the 2011 workshop. Capabilities that are only marginally satisfied by today’s technology are in yellow, while those requiring significant R&D are in red.

Parameter	LINAC (<5 yrs)	ERL (>5 yrs)
Photon energies (keV)	3-12	3-12
Average flux (ph/s in 10% BW)	$10^{14}$	$2 \times 10^{16}$
Repetition rate (MHz)	100	500
Laser average power (kW)	1	5
Laser pulse duration (fsec)	500	500
Storage cavity enhancement	1000	1000

A compelling application of Thomson scattering is generation of compact mono-energetic MeV gamma sources. Scattering from electron beams at 200-800 MeV energies can produce photons at 1.7-15 MeV. These photon energies are suitable for NRF or photo-fission interrogation, and are delivered with mrad divergence ideal for remote detection at hundreds-of-meters standoff with low radiation dose. The concept is supported by proof-of-principle experiments at LLNL [20]. Particularly exciting is anticipated miniaturization of such sources by obtaining the electrons from laser-wakefield accelerators. For example, a modest 300 MeV electron beam of 0.1 nC and 2% energy spread scattering with a 40 J, ps laser would produce  $\sim 10^8$  gammas at 1.7 MeV matched to the U-235 nuclear resonance fluorescence. Electrons at  $\sim 700$  MeV would access photo-fission. Electron beams approaching these requirements have already been generated using laser-plasma acceleration (LPA) in cm-scale plasmas. To produce electrons in the GeV range,  $\sim 50$  TW peak power is required. Such systems are today operational at 10 Hz; future kHz repetition will further benefit the Thomson X-ray source for such applications. The backscattering laser should produce  $\sim 10$  J with 1-100 ps pulse duration. A laser of this class has similar performance to the pump laser required for an optical-parametric-chirped-pulse-amplification OPCPA based solution for the laser-accelerator driver.

A novel proposal for coherent Thomson scattering in the  $\sim 1$  keV photon range is the “relativistic mirror” concept [67]. For a thin foil of nm scale thickness, a laser with intensity of  $10^{18} - 10^{19}$  W/cm<sup>2</sup> can remove the entire electron population. If the laser rise is single cycle, the entire sheet of electrons will preserve the initial thickness of the foil. A subsequent reflector foil will separate the electrons from the optical field, leaving them with a purely forward and narrow-spread momentum [68]. A counter-propagating laser will coherently backscatter from this “single microbunch” before Coulomb forces blow it apart. Cutting-edge few-cycle, intense lasers such as the Petawatt Field Synthesizer at MPQ Garching will enable first studies of this exciting concept.

## 1.3 Laser Applications for Medical Particle Beam Therapy

### 1.3.1 Introduction

The medical application of laser acceleration is discussed here primarily in the context of ion beam therapy with protons or carbon beams, with some discussion of the

application of electron beams. Worldwide the most common approach to radiation therapy is with photon beams (X-rays generated by electron accelerators), which benefit from the affordable cost and compact size of the devices. The advantage of ion beams lies in their Bragg peak property, which allows predominant and peaked irradiation in depth at the position of the tumor. This unique radiobiological advantage of protons (and, even more, carbon beams) is evidenced by the success of ion beam therapy in the more than 30 facilities in Europe, the USA, and Asia. Numerous proton facilities (primarily cyclotrons) are successfully in operation worldwide [69].

Only a few heavy ion facilities exist. The original site, the Berkeley Bevalac [70] is closed. Sites currently operating include Japan's HIMAC [71] and Germany's recently completed Heidelberg Ion Therapy facility [72]; others are recently finished or in construction. These facilities, with combined use of proton and carbon beams, rely on conventional accelerator technology, where a linear accelerator is used as the injector into a synchrotron. This technology has been developed to extremely high efficiency due to 3D scanning techniques for irradiation, and to proven high reliability (up to 98%). One of the drawbacks of synchrotrons is their large size and cost, which qualifies this approach for larger hospitals with three to five treatment rooms.

Laser acceleration has the potential to replace either cyclotrons or linac-and-synchrotron combinations for medical applications; see, for example, Bulanov and Khoroshkov [73] and Tajima et al. [74]. The benefits could be a significantly reduced system size and cost, possibly combined with further advantages (potentially facilitating gantry design, for example). On the other hand, it is not obvious that the high accuracy of spot scanning delivery by synchrotrons is the right approach for a laser system.

We therefore take for the current parameter study the reference case of the PSI cyclotron, which aims at a 3D scanning technique that has lower resolution (compared with synchrotrons). In particular, we examine the option of a 3D spot and energy scanning with passive formation by spreading the beam over the whole tumor volume and shaping it with adjustable collimators, as is commonly done with cyclotrons or synchrotrons. Specific parameters (like energy spread and total number of voxels) need to be adjusted to the particularities of laser acceleration, which include a much higher production energy spread than in cyclotrons or synchrotrons and a laser pulse rate that is within the reach of foreseeable technology.

### **1.3.2 Laser Particle Beams for Medical Applications**

#### **1.3.2.1 Ion Beam Production Mechanisms (including Targets)**

The laser acceleration of ions provides an acceleration gradient many orders of magnitude larger than that of conventional acceleration, of the order of 1 TeV/m. Several options exist in terms of target configurations and acceleration mechanisms [75]. Energetic proton and ion beams with high 6D phase space density have been produced in the last few years from thick metallic foils (e.g., few  $\mu\text{m}$  thick aluminum) irradiated by ultra-intense, short laser pulses. The results from most previous experiments are based on the Target Normal Sheath Acceleration [76] model (TNSA). Because these targets are relatively thick, the laser pulse is mostly reflected and the conversion efficiency of laser pulse energy to ion kinetic energy is normally less than 1%.

The dependence of maximum ion energy on laser intensity is a less-than-linear function. The maximum proton energy based on the TNSA mechanism has somewhat improved since its first discovery: from 58 MeV in the year 2008 [77] to, more recently, a 78 MeV cutoff energy for the exponential spectrum, with  $6 \times 10^{13}$  particles. The possibility of accelerating more monoenergetic ion bunches has already been demonstrated within the TNSA regime by restricting the ion source to a small volume, where the sheath field is homogenous. However, a very high laser intensity of  $>10^{22}$  W/cm<sup>2</sup> is required to accelerate protons to 200 MeV or above.

Because of the advantage in accelerating limited mass by laser pressure, experiments producing high-energy ions from sub-micrometer to nanometer targets much thinner than the ones in early experiments, and driven by ultrahigh contrast (UHC) short-pulse lasers have attracted a recent strong interest. A new mechanism for laser-driven ion acceleration was thus proposed, where particles gain energy directly from Radiation Pressure Acceleration or Phase Stable Acceleration (RPA/PSA); see for example Esirkepov et al. [78]. There are two key issues:

- 1) Generation of quasi-monoenergetic ion beams by reduction of the intrinsic energy spread. This is not a "must" as the required energy window must be filtered anyway.
- 2) Accelerating protons or C<sup>6+</sup> ions in laser-foil interactions to 250 MeV or 400 MeV per nucleon, respectively.

By choosing the laser intensity, target thickness, and density such that the radiation pressure equals the restoring force established by the charge separation field, the ions can be bunched in a phase-stable way and efficiently accelerated to a higher energy. In recent years, experiments with quasi-monoenergetic peaks of C<sup>6+</sup> at ~30 MeV were observed at MPQ/MBI [79], and beams of C<sup>6+</sup> at >500 MeV (exponential) and 100 MeV (quasi-monoenergetic) were observed at LANL [80]. Furthermore, at LANL quasi-monoenergetic protons at ~40 MeV were generated from nm-thin diamond-like carbon foils. Interpretation of these experiments in terms of RPA is, however, not conclusive. Theoretical study shows that the energies and intensities needed for medical proton/carbon applications may be generated from hydrogen/carbon foil (of submicron thickness) with a laser intensity of  $\sim 10^{21}$  W/cm<sup>2</sup> with sufficient ion abundance and a monoenergetic (peaked) energy distribution [81].

A step beyond the conventional TNSA mechanism is the so-called Break-Out Afterburner (BOA) mechanism. It was discovered theoretically in 2006. The main difference between TNSA and BOA (or RPA) is the decoupling of the ion acceleration from the driving laser field due to the thickness of the target. In contrast, for the RPA and BOA mechanisms, the electrons that are accelerating the ions are still interacting with the laser field. To use the maximum number of available electrons, the target must be dense enough so that the laser beam does not initially penetrate the target, but rather, couples to the electrons. At some point the target has to become "relativistically transparent" to the laser light. When the target becomes relativistically transparent, the light can directly interact with electrons, co-moving with the ions at the rear surface. Thus the BOA mechanism starts as normal TNSA, but then, during the rising edge of the laser pulse, the intensity couples to the already moving electron-ion front at the rear side of the target [82, 83]. Numerical simulations predict ion energies of hundreds of MeV for existing laser parameters and up to the GeV range for currently planned

systems. Recently, acceleration of protons up to energies of 100 MeV at the TRIDENT laser has been reported [84].

One important difference to TNSA is that in a mixture of target atoms, all of the accelerated ions propagate at the same particle velocity, governed by the slowest, i.e., the heaviest species present. Thus for high energy proton acceleration a pure hydrogen target is the ideal choice. For each laser pulse duration and intensity as well as for each target composition one can determine an optimum target thickness, based on the abovementioned physics.

Recently a mechanism of laser proton acceleration from double layer foils, the Directed Coulomb Explosion (DCE), which is an efficient combination of the RPA and Coulomb Explosion, was suggested [85]. In this regime a high-intensity laser pulse not only expels electrons from the irradiated area of the foil but also accelerates the remaining ion core, which begins to move in the direction of pulse propagation. Then the ion core experiences a Coulomb Explosion due to the excess of positive charges, transforming into a cloud expanding predominantly in the laser propagation direction. A strong one-dimensional longitudinal electric field moves ahead of it, which accelerates protons from the second layer. This mechanism predicts that 220 MeV protons can possibly be generated by a 500 TW laser pulse with the energy spread of about 3%.

An alternative method is laser driven proton acceleration in a hydrogen gas jet with density just above the critical density, which is  $10^{19}/\text{cm}^3$  for a  $\text{CO}_2$  laser [86]. This method has the characteristic feature of creating very narrow energy spreads (practically monoenergetic beams). In an experiment at the UCLA Neptune Laboratory, 22 MeV, nearly monoenergetic protons with energy spread of  $\sim 1\%$  have recently been achieved [87].

Table 21 summarizes the main proposed mechanisms. Relevance to therapy is signified by + or - based on existing experiments, simulation, and achieved kinetic energy.

**Table 21:** Mechanisms of laser proton acceleration and relevance to therapy

	<b>Experiments</b>	<b>Status</b>	<b>Theory</b>	<b>Relevance to Therapy</b>
TNSA	> 1999	$>10^{13}$ ions, $\sim 70$ MeV, robust, reproducible	Analytical + 2D/3D simulations	+
TNSA/BOA (Break-out- afterburner)	> 2011	100 MeV	2 D/3D simulations	++(+)
RPA	>2008	Experimental evidence not conclusive	2D/3D simulations >GeV	++(+)
Coulomb explosion	-	-	2D simulation	+
Gas Jet - RPA	2011	20 MeV monoenergetic	2D	++

### 1.3.2.2 Ion Beam Parameters to Treatment Area

The distance from the skin to the deepest tumors in the body determines the required particle energy. From the stopping range in water, the necessary energy for reaching deep tumors is calculated to be 250 MeV for protons and 400 MeV/u for carbon. The number of ions is defined by the dose requirements for killing cancer cells. The necessary total number per fraction (a single treatment lasting typically 1-10 minutes) is estimated to be  $\sim 1 \times 10^{11}$  for protons and  $\sim 2.5 \times 10^9$  for carbon for a 1 liter tumor volume. With reference to the commonly used hadron therapy schedules, the duration of a fraction is usually below 5 minutes, which we also adopt here as a goal.

For a standard 2 Gy dose and an assumed 1 cm<sup>2</sup> voxel area, the required number of particles is estimated to be  $\sim 10^9$  for protons and  $\sim 2.5 \times 10^7$  for carbon. The total dose on any tumor volume element must be defined with at least 5% accuracy. Due to the yet-unknown pulse intensity definition (intensity fluctuations in present experiments are significant) we consider that the total dose per volume element is delivered by the cumulative effect of (on average) 60 repetitive beams of the same kinetic energy. See the next section for details. In particular, we assume 4 gantry directions (fields) and 15 repetitions per field. In case of spot scanning we assume that 10×10 spots are sufficient for laterally uniform irradiation of a 100 cm<sup>2</sup> area. For passive formation lateral uniformity is assumed to be reached by 10 repetitive density profiles (using different boluses to adjust lateral density profiles).

It is assumed that 10 energy steps are sufficient to reach sufficient depth dose uniformity (similarly to the PSI cyclotron). The energy variation is not done by absorbers as with cyclotrons, but by magnetically filtering the desired energy window out of the usually broader production spectrum. For relatively monoenergetic production spectra, varying the laser intensity, which moves the peak of the spectrum, may be required. For a broad spectrum this may not be necessary.

In order to match approximately to the strongly reduced intensity needs for more proximal depth layers we apply a factor of ¼ to the total number of pulses. Results are summarized in Table 22. Note that the laser frequency for spot scanning had to be increased to 30 Hz to keep the duration per fraction below the 5 minute target.

**Table 22:** Suggested laser and ion parameters at treatment area for two proton reference cases

	Spot scanning	Passive formation	Comments
Protons / laser shot	$2 \times 10^7$	$2 \times 10^8$	reach 2 Gy by 15×4 repetitions
# transverse	10×10 spots	10 reps for lateral uniformity	
Energy steps	10	10	$\Delta E/E = \pm 5\%$
Reps specified dose (~30% energy jitter)	60	60	15 reps, 4 gantry directions
Total # shots per fraction	15,000	1500	¼ applied
Duration of fraction	8 min	2.5 min	
Laser rep rate	30 Hz	10 Hz	

The number of laser shots is reduced by a factor of 10 for passive formation, which has the advantage that lateral beam profiles can be shaped by boluses intercepting the beam.

In this report, for the purpose of estimating specifications for future laser systems, we assume an extended tumor size. However, for treatment of very early stage tumors that are much smaller in size, the required number of ions can be significantly reduced, as can the required energy range for treatment. We can use current or future imaging resolution limits to estimate the minimum tumor size that can be detected (located) and treated. In this case some laser specifications might also be lower and even present technology allows developing therapy system for animal tests. Also, for such small tumors, spot-scanning is less likely to be an appropriate delivery mode.

These requirements for proton intensities per shot must be compared with what laser acceleration can actually deliver. As experimental data in the energy range of interest are not yet available, we can only refer to theoretical projections. In an RPA-based computational study it was shown that over  $10^{10}$  protons can be expected in an energy window  $\pm 5\%$  and with sufficiently good ability for focusing, provided that protons are collected by a lens (solenoid) [81]. In comparison with numbers for spot or even passive formation in Table 22 there is still a large safety margin to account for surprises in the acceleration mechanism, or for optimization of laser pulse and/or target towards less proton output and possibly higher conversion efficiency (photons into protons).

It appears from present extrapolations of observed and simulated ion abundances that lasers produce more ions than needed—in particular for spot scanning. If reduction cannot be achieved by laser and target optimization, the overproduction needs to be absorbed and shielding of patients against neutrons can become an issue.

For carbon ions we assume the same ion parameters would apply, except that a factor of 1/40 can be applied to the ion numbers per bunch due to the enhanced relative biological effectiveness of carbon.

### **1.3.2.3 *Reproducibility and Reliability***

For irradiating tumor cells, very high reproducibility and reliability are required. In the event of exposure error, the ion beam would still deposit the excess energy into healthy cells surrounding the tumor. The total dose per voxel or volume element should be controlled to within  $\pm 3$  to 5%. In this sense, by increasing the number of laser shots (here assumed to be 60 on average), we can control the total dose error to the required value in spite of relatively large shot-to-shot dose fluctuation of  $< \pm 50\%$ . The accumulated dose has to be controlled after each shot and the repetitions stopped after 95% of the nominal dose is reached.

It is also essential to address the tumor motion problem (attributed to breathing, patient positioning and organ motion, for example). In this case, the total dose error is thought to be within  $\pm 20\%$  at present. For regular predictable motion such as that attributed to respiration, this is typically done with gated irradiation. However, spot-scanning delivery combined with tumor tracking can be more efficient and is under development.

#### 1.3.2.4 *Electron Beams for Radiotherapy*

Laser plasma accelerators provide electron beams with parameters of interest in many fields and in particular for radiotherapy [88]. The electron beam properties in the range of 150–250 MeV offer advantageous dosimetric characteristics compared with those calculated with conventional radiotherapy with 6 MeV energy photons. It was shown that electron beams produced with laser plasma accelerators are well suited for delivering a high dose peaked on the propagation axis, a sharp and narrow transverse penumbra, combined with deep penetration. Comparison of dose deposition with that of 6 MeV X ray beams showed a significant improvement of a clinically approved prostate treatment plan [89]. Laser plasma systems using commercial laser systems with tens of femtoseconds, few-joule laser pulses, and working at 10 Hz repetition rate can deliver the required dose in a few minutes and compete in size and cost effectiveness with conventional electron accelerators.

### 1.3.3 Requirements for Lasers for Ion Acceleration

The laser requirements are driven first and foremost by the particle energy requirement of hadron therapy, i.e., 250 MeV for protons and  $\sim 400$  MeV per nucleon for carbon. Achieving these energies will probably require laser-acceleration of ions in the RPA / PSA or BOA regimes. Laser parameters for diode pumped lasers assumed here are based on these mechanisms and summarized in Table 23 for “full energy” ions as required for deep tumors. Ion energies achievable in the TNSA regime do not scale favorably with laser intensity and the spectral yields from targets are typically quasi-exponential, not monoenergetic. While intensities beyond  $10^{22}$  W/cm<sup>2</sup> are required to reach the desired carbon energies, simulations indicate that 250 MeV of proton energy might be accessible at  $10^{21}$  W/cm<sup>2</sup> with optimum targets. However the optimal target thickness depends on laser intensity and it is very hard to make a thin, cryogenic liquid or solid hydrogen target, which will be required for efficient proton acceleration. Consequently, the optimal intensity for a proton machine might realistically be the same order of magnitude as for carbon.

Due to the nature of the target (very thin but of very high solid density), laser intensity contrast is one of the key requirements as is shown by the numbers given in Table 23. While the optimum laser pulse duration remains unclear, the newer acceleration mechanisms have been demonstrated at 45 fs and 500 fs, making it clear from both experiments and simulations that pulses with fast rise time are necessary to achieve highest efficiency, stable acceleration and a quasi-monoenergetic spectrum. Shorter rise time can improve the acceleration results. We assume a rise time of  $\leq 20$  fs is sufficient. Similarly a flat-top transverse pulse profile in the focal plane is a necessary requirement that must be developed. Altogether, these requirements equate to energy on target within a 5  $\mu$ m radius and flat-top focus of up to 150 J in the proton case and up to 1500 J in the carbon case.

If the CO<sub>2</sub> laser on gas jets proves feasible for the required energies, it may result in significantly lower laser intensity and power requirements. Suggested values of laser intensities are possibly down by a factor of 100, with 500 fs pulse duration, 25 J pulse energy, 50 TW peak power and frequency range of 30-300 Hz. This requires, however, dedicated laser development beyond what has been established.

For therapy applications these parameters must be obtained at the required rep rate and with  $\leq 1\%$  stability. For future use in hospitals, development of an overall system is needed, which includes a compact laser and devices for imaging and spatial filtering, a transport beam line with appropriate instrumentation, and a sophisticated beam delivery subsystem for treatment.

**Table 23:** Laser parameters for ion acceleration aiming at “full energy” ions.

	laser proton	laser carbon
Rep rate (spot/passive)	30 Hz / 10 Hz	
Laser intensity ( $\text{W}/\text{cm}^2$ )	$1-3 \cdot 10^{21}$	$1-3 \cdot 10^{22}$
Pulse duration (fs)	50-150	
Rise time (fs)	<20	
Contrast (5 ps / 500 ps)	$<10^{-8} / 10^{-12}$	$<10^{-9} / 10^{-13}$
Laser energy stability	1-5%	
Spot radius ( $\square\text{m}$ )	5	
Peak power (PW)	1-3	10-30
Pulse energy (J)	50-150	500-1500
Average power (kW) 10 Hz (30 Hz)	0.5-1.5 (1.5-4.5)	5-15 (15-45)
Laser cost assumption	<10 M€	~15 M€
Laser wavelength (nm)	800-1054	
Efficiency	1-10%	
Polarization	lp/cp	
Laser beam quality	diffraction limit	
Pulse stability	0.01	
Laser pointing ( $\square\text{rad}$ )	1-10	
Laser availability	12 h/day (50% duty factor)	
Failure rate	<2%	

### 1.3.4 Needed Roadmap for Laser Development

Developing laser systems that are adequate for driving medical plasma accelerators with the proposed required parameters will likely take another 10-20 years. There are several ongoing and near-term projects on this subject in the world. Those must have clear quantitative requirements to fulfill the declared and approved targets. Success with these ongoing projects could represent achievements in the specified time windows. Their time structure and the currently envisaged roadmap need to be brought to mutual balance.

The complete integrated accelerator system consists not only of the laser but also targets (sources), beam line instrumentation for diagnostics and control and a sophisticated delivery subsystem. Clearly these companion technologies must be developed in parallel with laser systems.

#### 1.3.4.1 Required Developments on Laser and Target Side

- 1) Laser + target specs as outlined in Table 23.
- 2) Robust acceleration mechanisms to required energies.
- 3) Reliability in energy *and* intensity spectrum.

- 4) Control of center energy for narrow production spectra.
- 5) Transverse emittance + position stability and failsafe control.
- 6) 10-30 Hz target replacement and positioning control.
- 7) An extremely thin but robust film or pneumatic target has to be developed for a carbon system.

#### **1.3.4.2 *Clinical Development***

- 8) Quality assurance of beam parameters to prevent overdose.
- 9) Beam delivery system development providing online dosimetry, field definition (scanning, etc.) and safety.

#### **1.3.4.3 *Laboratories Involved, Their Status and Plans***

The number of laboratories worldwide with programs in laser acceleration of protons or ions is increasing. Some of them have accompanying biophysical or medical programs/experiments, and a few are planning clinical programs based on laser acceleration. In Table 24 we give an overview of such laboratories that have some connection with biophysical or medical applications.

**Table 24:** Laser acceleration experiments and their therapy relevance (parameters contributed by U. Schramm, P. Bolton, Ch. Ma, J. Schreiber, V. Malka, M. Borghesi, M. Babzien)

	Operating facilities						Under or near construction / planning
	type of laser	J / fs / Hz	p / ion MeV	e <sup>-</sup> MeV	biophysics experiments	therapy relevant programs	J/fs/Hz (date)
<b>HZDR and Oncoray (Germany)</b>	DRACO 150 TW Ti:Sapphire	4.5 J / 30 fs / 10Hz (30J upgrade 1Hz 2012/13)	20		Dose controlled cell irradiation and dosimetry development	Depth dose planned, translational research	PENELOPE DPSSL 150J / 150fs 1 Hz (~2015)
<b>KPSI (Japan)</b>	J-KAREN 250 TW Ti:Sapphire	10 J / 30 fs / 30 min/	23	200	doublestrand breaks (2 MeV) Estimation of RBE with dose controlled cell irradiation	Development of source & beamline, assessment of PET diagnostics	
<b>Fox Chase Center (USA)</b>	150 TW Ti:Sapphire	4.5 J / 30 fs / 3min	6		Physics studies	Prototype studies	Planning an on-campus prototype facility
<b>MPQ &amp; LMU Munich (Germany)</b>	ATLAS 70 TW Ti:Sa LWS 20TW OPCPA	2 J / 25 fs / 5 Hz 0.1 J / 5fs / 10 Hz	8	600 50	Single shot radiation biology on cell level	Development of source, & beamline	60J/20fs/1Hz (~2015) 5J/5fs/10Hz(~2015) 0.5J/5fs/1kHz (~2015)
<b>LOA (France)</b>	Salle Jaune 30 TW Ti:Sapphire	1 J / 30 fs / 10 Hz (2 J upgrade 0.2 Hz 2012/2013)	14	250	Dosimetric properties Cell irradiation	Depth dose planned SAPHIR	SAPHIR 6 J / 30 fs (2012)
<b>QUB Belfast (UK)</b>	TARANIS 60 TW, Nd:Glass	15 J (2 beams) /500 fs/ 15 min	12		Cell irradiation: dose dependent effects on single shot basis		Ion beam lines planned
<b>GSI (Germany)</b>	PHLIX Nd glass	150J / 700 fs /10 <sup>-3</sup>	< 30		Double strand breaks (at 2 MeV)	Beam line collection & energy selection	PHLIX upgrade planned
<b>BNL (USA)</b>	CO <sub>2</sub>	5 J/5000 fs	5			Source R&D	

## 1.4 Laser Technology Development Roadmaps

### 1.4.1 Introduction

The laser technology roadmaps for future laser-based particle accelerators are defined by the requirements of each specific application, as summarized in Table 25. The main challenge for the laser technology is that the majority of these applications (with only a couple of exceptions) require extraordinarily high average laser driver power, ranging from approximately 10 kW up to ~0.5 MW. Although required pulse energy, duration and other performance characteristics have been met by a variety of existing laser drivers, none of these can currently provide such high average powers. In

fact, the majority of existing LPA drivers cannot even reach such powers by further gradual technology development; it is expected that substantially new technological developments and even breakthroughs will be required. The challenge is further compounded by the need for high electrical-to-optical conversion efficiencies so that the “wall plug” electrical-power requirement for an accelerator facility is acceptable.

Table 25 also summarizes possible candidate laser technologies best suited for each particular application. There follows a detailed review of the five, summarizing current state of the art, anticipated challenges, and required R&D for each.

## 1.4.2 Fiber Lasers for Laser Based Particle Acceleration

For laser-based accelerators to be broadly accepted for use, they must be robust tools with low maintenance requirements, turnkey operation and high wall-plug efficiency. To date, fiber laser systems offer the most potential to attain the combination of reliability and efficiency ultimately required for a user facility, on a par with RF based accelerators. Further, because they are waveguide based, the beam quality of fiber lasers is (if not perfect) typically superior to that of other lasers of similar power and pulse energy. However, while fiber lasers commonly attain 30% wall plug efficiency in the robust turnkey, low maintenance,  $M^2 < 1.1$ , commercially available form needed for a demanding application, this has been true only of continuous wave lasers to date.

Laser based particle accelerators will in most cases require ultrafast pulses ( $< 100$  fs) with high contrast ( $> 10^{10}$ ), high pulse energy ( $> 10$  J), high average power ( $\sim 100$  kW), and high efficiency ( $> 30\%$  wall-plug), along with excellent beam quality and pointing stability. While fiber lasers are great CW lasers, they simply cannot attain pulse energies greater than a few millijoules with good beam quality. However, once they can make a single pulse of a given energy, the repetition rate and average power will typically scale to quite high values with little to no additional R&D; this is not true of most other laser systems. Further, the primary (but not the only) focus of development to date for fiber laser systems has been on making better CW lasers. Thus, while mJ fiber laser with sub-picosecond pulses have been demonstrated, critical issues such as pulse contrast and  $< 100$  fs pulse widths have not been adequately addressed. Further, to attain joule-class energies, a fiber laser system will need to be able to combine the outputs of multiple, high-quality individual lasers into a single beam. Thus development of fiber laser beam combination techniques will be critical to the future success of laser based particle accelerators.

### 1.4.2.1 *Fiber Laser State-of-the-Art*

In 1985, the University of Southampton rediscovered fiber lasers [90]. Since then, developments in low loss rare earth doped optical fiber technology [91, 92] combined with improved reliability, brightness, efficiency and packaging of diode pump lasers [93-95] has quickly led to very-high-power fiber laser systems [96-98]. These systems leverage the waveguide properties of optical fiber in order to achieve exceptional wall plug efficiencies ( $> 30\%$ ) and diffraction limited beam quality with high average output powers ( $> 10$  kW).



Pulsed fiber laser systems with pulse widths of a few nanoseconds are limited to around 4 MW peak power in a single mode due to self focusing [99]. This value has been attained with 1-ns pulses, and high quality beams with >4 mJ output have been demonstrated from 100- $\mu\text{m}$ -class core diameter fiber rods [100]. While the results from fiber rods have been impressive, from the standpoint of compact packaging a more flexible form factor may be desirable in the long run. Furthermore, a bent waveguide may only be useful up to 50  $\mu\text{m}$  mode field diameter, after which the process of bending itself will likely limit further scaling. NKT Photonics currently offers a 40  $\mu\text{m}$  core, 30  $\mu\text{m}$  mode field diameter photonic crystal fiber that has many desirable properties [101]. Further, Galvanauskas et al. [102] have recently demonstrated a “chirally coupled core” fiber with a 55  $\mu\text{m}$  core diameter. Thus, in terms of energy scaling of nano-second pulses, the limits of single aperture fiber lasers may be close to being reached.

Ultrafast fiber lasers have demonstrated significant powers and pulse energies approaching the limits discussed with regards to nanosecond pulses above. Commercial fiber laser systems with up to 100  $\mu\text{J}$  pulse energies and sub-picosecond pulses are currently available from a number of vendors [103]. Given the current rate of development, one could reasonably expect to see mJ-class commercial systems with sub-picosecond pulses available in the next 5 years.

On the R&D front, a 1mJ, sub-picosecond chirped pulse amplification (CPA) fiber laser was first demonstrated in 2001 [104]. Recent results with fiber rods have demonstrated 11W of average power with 2.2 mJ pulse energies and <500 fs pulses with the best quality optical pulses from a fiber laser system to date [105]. Similar rods have been employed to amplify non-stretched pulses to the 1  $\mu\text{J}$  level [106]. These latter systems experience significant self-phase modulation, which can in turn be used to compress the output pulses to <50 fs, albeit with significant pulse pedestal. Systems with a very small amount of chirp (<100 ps) have been shown to achieve a few hundred nanojoules of pulse energy in <250 fs pulses with excellent pulse fidelity [107]. Low energy pulses have been generated via CPA using chirped volume Bragg gratings (CVBG) and have attained <200 fs pulse width, which is a promising technology for significantly reducing the size of CPA systems [108].

Continuous wave fiber laser beam combination systems have been demonstrated at the multi-kW level. Typically these systems employ either a coherent beam combination scheme with active phase locking [109-112] or a wavelength multiplexing scheme [113-118] or some combination thereof. Up to 64 unit cells have been successfully demonstrated [119]. In the case of coherently combined systems, packing fraction is important to keeping most of the power in the central lobe in the far field, or an additional beam combining optic is required to improve the far field [120, 121].

Development of beam combination schemes for ultrafast fiber lasers is relatively recent with only three research groups reporting results to date [122-124]. So far, most results have employed an active phase control scheme with one demonstration of a passive scheme [125]. To date, 4 channels have been combined with <600 fs pulse width and 93% combining efficiency [122]. The other two groups reporting results have demonstrated combination of two unit cells thus far. However, the use of either a 50% splitter as the recombining element [123] or a polarization beam splitter as the recombining element [124] enabled combination efficiencies as high as 97%. Recent progress of coherent combination of femtosecond fiber CPA systems resulted in 100-W-class average power and 3 mJ pulse energy [125]. These experiments suggest that

coherent combination is feasible at high average power (implying high thermal load) and high nonlinearity (i.e., high B-Integral).

#### 1.4.2.2 *Fiber Laser Technology Challenges*

The critical R&D path needed to bring fiber lasers from their current state of the art to a technology readiness level suitable for most accelerator applications is discussed next. For some applications, such as dielectric laser accelerators, almost no R&D is needed, as the industrial fiber laser base will likely produce the required systems through incremental improvements, or already produces the required systems.

However, most applications will require significantly more pulse energy, pulse quality, and better than any known laser system is presently capable of producing. As fiber lasers are the most likely to be useful from a maintenance and reliability standpoint, and have a high probability of attaining the critical requirement for wall-plug efficiency, it is logical to invest in the R&D required to bridge the gap between present performance and laser particle accelerator system requirements.

It was the assessment of the working group that much of the required R&D is unlikely to be pursued by commercial industry on its own. Further, the nature of much of the needed R&D is such that it is best pursued via collaborations led by universities and national laboratories, with industry being brought into the mix as the technology matures further. R&D issues, in order of critical importance, are:

- Beam combining: schemes for coherently summing the outputs of many fiber lasers.
- Unit cell development: high contrast, ultrafast fiber lasers with <100fs pulse width.
- Wall plug efficiency: demonstrations of high wall plug efficiency in pulsed operation in the range of 10 kHz – 25 kHz repetition rate.
- Reliability at high energy and high average power.
- Cost control with simply manufactured unit cells.

Beam Combination Challenge: To attain pulse energies on the order of 50 J – required for laser plasma acceleration, for example – a fiber laser system would need to combine on the order of 50,000 unit cells with 1-mJ energies, 12,500 unit cells with 4-mJ energies, or 5,000 unit cells for 10-mJ energies (which might be attainable with 2-3 ns stretches).

A generic schematic of one way this might be done is shown in Figure 13. A pulse stretcher stretches pulses from a mode-locked oscillator. This stretcher needs to include dispersion control for the amplifier chain that follows it as well as for the output compressor. The pulses are pulse-picked to reduce the repetition rate to the target repetition rate and then amplified in a series of preamplifiers. The amplifiers are assumed to include key components such as isolators, acousto-optic modulators and band-pass filters as needed. The pulses are then split in a splitter and coupled to the unit cells. Each unit cell will include a phase control actuator (assuming phase control is required) and additional power amplifiers to bring the pulses to full energy. The pulses are then recombined into a single output beam and compressed. A portion of the output beam will be sampled and employed as feedback to permit phase locking electronics to create a feedback signal for the phase control actuators.

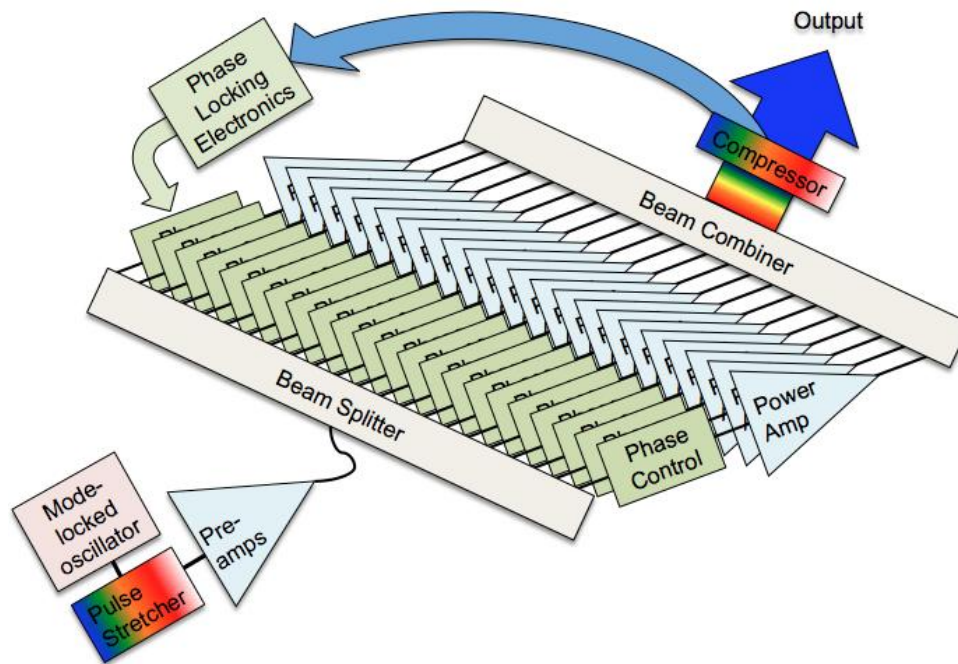


**Figure 13:** Conceptual outline of a coherently combined fiber laser array.

The number of unit cells required represents a significant advance:  $1000\times$  the current state of the art pulsed demonstrations and close to  $100\times$  the best continuous wave demonstrations. Thus the challenge here is the demonstration of robust schemes for beam combination of order 10,000 unit cells that employ technology that will be cost effective at these scales. This is a basic research problem best pursued by a combination of universities and national laboratories until a clear pathway is formed, at which point industry should be brought into the collaboration to assist with determining methods for cost control.

Advanced approaches to beam combination: The generic approach for coherent beam combination through active phasing illustrated in Fig. 13 can be implemented in different configurations with different advantages and disadvantages. These have been investigated in depth for the cw case, and while some configurations work equally well for ultrafast pulses, the norm is that the inherently broad linewidth brings additional issues. As mentioned, the aperture-tiling approach suffers from side-lobes due to imperfect aperture filling (i.e., packing fraction). While that can conceivably be addressed with diffractive optics and phase-plates, the strong dispersion of such elements may lead to degraded beam quality and contrast ratio. There are similar concerns for other combination schemes relying on diffractive elements and phase plates. For example, the use of Damman gratings for stacking rather than tiling beams avoids the filling problem [126], but may suffer from dispersion. A beam-splitter tree [121] can avoid both the dispersion and the filling problem, but may be prohibitively deep in case of a large number of arms.

On the other hand, beam combination can also conceivably bring important advantages, beyond power scaling. One advantage is the possibility that the superposition (i.e., combination) of a large number of constituent beams might reduce the noise. If so it might be possible to improve the contrast ratio of the combined and

compressed pulses. Furthermore, it is possible to simultaneously compress and combine pulses by coherent spectral stitching of multiple trains of longer, possibly transform-limited, pulses in multiple spectrally narrower beams. As a bonus, this opens up for the synthesis of shorter pulses, with broader spectra than can be supported by a single type of gain elements and with precise control of the electric field [127, 128]. The most obvious way is to combine two spectrally disjoint beams in a dichroic mirror, while a cascade of mirrors can be used to combine several beams. More attractive would be to combine a large number of pulse trains into a train of compressed pulses in a single element (e.g., a volume grating), but whether such an element can be realized is an open question. In any case the combination and compression problem may well be eased by the possibility to use a mixture of combination approaches, e.g., a first step with, say 16 Dammann gratings which each combines a number of spectrally disjoint and narrow beams followed by a shallow tree of dichroic mirrors to combine the resulting 16 beams. In all cases, the overall size of the combination and compression stage as well as power densities and damage warrant careful attention.

Unit Cell Challenge: Sub-100fs, High Contrast, Efficient and Good Beam Quality: Presently fiber lasers that produce millikoule pulse energies typically have pulse widths of more than 500 fs. Due to high B-integral (self phase modulation on the chirped pulse) and inadequate dispersion management, these 500-fs pulses tend to have contrast much less than the  $10^{10}$  required for the wakefield accelerator application. While beam quality is generally acceptable, it is obtained from fiber rods that are stiff and inflexible and likely to constrain packaging options (at least in their current format). Further, systems demonstrated to date typically have optical-to-optical efficiencies much less than those attained by CW fiber lasers, particularly at relevant repetition rates (10-20 kHz). This is because attempts to minimize B-integral and dispersion typically lead to short, large core fiber amplifiers that suffer from both incomplete pump absorption and inadequate gain saturation in the 10-20 kHz regime. Little R&D has been performed to address these issues.

Maximum Wall Plug Efficiency Challenge: Overall wall plug efficiency is a product of the efficiency of the individual unit cells, the beam combination system, and the electrical drive and cooling systems for the laser. Furthermore, there may be an interplay between the laser system and particle accelerator scheme that impacts overall-system wall-plug efficiency. This is most apparent in terms of the laser wavelength. Fiber lasers can operate efficiently at both 1  $\mu\text{m}$  and 2  $\mu\text{m}$ . Impact of wavelength selection on the accelerator performance as well as the laser performance should be studied and understood prior to the construction of a large system. In the long run, the commercial companies that will manufacture large numbers of these systems can best address this issue. However, in the near term, universities and national laboratories could be helpful in assessing the impact upon these issues of R&D pathways developed in the two preceding challenges, as well as determining the optimum wavelength for maximum overall system efficiency.

Reliability at High Energy and High Average Power: High average power fiber lasers with good reliability are now commercial products. However, these systems do not operate with pulsed light, where high peak powers can lead to additional reliability issues. The long-term aging impact of pulsed laser effects needs to be studied and

understood prior to deployment of a full system. Additionally, a beam combination system will require a high-energy beam combiner with high reliability. Finally, these systems may require additional high-energy, high average power components in order to operate as all-glass monolithic systems, particularly optical isolators and temporal gating devices such as acousto-optic modulators.

Cost Control with Simply Manufactured Unit Cells: A 10 TeV accelerator facility will probably have the most aggressive cost controls. Such a facility will require a significant number of laser systems to drive the full accelerator. For example, if the cost of a 10-TeV accelerator is capped at \$10B and half of that is devoted to constructing 10-GeV, stages, then the 1000 stages, each with its own laser, must cost less than \$5M apiece. As the laser is likely to represent the majority of this price, a cost target for the laser may be \$4M. If this laser requires 50,000 1-mJ unit cells, they must cost less than \$80 each. Higher-pulse-energy unit cells would be proportionately fewer but could cost more. Given the volumes of unit cells required (>5M), achieving the required price point is not inconceivable. However, simplicity in the unit cell design will be a must in order to keep the manufacturing costs contained.

**1.4.2.3 Roadmap**

Figure 14, below, details a 10 year plan for addressing the challenges listed above.

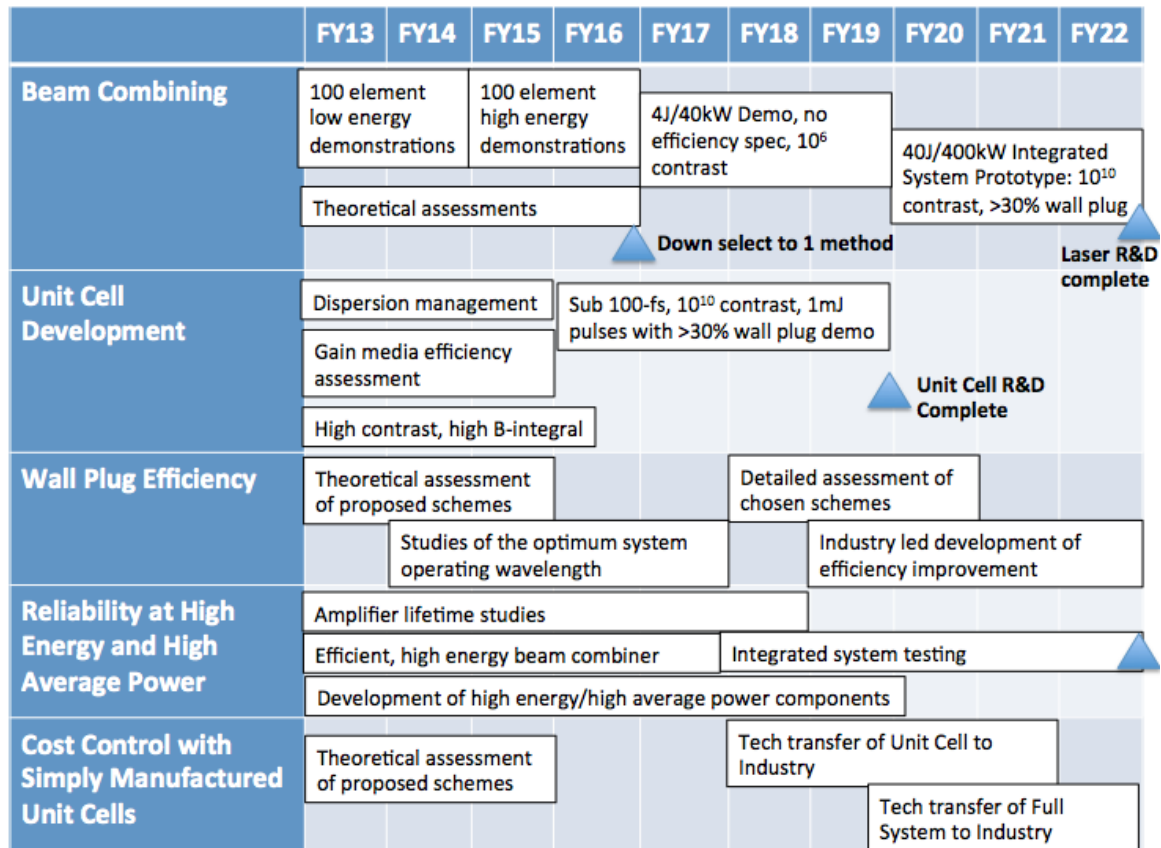


**Figure 14:** Fiber Technology Development Roadmap

Beam Combination: This roadmap is designed to quickly scale the number of unit cells from the current 4 to 100, first at low energy, then quickly to higher energy. It is

assumed that these demonstrations will employ unit cells based upon existing state of the art. That is, they will deliver 500 fs-1 ps pulse widths and possibly have significant pedestals relative to the desired  $10^{10}$  contrast requirement. Further, these demonstrations will only consider efficiency of the beam combination scheme, and not the underlying unit cell's efficiency and cost. A low energy unit cell today might cost \$30k, for a total system cost of nearly \$3M. Additional support for 2-3 scientists to perform work using the system might bring an R&D effort into a range of \$2-3M/year over a 4-year period. Development of several concepts at lower unit cell numbers, in order to generate an early competition for the best ideas, should be a fruitful undertaking at this stage.

A 4 J, 40 kW system demonstration would require improved engineering and would presumably begin to take advantage of improved unit cells. This system might be useful for some interim particle accelerator experiments when complete. As several thousand unit cells may be involved, with significant engineering wrapped around the system, the cost may be on the order of \$10M/year for four years. This very preliminary cost estimate assumes cost reduction of unit cells to \$3k each (from \$30k each in the earlier efforts.) This requirement will force the beginning of cost reduction efforts.

Once this prototype is complete, the essential knowledge to construct a full scale 40 J/400 kW/40 fs high contrast laser should exist. This will likely be a larger undertaking and enable a 10 GeV accelerator with significant luminosity upon completion. Up to 40,000 unit cells might be required for this effort. Assuming ongoing cost reductions, the cost per unit cell could conceivably drop to \$1k each. Given the laser would require significant additional engineering and an appropriate facility. The budget for this prototype effort would likely be on the order of \$50M/year. It is expected that technology would be transferred to industry as part of this effort and production systems for a TeV class accelerator would be produced by industry at significantly less cost, in volume, post 2022.

Unit Cell Roadmap: There is no point in combining the outputs of lasers that cannot meet the end user requirements. Thus in parallel to beam combination experiments, significant work needs to be put into improving pulse quality and laser efficiency early. To this end, small scale experiments and R&D are needed to improve the dispersion management of fiber lasers. This might cost \$1M/year to simply look at stretching low energy pulses to 1-2 ns, run them through 40-50 m of fiber and some fiber components, and then recompress these pulses with good contrast.

An important issue with current pulsed laser systems is that they are not as efficient as their CW counterparts. This is because the fluence at 10-20 kHz repetition rates is not high enough to saturate the gain medium when a system is designed to operate at low (<6 radians) B-integral. However, rare earth ions other than ytterbium (such as neodymium, erbium or thulium) might offer lower saturation fluence and thus significantly improve the overall system efficiency without requiring the system to operate at excessively high B-integral. This could be a small-scale effort that would heavily leverage modeling capability to reduce to one the number of competing materials to be studied in a demonstration experiment. This undertaking is likely to cost ~\$1M/year for 5-10 years.

If that is not technically feasible, it will likely be necessary to compress pulses with good pulse contrast at B-integrals as high as 30 radians. Learning to do this is a significant R&D effort that may require new inventions. It might be a 3-4 year effort, costing \$2-3M/year in equipment and personnel, with efforts from 2-3 R&D groups.

Assuming these efforts are successful, a well-engineered unit cell showing good pulse contrast, sub-100-fs pulse widths, and >30% wall plug efficiency (counting all electrical inputs to the system), delivering 1 mJ/pulse at 20 kHz, should be constructed as a demonstration. An effort costing not more than \$2M/year over 4 years should be able to demonstrate a system such as this as a well-engineered device.

Wall Plug Efficiency: In the early years, what is predominantly needed here is a paper study examining and clearly detailing all the issues. This might be cost as little as \$250-\$500k and be done by a single PI. Additionally, R&D teams working on the particle acceleration schemes and on the laser schemes should look collaboratively at the overall system to understand how to maximize wall-plug efficiency. Once high-unit-cell beam combination demonstrations had been completed, a second study or an independent assessment of wall-plug efficiencies may also be useful. Finally, as the unit cell development activity begins to wind down, industry should be heavily engaged in order to improve component efficiencies for the single unit cell and critical parts of the beam combining system.

Reliability at High Energy and High Average Power: There are quite a few high-average-power lasers and quite a few high-energy lasers; however, there are few if any lasers with both those attributes. Further, there is reason to believe that such systems may have unique reliability issues due to the combination of high energy and many orders of magnitude more pulses than current high energy systems. Overcoming photo-darkening has been key to the success of CW fiber lasers. It will be necessary to validate that in the pulsed regime, this issue is no worse than in CW and that no new issues arise. To do this properly, several groups would need to study the effects over a period of several years. This is likely a \$1-2M/year, 5-year effort.

In addition to the amplifiers, it will be necessary to develop monolithic all-glass components such as optical isolators and couplers that can withstand the required energies and average powers. As each individual unit cell may be of relatively low average power, this may not be a difficult undertaking for most components and more a matter of validating that the pulse energy effects are not too detrimental.

However, the final beam combination optics will see quite high powers and energies; development of an efficient beam combiner and understanding the safe operating fluence for this combiner may be a significant undertaking. It might require a team of optical scientists and engineers with a facility for fabricating the required components. Assuming existing facilities can be employed, this may cost as little as \$1-2M/year for four to five years.

Cost Control: Cost control is critical in the long run, but should probably be of minimal influence in the next 4-5 years; much cost-reducing technology development can occur in that time frame for other reasons. This we suggest only a small paper study to assess the potential end cost of various system concepts. As the R&D from the abovementioned efforts begins to generate significant results, involving industry more and more, and having them focus on cost reduction efforts, will likely be critical to final success.

### 1.4.3 Solid-State Laser Technology Development Plan

Solid-state lasers have played an important role in the history of laser research and development, as evidenced by the first laser demonstration in 1960, which used sapphire as the host material. In this section, the term solid-state laser refers to a class of optically pumped laser in which active ions are doped in a crystalline or ceramic host material. Other types of lasers using solid-state media, such as optical fiber or glass host materials, are considered in other sections.

Diode-pumped solid-state lasers are an attractive enabling technology for accelerator applications because of their potential for peak power scaling at high average power in a single aperture. This section is meant to address some of the challenges associated with solid-state laser development for these applications, as well as to highlight areas for further investment. These challenges can be summarized as follows:

- Operation at high average power (kilowatt or greater) with near-diffraction-limited beam quality and high efficiency;
- Availability of large aperture gain media;
- Operation at high peak and high average power with sub-picosecond pulse duration and high efficiency;
- Coherent combining.

Some of the challenges are general to solid-state laser development, and not necessarily specific to the ultrashort pulse systems required for accelerators. These more general challenges are associated with achieving high average power.

For example, a particular challenge is to improve the beam quality of solid-state lasers with average output powers in the multi-hundred-watt or kilowatt regime. Central to this challenge is the removal of waste heat from the active medium. If the crystal tends to store too much heat, problems of efficiency, stability or even fracture of the gain medium may occur. The fundamental source of waste heat is the quantum defect, the energy difference between the pump and laser wavelength which is deposited in the medium through nonradiative transitions. This quantity is material-dependent; for example, the quantum defect of Yb-doped materials is small (e.g., 9% for Yb:YAG, assuming a pump wavelength of 940 nm and laser wavelength of 1030 nm), meaning that the amount of generated heat is intrinsically low. For comparison, the quantum defects for Nd:YAG (assuming pump wavelength of 808 nm and laser wavelength of 1064 nm) and Ti:sapphire (assuming pump wavelength of 532 nm and laser wavelength of 800 nm) are 0.24 and 0.34, respectively.

Thermo-optic material properties also play a critical role in the design of solid-state lasers that can operate at high average power with near-diffraction-limited beam quality. The ideal material exhibits a high thermal conductivity, a small change in refractive index with temperature, and a low coefficient of thermal expansion. One general strategy to improve these thermo-optic material properties is through cooling below room temperature. While general temperature dependence is known, measurements are required in order to provide accurate, quantitative values. Clearly, this data is needed in order to make critical assessments as to the desirability of various host materials and to provide engineering inputs for thermo-optic performance. However, material property measurements are typically only performed at room temperature. Future investment is necessary to identify new candidate materials as well as to perform further temperature-

dependent characterization of existing materials.

Another challenge is the availability of large-aperture gain media. For simultaneous pulse energy and average power scaling, this will be a critical need. Compared to single crystals, ceramic laser materials can be fabricated in large sizes, and can be co-sintered to produce composite gain media with more advanced gain element designs that would otherwise be difficult to fabricate with single-crystal material. To date, only ceramic YAG has been developed to the point of commercial availability. The sesquioxides (e.g.,  $\text{Y}_2\text{O}_3$ ,  $\text{Sc}_2\text{O}_3$ ,  $\text{Lu}_2\text{O}_3$ ) are under development, but still far from commercial availability. Other material types, such as fluorides, may offer particular advantage for high peak power systems. Continued development of large aperture ceramic laser gain media of high optical quality (high transparency and low scattering loss) will be important.

In addition to laser material considerations, there are efforts focused on optimizing the geometry of the gain element for high-average-power, diffraction-limited solid-state lasers. Different geometries include rod, slab and thin disk. Each geometry has advantages and disadvantages, and working through this design space is important for future high-average power systems. Innovations in this area could substantially improve diffraction-limited average powers. In addition, there is research into compensating for thermo-optic distortion with active or passive means and combining multiple lower-power lasers.

Ultrashort-pulse solid-state lasers, such as the ones required for accelerator applications, must confront additional challenges to those that are faced by high-average-power lasers. High peak power may result in undesired nonlinear effects as well as damage of optical components, and is usually mitigated by temporally broadening the pulses during amplification, known as chirped pulse amplification. It is interesting to note several inherent trades that exist in ultrashort solid-state lasers, and to discuss briefly the consequences and implications these trades may have on the laser system design.

For example, rare-earth doped materials with high thermal conductivity tend to have a narrow emission bandwidth. In general, the high electron-phonon coupling that is needed to obtain a broad emission band tends to limit thermal conductivity, presenting a trade between short pulse duration and average power scalability. Another approach to broad emission is to use structurally disordered hosts, such as mixed composition crystals and glasses, which leads to inhomogeneous broadening. However the structural disorder leads to short phonon scattering lengths and therefore poor thermal conductivity. These are general trends, and research into materials that can break the trend lines in the regime of simultaneously high peak and high average power will be important.

A second trade exists between the desire to operate at a high fluence to improve efficiency and the desire to operate at low fluence to mitigate the risk of optical damage and maintain a low B-integral. The latter also requires minimizing gain element length and choosing a material with a low nonlinear index of refraction. Optimizing this trade space is a difficult problem. Even with chirped pulse amplification, the saturation fluence can be significantly higher than the damage threshold, limiting extraction efficiency. Some material properties are of particular interest for this application. For example, materials with low nonlinear index of refraction that maintain a relatively high thermal conductivity at high dopant concentrations are of interest, despite the general trend of a decrease in thermal conductivity with increasing dopant concentration. Such a

material would balance the need for materials with high thermal conductivity with the need for a short gain element to maintain a low B-integral.

In addition to the materials-related challenges, there are system-level design approaches worthy of further investment that may enable high-average-power ultrashort-pulse solid-state laser systems. For example, one can exploit the use of multiple laser host materials to provide a composite gain bandwidth. This can provide a broad emission bandwidth for the system, while using materials with relatively high thermal conductivity and capability of high average power handling.

Another system-level design decision will involve the operating temperature of the gain media. Cryogenic cooling typically reduces the saturation fluence, to the benefit of extraction efficiency. However, this generally comes at the expense of reduced gain bandwidth, and therefore an increase in the minimum pulse duration achievable.

It may be that the optimal approach to system design begins at low average power with room temperature gain media and/or media with low thermal conductivities, and continues through further stages of amplification with media at lower temperatures and higher thermal conductivities. Further research is needed to explore this large design space.

It is also worth investigating other system-level design strategies for high average power in ultrashort laser systems. One such strategy is the use of coherent beam combining of multiple solid-state lasers, whereby a higher average and peak power can be achieved than might otherwise be possible from a single aperture. To enable this, measurements on the phase noise of such systems will be necessary, followed by some system-level demonstrations.

#### **1.4.4 High Average Power OPCPA for Laser Plasma Accelerator Applications**

##### **1.4.4.1 *Optical Chirped Pulse Amplification***

Optical Parametric Chirped Pulse Amplification (OPCPA) [129, 130] is an ultrashort pulse amplification approach that uses phase-matched optical parametric interactions in a nonlinear crystal to convert pulse energy from nanosecond-long pump pulses into energy of duration-matched stretched ultrashort pulses, which subsequently are compressed to produce high energy femtosecond optical pulses. The principal difference between OPCPA and an optical-inversion based gain medium is that there is no energy storage during optical parametric amplification. This brings a very different set of advantages and disadvantages compared to optical-inversion amplifiers.

Overall, when seeking very high intensities and very short pulse durations, the advantages of OPCPA far outweighs its disadvantages, which is the main reason why over the last thirteen years OPCPA has seen very rapid development and have been extensively used in a number of multi-TW and PW class laser facilities [131-137].

One of the principal advantages of OPCPA is, in general, much larger bandwidth and, subsequently, much shorter achievable pulse durations, compared to inversion-based amplifiers. Indeed, pulse durations of only a few optical cycles have been reported with various OPCPA systems [137-140], and multi-TW peak powers are achievable with pulse durations at around 30 fs [138]. Furthermore, since there is no energy storage in the medium, quantum efficiency is in principle very high—each pump photon is “cut” into one signal and one idler photon. Consequently, no pump power is directly deposited in the gain medium, and thermal loading in OPCPA only occurs due

to (usually small) material absorption at pump, signal or idler wavelengths. As a result, thermal loading is orders of magnitude smaller compared to conventional energy-storage amplifiers, and, in principle, correspondingly higher average powers can be achieved in OPCPA.

Negligible thermal lensing typically results in higher output beam quality. Also, due to the absence of energy storage as well as need to phase-match, OPA is immune to parasitic side-lasing, which usually limits high-power pumping of conventional inversion-based optical amplifiers. Finally, OPA is a high-gain process, which usually requires a much shorter material path. This, in combination with the fact that typically OPA crystals can be grown to a larger aperture at a lower cost, leads to much smaller nonlinear distortions in the compressed-pulse temporal shape [141]. Indeed, pre-pulse contrast ratio of down to  $4.4 \cdot 10^{-11}$  has been achieved with high-intensity OPCPA, which is orders of magnitude better than the contrast achieved at TW-PW peak powers with energy-storage CPA systems [142].

The main disadvantage of OPCPA is associated with the limited pump-to-signal energy conversion efficiency. Although quantum efficiency is high, the quantum defect (i.e., ratio between pump and signal optical frequencies) is generally quite low, with typical values in the range from 50-70%.

Furthermore, since there is no energy storage, conversion efficiency is directly determined by the spatial and temporal properties of the pump. Nonlinear back-conversion from signal to pump can occur after the pump has been completely depleted, which means that, for example, with Gaussian beams and pulse shapes, it is impossible to achieve complete power extraction across the full spatial and temporal profile of the pump. A complete energy extraction can only be achieved with specially-shaped flat-top beams and square temporal pulse profiles [143]. Typically, reported OPCPA conversion efficiencies are in the 25-35% range [143]. Also, in many cases, pump light is first converted to the second harmonic, which then is used to pump OPA, which approximately halves the overall plug-to-power conversion efficiency [144].

#### **1.4.4.2 High Average Power OPCPA**

Since there is no pump power or energy storage in OPCPA systems, achievable peak and average powers and pulse energies are directly related to the corresponding performance characteristics of a pump laser. Therefore, a single-laser pumped OPCPA would have the same power limitations as the pump laser. For example, solid-state laser pumping would be limited in average power, while fiber-laser pumping would be limited in pulse energy. The advantage here only comes in cases when nanosecond pulsed lasers have better achievable performance characteristics compared to their ultrashort-pulse counterparts.

However, since the phase difference between pump and signal is transferred to the idler, [143] OPA can be pumped with multiple beams, thus in effect providing an avenue to combine multiple pump lasers [144-148] and to exceed the power characteristics of each individual pump. Multiplexing of multiple pump beams into a single amplified signal beam can be achieved through vector phase-matching, when each pump beam enters the nonlinear crystal at a different angle [144]. For example, some demonstrated OPA phase-matching geometries [144-148] allow positioning of pump beams symmetrically with respect to each other in a cone, with the cone apex constituting the intersection of all pump and idler beams and the single signal beam.

Such beam-combining OPCPA geometries permit use of either solid-state or fiber-laser pumps. Reaching 10 kW of OPCPA output power would require combining tens of solid-state laser pumps, while achieving joules of combined energy would require hundreds of fiber laser pumps.

Even though thermal loading of an OPCPA crystal is much smaller than that of a pumped energy-storage gain medium, when tens of kW of average pump power are applied to a nonlinear crystal, even a small amount of residual absorption could produce significant thermal effects, which could distort OPA output beam or degrade phase-matched pumping conditions. This thermal loading will depend on nonlinear-crystal losses at pump, signal and idler wavelengths. If all three wavelengths are well within the transparency range of a particular crystal, estimates show [148] that 10 kW of average power should be achievable with existing material choices.

#### **1.4.4.3 OPCPA for Laser Plasma Accelerator Applications**

Due to the above-described properties, high average power OPCPA becomes advantageous over other approaches when:

- Very short pulse durations (much shorter than 100 fs) are needed. Such pulse durations are difficult to reach with other high average power laser systems, due to the limited number of available broad-band material choices.
- Very high pre-pulse contrast is needed. OPCPA is clearly superior to other approaches in this regard.

Additionally, OPCPA offers the advantage of more flexibility in choosing an operating wavelength. Pump and signal wavelengths can in many cases be chosen by selecting a suitable phase-matching geometry with available nonlinear materials. This is a significant advantage for those laser-plasma acceleration applications that require longer operation wavelengths (e.g., 1-2  $\mu\text{m}$ ).

Therefore, as inspection of laser requirements presented in Table 25 reveals, these advantages and the principal limitation associated with relatively low plug-to-optical efficiency make high average power OPCPA best suited for (i) “intermediate” 1-GeV LPA sources operating at 1 kHz, (ii) FEL drivers, (iii) FEL seeders, and (iv) high-luminosity hard X-ray sources. Indeed, all these applications require approximately 10-fs to 30-fs pulses, with 1-3 J pulse energy, pre-pulse contrast of  $10^9$  to  $10^{10}$ , and repetition rates from 1 to 10 kHz. An exception is the parameter set for FEL seeders, which require somewhat longer pulses of <50 fs and lower energy of 1-10 mJ, but at much higher repetition rates of 100 kHz to 1 MHz. Most importantly, all these applications require average laser-driver power below 10 kW, and, therefore, overall power consumption of the system should be acceptable even at somewhat lower plug-to-optical efficiencies of >5%.

#### **1.4.4.4 OPCPA Development Roadmap**

Although single-laser pumped OPCPA has already reached the parameters required for the applications envisioned here in terms of pulse energies (>1 J), pulse durations (10-50 fs), and pre-pulse contrast (down to  $10^{10}$ ), but scaling of this approach to high average powers (and high repetition rates) requires significant further R&D. Primarily, this research has to explore beam-combining options as well as sustaining high average powers in nonlinear crystals. Note that OPA beam combining has been demonstrated

[142-146], but its scalability has not been explored yet. In more detail, the following general topics need to be addressed:

- Scalability of pump-beam numbers in various OPA beam-combining geometries. It is essential to explore the possible multiple-beam OPA pumping geometries and the maximum numbers of pump beams that can be accommodated in each phase-matching geometry. As part of this exploration, it is important to verify that broad gain bandwidths are compatible with these multiple-beam pumping approaches. It is also necessary to determine possible material as well as pump and signal wavelength choices, compatible with beam-combining geometries. It is also important to consider detrimental effects associated with parametric self-diffraction [148], which under certain conditions can cause degradation in OPA efficiency and output beam quality.
- Peak power scalability in beam-combined OPA. Combining multiple pump beams can result in unacceptably high peak intensities inside the nonlinear crystal, leading to optical damage. This could be addressed by simply increasing transverse size of pump and signal beams, but it is essential to determine whether this spot size scaling is compatible with various multiple-beam combining geometries.
- Average power handling of nonlinear crystals. Thermal loading of nonlinear materials will be the ultimate factor limiting achievable OPA output powers. It is essential to determine power scalability of each identified pump-combining geometry and material choice. Primarily this will be addressed by determining residual absorption at pump, signal and idler wavelengths, and by exploring thermal loading occurring due to this absorption at high optical powers.

## 1.4.5 CO<sub>2</sub> Laser Technology for Accelerator Applications

### 1.4.5.1 *Applications of CO<sub>2</sub> Laser Technology*

#### Medical Ion Therapy:

Using the radiation pressure acceleration (RPA) mechanism of generating proton beams from gas jet targets, CO<sub>2</sub> systems have already demonstrated the benefits of longer wavelength operation, specifically higher charge and operation at gas jet versus solid target densities. Parameters achieved at BNL experiments so far with an input laser of 5 J in 5 fs include a total of 10<sup>10</sup> protons with an energy of 5 MeV and 2-4% rms energy spread. Further scaling of proton energy, as well as using different gases for accelerating heavier ion species, would extend the method to the medically interesting regime for cancer treatment facilities. RPA appears to be well enough understood theoretically to attempt such experiments as soon as possible. Longer term studies aimed at increasing repetition rate and delivery methods for high-charge ion beams would be the final step before construction of an operating treatment center utilizing CO<sub>2</sub> lasers.

#### Moderate energy LPA electron source:

Because the critical plasma density for LPA is an order of magnitude lower at 10 μm than at near-IR wavelengths, applying a CO<sub>2</sub> system to laser wakefield acceleration corresponds to operation at a longer plasma wavelength. Furthermore, when operating

in the “bubble regime” where plasma electrons may be trapped and accelerated with small energy spread and emittance, the charge is proportional to the laser wavelength and square root of laser power. Therefore, a CO<sub>2</sub> laser at 10× longer wavelength is capable of accelerating the same charge per laser pulse as a near-IR system of 100× greater power. Furthermore, the range of densities over which the plasma bubble forms is very small for near-IR systems, making stability of the process a concern, while at 10 μm, stable operation should be much easier to achieve. However, accelerating gradient is lower; therefore use of a CO<sub>2</sub> laser is not applicable to machines designed to achieve very high energies. In smaller electron accelerators where higher charge and compact, reliable operation are important, CO<sub>2</sub> technology becomes very attractive.

#### Polarized Proton Source for Linear Collider:

Current designs for a polarized positron source at next generation linear colliders such as an ILC have very difficult requirements for the positron conversion targets. Mercury jets or other solid targets must dissipate significant energy from the incident electron beam of a few to several MeV, since only a small fraction of the incident energy is converted to positrons. Substituting a Compton backscatter gamma ray source and subsequent pair-production target relaxes the target constraints significantly. In order to provide laser-electron interactions at the repetition rate of a collider, regenerative cavities would be needed. Furthermore, multiple cavities and interaction points could be synchronized to achieve the required number of positrons. Such a regenerative cavity has already been demonstrated at BNL, producing a 3 μs long pulse train with a envelope flatness of 3% rms. Further tests are required to demonstrate stable temporal and spatial profiles of the circulating pulses.

#### Compact X-ray/gamma source:

Applying CO<sub>2</sub>-driven LPA as described above to generate the electrons that scatter photons in a Compton backscattering configuration results in a very compact and reliable system. The same laser may be used for both LPA electron and incident photon sources by splitting the laser output into two branches with equal path lengths. For a given laser power, the number of photons reaching the interaction point is 10× higher for CO<sub>2</sub> than for near-IR lasers, so once again CO<sub>2</sub> systems can produce results similar to those of solid-state lasers with much higher peak powers. Furthermore, the ability to focus a near-IR laser beam down to approximately 10× smaller spot size and consequently higher scattering yield is difficult to achieve in practice, since electron beam focusing rarely permits spot sizes of 1 μm in a typical interaction point geometry. Therefore, such a machine provides several practical benefits that fit well with the needs of a small facility for medical/industrial/scientific applications at medium repetition rates.

### ***1.4.5.2 Current State-of-the-Art, Challenges, Identifying Path of Technological Solution***

The two established short-pulse CO<sub>2</sub> laser systems operating at BNL and UCLA are somewhat different in design. The BNL-ATF final amplifier is capable of operation at higher pressure, with current pulse parameters of 5 J and 5 ps. Further improvements including shorter seed pulse and chirped pulse amplification (CPA) will increase power to greater than 10 TW in the next few years. The UCLA Neptune laser operates in a

regime in which power broadening of the gain spectrum allows direct amplification of 100-J, 3-ps pulses in the final amplifier.

Identifying technological breakthroughs needed

Further demonstration of optical pumping of a CO<sub>2</sub> laser at 2.9 μm using ErCr:GGG solid-state lasers may enable very high pressure amplifiers to operate at 20-25 bar at which the rotational lines fully overlap into a smooth gain spectrum adequate for sub-ps pulse amplification. Optical pumping also allows higher gain since a single vibrational band may be pumped, in contrast to the uniform pumping of all bands achieved with electric discharge pumping.

Identifying proof-of-principle experiments and validation modeling

CO<sub>2</sub> laser development has reached a level where the benefits to be realized from CPA should be demonstrated. As with solid-state systems, management of non-linear effects is critical to further advances in peak power. Furthermore, power (Stark) broadening of the rotational line structure, as utilized to amplify 3-ps pulses in the UCLA Neptune amplifier, should be further investigated through simulations.

Achievable key parameters:

- **Efficiency**  
Efficiency is inherently poor in current research lasers amplifying a single short pulse because the time scale for energy transfer into depleted rotational lines is very long relative to the pulse length. A train of pulses could increase extraction efficiency, as can regenerative amplifiers. The requirement for multiple pass energy extraction becomes more challenging in the final stage as the optical configuration becomes more complex and optical losses increase in either regenerative or multipass configuration, limiting efficiency. Present efficiency is  $\sim 2 \times 10^{-3}$  in a single pulse after several passes through the final stage amplifier.
- **Power/energy**  
Energy is primarily limited by the aperture of the pumped gain region between the discharge electrodes. Also, high gas pressure is required to pressure broaden the individual rotational lines into a continuous gain spectrum. However, increasing the gas pressure and aperture is not possible beyond current levels because a uniform electrical discharge is increasingly difficult to produce above approximately 10 cm aperture and 10 bar pressure. One possible technological solution to remove this limitation is to use electron beam or optical pumping. Recent work suggests that ErCr:YSGG lasers are good candidates for optical pumping. The challenge then essentially becomes one of efficient high-energy operation of the pump laser.
- **Pulse width**  
Sub-picosecond pulses require more sophisticated manipulation of the CO<sub>2</sub> gain medium such as gas mixtures utilizing both oxygen and carbon isotopes to provide additional bandwidth.

- **Beam quality**  
Gas lasers such as CO<sub>2</sub> systems suffer little beam distortion from thermal effects, and are capable of producing gaussian beam profiles independent of pumping level. Typical beam distortions arise from optical damage and can be managed by proper system design to achieve low M<sup>2</sup> values and near diffraction-limited focal spot sizes. As with all high power lasers, beam self focusing and breakup from accumulated non-linear phase shift must also be given careful consideration. Calculations of accumulated B-integral are necessary, as there exists a smaller selection of optical materials for fabricating active and passive optical components to optimize system performance.
- **Cost estimate of a system designed for each particular application**  
The basic pressure vessel plus associated gas handling hardware, HV generator and electrical equipment to achieve several joules of output is clearly a function of the design. Using a single seed laser for multiple amplifiers can reduce unit cost considerably. Overall system cost of around \$1M is approximately ~30-50% seed laser system and the remainder for amplifier stages and optics. Final-stage, large-aperture amplifiers constructed in significant quantities could in principle cost as little as \$200-\$300k each, which is very comparable to solid-state technology. However, the market is not yet large enough to support any mass production, so it is difficult to predict actual future costs.

*Timeline / milestones for the roadmap*

- Within two years, demonstrate scaling of peak power via CPA.
- Within two years, validate RPA scaling to 250 MeV ion energy for medical applications.
- Within five years, extend peak power to the 100-300TW level useful for a compact gamma source.

## 1.4.6 Facility Class Lasers for Particle Accelerator Applications

### 1.4.6.1 Introduction and State-of-the-Art

“Facility Class” lasers are laser systems that require their own building or facility and a dedicated team of scientists, engineers and technicians. Examples of the more well known of these lasers are the National Ignition Facility (NIF) at Lawrence Livermore National Laboratory, the Omega Laser and Omega EP at the Laboratory for Laser Energetics, and Laser Mégajoule in Bordeaux, France. A more complete and up-to-date list of facilities can be found at the ICUIL website [149]. Beamlines of these lasers systems typically produce hundreds of joules at over 20 kJ of pulse energy, and by direct chirped pulse amplification achieve pulse widths as short as 1 ps, while laser pumped laser systems, OPCPA, and Ti:Sapphire can attain much shorter pulse widths. While these lasers are awe-inspiring in their pulse energy and peak power, they are typically very limited in repetition rate, with the majority firing shots once every few hours. The fastest repetition rates for these high-energy systems may reach 10 Hz, but this is not common at present.

The large apertures of these systems lead to beams that are not diffraction limited. In practice the beams are often spatially sculpted to be flat tops, with a goal of achieving a flat phase front with minimal contrast (high-frequency spatial noise) at the system output. When focused, most of the energy from a shot of a well engineered system will typically fall within an circle a few times bigger than the diffraction limit, with significant hot-spots that change location from shot to shot within this circle. Due to the long time between shots and scale of the typical facility, significant pointing jitter can increase the expected spot size further if one considers a spot as the range of spatial points the laser pulse might strike. Finally, to attain energies higher than 10-20 kJ per pulse, these lasers typically incoherently combine the output of multiple beam lines via spatial multiplexing, leading to even larger spot sizes.

To date, the majority of these systems have been flash-lamp pumped lasers based upon neodymium-doped phosphate laser glass. Cost constraints have traditionally driven the choice of flash-lamp pumping, and this in turn drives the choice of neodymium-doped phosphate glass. The high heat load from the flash-lamp pumping process has been one of the major repetition rate limiters. This process also tends to have very poor system efficiency. However, for the experiments performed at these facilities, this has not been a concern.

The primary R&D focus for these systems is the cost-effective conversion of the pump source from flash-lamps to diode lasers. This is needed in order to significantly increase the repetition rate (typical goals are of order 10 Hz) and correspondingly increase the efficiency of the system. The latter will be required to minimize the operating cost of the facility once the repetition rate and thus the average power increases significantly.

The most advanced demonstration of this type of laser completed to date is the Mercury laser system at Lawrence Livermore National Laboratory [150]. This diode pumped solid state laser system produced peak energy of 60 J at 10 Hz and 1047 nm, and 32 J at 523.5 nm in 10 ns pulses at a nominal electrical-to-optical efficiency of 5%. This system was based upon ytterbium doped SFAP crystals as the gain media, and employed a novel laser architecture with high speed flow of turbulent helium over the face of the crystals to remove excess heat from the laser gain medium with minimal distortion of the beam wave front. As a result the Mercury laser is able to attain a beam quality that is less than  $5\times$  the diffraction limit. A proposed follow-on (which remains uncompleted due to lack of funding) would employ the Mercury laser to pump a Ti:Sapphire laser system capable of attaining petawatt peak pulses (15 J, 15 fs) with sufficient beam quality to attain focused spots with  $10^{23}\text{W}/\text{cm}^2$  intensity at 10 Hz, showing the extreme optical power densities attainable with a facility-class laser [151].

Building on the Mercury laser technology, LLNL is currently designing a diode-pumped successor to the NIF laser capable of operating at 16 Hz [152]. Laser for Inertial Fusion Energy (LIFE) utilizes beamlines each capable of producing 8.1 kJ laser pulses at 1053 nm, with a few-nanosecond pulse duration, at 18% electrical efficiency. The design size for a single beam line is  $1.35 \times 2.2 \times 10.5$  m. Currently LIFE designs, planning, and detailed R&D roadmaps are being developed at LLNL under internal laboratory-directed funding. Execution of these plans and actual construction of a LIFE laser beam line is awaiting funding. Once complete, such a laser would make an excellent pump laser for femtosecond OPCPA or Ti:sapphire laser systems or, through direct CPA, to a picosecond laser system. In either case, conversion of the long pulse laser to a short pulse system results in a significant pulse energy reduction (3-10 $\times$ ).

### 1.4.6.2 R&D Challenges

The LIFE laser development program (when funded) will address most of the critical R&D issues for this type of facility-class laser for the next 10 years. These R&D issues include: cost and availability of pump diode lasers and diode laser drivers; thermal management of the laser gain media to minimize impact on beam quality; minimizing system footprint (a major facility cost driver); high-energy repetition-rated Pockels cells; and demonstration of a complete operational beam line. Converting a LIFE laser into a short pulse laser system (as required for most particle accelerator applications) would require additional R&D beyond the LIFE laser system. Once complete, lessons learned from the LIFE laser beam line development program may be employed to develop laser systems with several times more energy and/or average power.

Diode Laser R&D Challenges: Facility-class lasers will employ diode lasers that operate in a pulsed mode at low repetition rate. The technical viability of these diode lasers has been shown through the Mercury laser program (even-more-advanced diode laser technology is available today). However, a facility-class laser will require so many of these diode lasers that their cost will drive the cost of the facility. Thus reducing the diode laser cost to an acceptable level is a critical technical challenge to be overcome. This is believed to be an attainable goal and the diode laser community and LLNL have jointly authored a publication [153] detailing how the cost goals might be achieved.

Laser Architecture R&D Challenges: The two key challenges for the laser architecture are how to minimize the laser footprint (a facility cost driver) and how to extract enough heat from the laser gain medium to prevent beam quality degradation. Laser footprint is driven in large part by the size of the spatial filters between gain stages. Thus the ability to make more compact spatial filters is key to a reduced system footprint. Aggressive cooling such as that demonstrated in the Mercury laser system can minimize thermal impacts, but choice of gain media and system architecture to minimize or eliminate thermal degradation of the laser beam are also critical to overall system performance. There may be a number of approaches to this problem worth considering.

High Energy Repetition Rated Pockels Cells: In large aperture facility class laser systems a laser pulse typically passes through the gain media multiple times. This both increases the effective gain of the system (which is critical, given the large pulse energies involved) and provides for efficient conversion of pump power to laser power by ensuring all possible laser energy is extracted from the gain media. Furthermore, to minimize diode laser cost by minimizing total required diode laser power, the diode laser pump is typically run for the full upper-state lifetime of the gain media. To prevent loss of laser energy through parasitic lasing and to enable multiple passes through the gain media, Pockels cell switches are required. Development of large aperture Pockels cells capable of operating at 10-20 Hz repetition rates or higher is thus a key technology goal.

Demonstration of a Complete Beam Line: Many lessons were learned in the construction of the Mercury laser system. However, any future facility based upon high-energy, high-repetition-rate laser systems would need to first construct a single laser beam line in order to validate the proposed technology operates as designed and to

work out any issues that may arise in the laser system. Thus the demonstration of a complete beam line is a critical final step in any realistic development plan.

*Technology for Short Pulses:* A diode pumped high energy, facility class laser typically is designed to operate in the few nanosecond pulse width regime. Short pulses, down to a few hundred fs, may be possible via direct application of CPA to the laser system. Typically grating damage thresholds and other laser design considerations result in significant reduction of output pulse energy in performing this operation. Further development of large-aperture, high-damage-threshold dielectric gratings would be beneficial to this goal. Shorter pulse widths (less than 100 fs) may be attainable with a facility-class laser via two additional R&D paths. First, one might consider the design and development of Ti:Sapphire laser technology utilizing the frequency doubled output of the facility class laser as a pump laser system would also be a viable R&D path. Second, it is conceivable that a facility-class laser could be employed as a pump laser for an OPCPA system in order to attain sub-100-fs pulse widths.

#### **1.4.6.3 Summary and Applicability to Particle Acceleration**

A review of the requirements for the various accelerator applications suggest that facility-class laser technology may be useful for some gamma-gamma collider applications, medical laser applications and possibly some proposed laser wakefield accelerator schemes based upon high pulse energy, lower repetition rates (tens to hundreds of Hz). In the LPA case, a Ti:Sapphire laser intermediary would be required, which would severely limit efficiency of the overall system. The best match of requirements and technology for facility-class lasers is likely in the medical laser applications. However, it should be noted that the system described here are fundamentally diode-pumped solid-state lasers, so lessons learned in developing these systems may be applicable to high repetition rate systems with more-modest pulse energy (<100 J).

There exist several proposals for accelerators, which operate in excess of 1 kHz (Table 25). At these frequencies, the diode technology changes from pulsed format to CW format, with a driver cost that is roughly 10× higher than that of pulsed diode systems due to necessarily lower power per bar as well as microchannel packaging required for thermal management. Likewise, thermal management of the gain media and of all laser hardware becomes paramount. Material selection will be limited to robust materials with high thermal conductivity and fracture toughness. While the diodes in this situation can be long lived, the solid state laser system is still subject to a pulsed energy threat. Where possible, the peak power on the optics needs to be limited to below GW levels, where long term degradation would probably occur at these very high repetition rates.

For example if we assume that an LIFE-like laser system is capable of 30 gigashots before optics need to be replaced (~60 yrs at 16 Hz), then at 1 kHz, the replacement time is 1 yr, and at 15 kHz only 23 days. With these statistics in mind, laser designers for these accelerators will need to make an effort to format pulses to mitigate peak power on optics and choose gain media with low saturation cross sections. Large optics will need to be utilized to spread the power load on CPA components like gratings that are very temperature sensitive. Therefore, accelerators requiring high energy (> 10 J) and high repetition rate (> 100 Hz) will require extensive design to achieve efficiency, thermal robustness, and longevity.

For lasers with repetition rates slower than hundreds of Hz, the development of a LIFE or similar laser system would be complementary to many laser based particle accelerator needs. R&D specific to converting such a LIFE-like laser system to short pulse capability would still be required, in order to enable use of these systems in particle accelerator applications. This latter R&D may need to be directly funded by the particle accelerator community, as this development is not within the known scope of an existing facility.

## 1.5 References

1. W.P. Leemans and E. Esarey, *Physics Today* **62**, 44 (2009).
2. T. Tajima and J.M. Dawson, *Phys. Rev. Lett.* **43**, 267 (1979).
3. E. Esarey, C.B., Schroeder, W.P. Leemans, *Rev. Modern Phys.* **81**, 1229 (2009).
4. W.P. Leemans *et al.*, *Nature Physics* **2**, 696 (2006).
5. C.B. Schroeder, E. Esarey, C.G.R. Geddes, C. Benedetti, and W.P. Leemans, *Phys. Rev. ST Accel. Beams* **13**, 101301 (2010).
6. A. Pukhov and J. Meyer-ter-Vehn, *Appl. Phys.* **B 74**, 355 (2002).
7. W. Lu *et al.*, *Phys. Rev. ST Accel. Beams* **10**, 061301 (2007).
8. K. Nakajima *et al.*, *Phys. Rev. ST Accel. Beams* **10**, 061301 (2007).
9. T. Tajima and A. Chao, private communication; H. C. Wu, T. Tajima, D. Habs, A. Chao, J. Meyer-ter-Vehn, *Phys. Rev. ST Accel. Beams* **13**, 101303 (2010).
10. M. Rosing and W. Gai. Longitudinal and transverse wake field effects in dielectric structures. *Phys. Rev. D*, 42:1829–1834 (1990).
11. A. Mizrahi and L. Schachter. Optical Bragg accelerators. *Phys. Rev. E*, 70:016505 (2004).
12. X. E. Lin. Photonic band gap fiber accelerator. *Phys. Rev. ST-AB*, 4:051301 (2001).
13. R. H. Siemann. Energy efficiency of laser driven, structure based accelerators. *Phys. Rev. ST-AB*, 7:061303 (2004).
14. P. Bermel, R. Byer, B. Cowan, J. Dawson, R. J. England, R. Noble, M. Qi, R. Yoder, *et al.* *Proceedings of the ICFA Mini-Workshop on Dielectric Laser Acceleration*, Menlo Park, CA (2011).
15. K. Soong, R. L. Byer, C. McGuinness, E. Peralta, E. Colby, "Experimental Determination of Damage Threshold Characteristics of IR Compatible Optical Materials," *Proceedings of the 2011 Particle Accelerator Conference*, New York, NY (2011).
16. R. J. England, *et al.* "Experiment to Demonstrate Acceleration in Optical Photonic Bandgap Structures," *Proceedings of the 2011 Particle Accelerator Conference*, New York, NY (2011).
17. ATLAS Collaboration, "Performance of the ATLAS Trigger System in 2010", CERN-PH-EP-2011-078 (2011).
18. A. Chao, *Physics of Collective Beam Instabilities in High Energy Accelerators*, John Wiley&Sons (1993).
19. Z. Wu, C. Ng, C. McGuinness, E. Colby, "Design of On-Chip Power Transport and Coupling Components for a Silicon Woodpile Accelerator," *Proceedings of the 2011 Particle Accelerator Conference*, New York, NY (2011).
20. E. R. Colby, R. J. England, R. J. Noble, "A Laser-Driven Linear Collider: Sample Machine Parameters and Configuration," *Proceedings of the 2011 Particle Accelerator Conference*, New York, NY (2011).
21. R. H. Siemann, "Energy efficiency of laser driven, structure based accelerators," *Phys. Rev. ST-AB* **7**, 061303 (2004).

22. S. M. S. Sears, et al., "Production and characterization of attosecond electron bunch trains," *Phys. Rev. ST-AB* **11**, 061301 (2008).
23. P. Hommelhoff, et al., "Field Emission Tip as a Nanometer Source of Free Electron Femtosecond Pulses," *Phys. Rev. Lett.* **96**, 077401 (2006).
24. Private communication.
25. RDR, <http://www.linearcollider.org/about/Publications/Reference-Design-Report>
26. D. Asner *et al.*, "Higgs physics with a  $\gamma\gamma$  collider based on CLIC 1", *Eur. Phys. J. C* **28**, 27–44 (2003).
27. R. Tomas, "Overview of the Compact Linear Collider", *Phys. Rev. ST Accel. Beams* **13**, 014801 (2010). Two parameter sets for  $E_{CM} = 0.5$  and 3 TeV are given. Here, the former is used.
28. Private communication.
29. For example, E. Saldin *et al.*, Proc. PAC2009, Vancouver, BC, Canada, WE6PFP083.
30. For example, G. Klemz *et al.*, "Design study of an optical cavity for a future photon collider at ILC", *Nucl. Instr. Meth. A* **564**, 212 (2006).
31. J. Urakawa, "Development of a compact x-ray source based on Compton scattering using 1.3 GHz superconducting RF accelerating linac and a new laser storage cavity", submitted to *Nucl. Instr. Meth. A*.
32. W. Sandner, private communication.
33. O. Brüning (ed.) et al, "LHC Design Report". CERN-2004-003-V-1.
34. C. Adolphsen et al., "A Large Hadron Electron Collider at CERN – Report on the Physics and Design Concepts for Machine and Detector". CERN-LHeC-Note-2011-003 GEN.
35. EuroNNAc workshop, CERN, Switzerland, 3 – 6 May, 2011: <http://indico.cern.ch/event/EuroNNAc>
36. W.P. Leemans *et al.*, "The Berkeley Lab Laser Accelerator (BELLA): A 10-GeV laser plasma accelerator," Proc. 14th Advanced Accelerator Concepts Workshop, Annapolis, Maryland, 13-19 Jun 2010. Published in AIP Conf.Proc.1299:3-11,2010.
37. F. L. Zheng et al., *Euro. Phys. Lett.* **95**, 55005 (2011).
38. F. L. Zheng et al., "Generating sub-TeV quasi-monoenergetic proton beam by an ultra-relativistically intense laser in the snowplow regime," arXiv:1101.2350v2 [physics.plasm-ph] 17 Jan 2011.
39. X. Q. Yan et al., *Phys. Rev. Lett.* **103**, 135001 (2009).
40. A. Henig et al., *Phys. Rev. Lett.* **103**, 245003 (2009); B. Aurand *et al.*, to be published.
41. H. A. Bethe and E. E. Salpeter, *Quantum Mechanics of One- and Two-Electron Atoms*, pp 295-322, Springer-Verlag (1957).
42. A. N. Grum-Grzhimailo et al., *Phys. Rev. A* **81**, 043408 (2010).
43. S. Borbély et al., *Phys. Rev. A* **77**, 033412 (2008).
44. S. Geltman, *J. Phys. B: At. Mol. Opt. Phys.* **33**, 1967 (2000).
45. J. Bauer et al., *J. Phys. B: At. Mol. Opt. Phys.* **34**, 2245 (2001).
46. G. A. Kyrala and T. D. Nichols, *Phys. Rev. A* **44**, R1450–R1453 (1991).
47. P. Zeitoun, M. Fajardo, and G. Lambert, "Coherent and compact", *Nature Photonics* **4**, 739 (2010).
48. S. Schulz et al., "All-optical synchronization of distributed laser systems at Flash", in Proceedings of PAC 2009, number TH6REP091, page 4174, Vancouver (Canada), 2009.
49. E. Saldin, E. Schneidmiller, Yu. Shvyd'ko and M. Yurkov, *NIM A* **475**, 357 (2001).
50. G. Geloni, V. Kocharyan and E. Saldin, "Scheme for generation of highly monochromatic X-rays from a baseline XFEL undulator", DESY 10-033 (2010).
51. G. Lambert et al., "Injection of harmonics generated in gas in a free-electron laser providing intense and coherent extreme ultraviolet light", *Nature Physics* **4**, 296 (2008).
52. D. Ratner, A. Chao and Z. Huang, "Two-chicane compressed harmonic generation of soft x rays", *Phys. Rev. ST AB* **14**, 020701 (2011).

53. L.-H. Yu et al., “High-Gain Harmonic-Generation Free-Electron Laser”, *Science* **289**, 932 (2000).
54. G. Stupakov et al., “Using the beam-echo effect for generation of short-wavelength radiation”, *Phys. Rev. Lett.* **102**, 074801 (2009).
55. P. Schmüser, M. Dohlus and J. Rossbach, *Ultraviolet and Soft X-Ray Free-Electron Lasers*, Springer Verlag, 2008.
56. E. L. Saldin, E. A. Schneidmiller, and M. V. Yurkov, “Study of noise degradation of amplification process in a multistage HGHG FEL,” *Optics Comm.* **202**, 169 (2002).
57. L. Giannessi, “Harmonic generation and linewidth narrowing in seeded FELs,” in *Proceedings of the 2004 FEL Conference*, 37 (2004).
58. G. Stupakov, “Noise amplification in HGHG seeding,” and G. Stupakov, Z. Huang, and D. Ratner, “Noise amplification in echo-enabled harmonic generation (EEHG),” in *Proceedings of the 2010 FEL Conference* (2010).
59. G. Geloni, V. Kocharyn, and E. Saldin, “Analytic studies of constraints on the performance for EEHG FEL seed lasers”, DESY 11-200 (2011).
60. N. Yampolsky, “Description of modulated beam dynamics,” in preparation (2011).
61. A. McPherson et al., “Studies of multiphoton production of vacuum-ultraviolet radiation in the rare Gases”, *JOSA B* **4**, 595 (1987).
62. X.F. Li, A. L’Huillier, M. Ferray, L.A. Lompre, and G. Mainfray, “Multiple-harmonic generation in rare gases at high laser intensity” *Phys. Rev. A* **39**, 5751 (1989).
63. J. Rothhardt et al., “High average and peak power few-cycle laser pulses delivered by fiber pumped OPCPA system”, *Opt. Express* **18**, 12719 (2010).
64. A. Willner et al., “A new XUV-source for seeding a FEL at high repetition rates”, in *Proceedings of SPIE Optics + Optoelectronics*, Paper 8075-20, Prague (2011).
65. J. Pupeza et al., “Power scaling of a high-repetition-rate enhancement cavity”, *Opt. Lett.* **35**, 2052-2054 (2010).
66. F. Albert et al., “Isotope-specific detection of low-density materials with laser-based monoenergetic gamma-rays”, *Optics Letters* **35**, 354 (2010).
67. J. Meyer-ter-Vehn and H.-C. Wu. *Eur. Phys. J. D* **55**, 433 (2009).
68. H.-C. Wu, J. Meyer-ter-Vehn, J. Fernandez, B.M. Hegelich, “Uniform Laser-Driven Relativistic Electron Layer for Coherent Thomson Scattering”, *Phys. Rev. Lett.* **104**, 234801 (2010).
69. H. Eickhoff and U. Linz, *Reviews of Accelerator Science and Technology* **1**, 143 (2008).
70. W.T. Chu et al., *Rev. Sci. Instrum.* **64**, 2055 (1993).
71. Y. Hirao et al., *Nucl. Phys. A* **538**, 541c (1992).
72. T. Haberer et al., *Radiother. Onc.* **73**, 186 (2004).
73. S. V. Bulanov and V. S. Khoroshkov, *Plasma Phys. Rep.* **28**, 453 (2002).
74. T. Tajima, D. Habs and X. Yan, *Reviews of Accelerator Science and Technology* **2**, 201 (2009).
75. M. Borghesi, J. Fuchs, S. V. Bulanov, A. J. Mackinnon, P. K. Patel and M. Roth, *Fusion Sci. Technol.* **49**, 412 (2006).
76. S. C. Wilks et al., *Phys. Plasmas* **8**, 542 (2001).
77. R.A. Snavely et al. *Phys. Rev. Lett.* **85**, 2945 (2000).
78. T. Esirkepov, M. Borghesi, S. V. Bulanov, G. Mourou and T. Tajima, *Phys. Rev. Lett.* **92**, 175003 (2004).
79. S. Steinke et al., *Phys. Rev. Lett.* **105**, 215001 (2010).
80. A. Henig et al. *Phys. Rev. Lett.* **103**, 245003 (2009).
81. I. Hofmann, J. Meyer-ter-Vehn, X. Yan, A. Orzhekovskaya and S. Yaramishev, *Phys. Rev. ST-AB* **14**, 031304 (2011).
82. L. Yin et al., *Phys. Plasmas* **14**, 056706 (2007).
83. B. J. Albright et al., *Phys. Plasmas* **14**, 094502 (2007).

84. M. Hegelich, presented at 53rd annual meeting of the APS Division of Plasmas, Vol. **16**, No. 16 (2011).
85. S. S. Bulanov et al., *Med. Phys.* **35**, 1770 (2008); S. S. Bulanov, et al., *Phys. Rev. E* **78**, 026412 (2008).
86. D. Haberberger et al., *Opt. Exp.* **18**, 17865 (2010).
87. D. Haberberger et al., *Nature Physics* **7**, 2130 (2011).
88. V. Malka et al., *Nature Physics* **4** (2008).
89. Fuchs et al., *Phys. Med. Biol.* **54**, 3315-3328 (2009).
90. R.J. Mears, L. Reekie, I.M. Jauncey and D.N. Payne, "Low noise erbium doped fiber amplifier operating at 1.54  $\mu\text{m}$ ," *Electronics Letters*, vol. **23**, pp. 1026-1027 (1987).
91. B.J. Ainslie, S.P. Craig and S.T. Davey, "The absorption and fluorescence spectra of rare earth ions in silica based monomode fiber," *Journal of Lightwave Technology*, vol. **6**, pp. 287-293 (1988).
92. H.M. Pask, R.J. Carman, D.C. Hanna, A.C. Tropper, C.J. Mackechnie, P.R. Barber and J.M. Dawes, "Ytterbium-doped silica fiber lasers: versatile sources for the 1-1.2 $\mu\text{m}$  region," *IEEE Journal of Selected Topics in Quantum Electronics*, vol. **1**, pp. 2-13 (1995).
93. S.L. Yellen, A.H. Sheppard, R.J. Dalby, J.A. Baumann, H.B. Serreze, T.S. Guido, R. Soltz, K.J. Bystrom, C.M. Harding and R.G. Waters, "Reliability of GaAs-based semiconductor diode lasers:0.6-1.1 $\mu\text{m}$ ," *IEEE Journal of Quantum Electronics*, vol. **29**, pp. 2058-2067, (1993).
94. P. Leisher, M. Reynolds, A. Brown, K. Kennedy, L. Bao, J. Wang, M. Grimshaw, M. DeVito, S. Karlsen, J. Small, C. Erbert, R. Martinsen and J. Haden, "Reliability of high power diode laser systems based on single emitters," *Proceedings of the SPIE*, vol. 7918, pp. 791802-1-7 (2011).
95. T. Koenning, K. Alegria, Z. Wang, A. Segref, D. Stapleton, W. Fassbender, M. Flament, K. Rotter, A. Noeske and J. Biesenbach, "Macro-channel cooled, high power, fiber coupled diode lasers exceeding 1.2kW of output power," *Proceedings of the SPIE*, vol. **7918**, pp. 79180E-1-8 (2011).
96. V. Gapontsev, V. Fomin and A. Yusim, "Recent progress in scaling of high-power fiber lasers at IPG Photonics," *22nd Solid State and Diode Laser Technology Review Technical Digest*, 29 June-2 July, 2009, pp. 142 (2009).
97. G.D. Goodno, L.D. Book and J.E. Rothenberg, "Low-phase-noise, single frequency, single-mode 608W thulium fiber amplifier," *Optics Letters*, vol. **34**, pp. 1204-1206 (2009).
98. D.J. Richardson, J. Nilsson and W.A. Clarkson, "High power fiber lasers: current status and future perspectives [Invited]," *Journal of the Optical Society of America B*, vol. **27**, pp. B63-B92 (2010).
99. M.Y. Cheng, Y.C. Chang, A. Galvanauskas, P. Mamidpudi, R. Changkakoti and P. Gatchell, "High-energy and high-peak-power nanosecond pulse generation with beam quality control in 200- $\mu\text{m}$  core highly multimode Yb-doped fiber amplifiers," *Optics Letters*, vol. **30**, pp. 358-360 (2005).
100. F. Di Teodoro, M.J. Hemmat, J. Morais and E.C. Cheung, "High peak power operation of a 100 $\mu\text{m}$  core, Yb-doped rod type photonic crystal fiber amplifier," *Fiber Lasers VII: Technology, Systems, and Applications*, Proc. SPIE, vol. **7580**, pp. 758006 (2010).
101. See product sheet DC-200/40-PZ-Yb-03 at <http://www.nktphotonics.com/dcfibers?cid=5215>
102. A. Galvanauskas, report at 2nd Joint ICFA-ICUIL Workshop on "High Power Laser Technology for Future Accelerators," September 20-22, 2011.
103. Raydiance (<http://www.raydiance.com/>), IMRA (<http://www.imra.com/>), Calmar (<http://www.calmarlaser.com/>), Polar Onyx (<http://www.polaronyx.com/>), Fianium (<http://www.fianium.com/>), Active Fiber Systems (<http://www.afs-jena.de/>)

104. A. Galvanauskas, Z. Sartania and M. Bischoff, "Millijoule femtosecond all-fiber system," CLEO 2001, paper CMA1, 2001).
105. T. Eidam, J. Rothhardt, F. Stutzki, F. Jansen, S. Hadrich, H. Carstens, C. Jauregui, J. Limpert and A. Tunnermann, "Fiber chirped-pulse amplification system emitting 3.8GW peak power," *Optics Express*, vol. **19**, pp. 255 (2011).
106. Y. Zaouter, D.N. Papadopoulos, M. Hanna, J. Boulet, L. Huang, C. Agueraray, F. Druon, E. Mottay, P. Georges and E. Cormier, "Stretcher-free high energy nonlinear amplification of femtosecond pulses in rod-type fibers," *Optics Letters*, vol. **33**, pp. 107-110 (2008).
107. J.W. Dawson, M.J. Messerly, H.H. Phan, J.K. Crane, R.J. Beach, C.W. Siders and C.P.J. Barty, "High-energy, short-pulse fiber injection lasers at Lawrence Livermore National Laboratory," *IEEE Journal of Selected Topics in Quantum Electronics*, vol. **15**, pp. 207-219 (2009).
108. M. Rever, S. Huang, . Yabus, V. Smirnov, E. Rotari, I. Cohanoshi, S. Mokhov, L. Glebov and A. Galvanauskas, "200 fs, 50W fiber-CPA system based on chirped volume Bragg gratings," CLEO/IQEC (2009).
109. V. A. Kozlov, J. Hernández-Cordero, and T. F. Morse, "All-fiber coherent beam combining of fiber lasers," *Opt. Lett.* **24**, 1814-1816 (1999).
110. T. M. Shay, J. T. Baker, A. D. Sancheza, C. A. Robin, C. L. Vergien, A. Flores, C. Zerinque, D. Gallant, C. A. Lu, B. Pulford, T. J. Bronder, and A. Lucero, "Phasing of High Power Fiber Amplifier Arrays," in *Advanced Solid-State Photonics*, OSA Technical Digest Series (CD) (Optical Society of America, 2010), paper AMA1.
111. Eric C. Cheung, James G. Ho, Gregory D. Goodno, Robert R. Rice, Josh Rothenberg, Peter Thielen, Mark Weber, and Michael Wickham, "Diffractive-optics-based beam combination of a phase-locked fiber laser array," *Opt. Lett.* **33**, 354-356 (2008).
112. Radoslaw Uberna, Andrew Bratcher, Thomas G. Alley, Anthony D. Sanchez, Angel S. Flores, and Benjamin Pulford, "Coherent combination of high power fiber amplifiers in a two-dimensional re-imaging waveguide," *Opt. Express* **18**, 13547-13553 (2010).
113. S. J. Augst, A. K. Goyal, R. L. Aggarwal, T. Y. Fan, and A. Sanchez, "Wavelength beam combining of ytterbium fiber lasers," *Opt. Lett.* **28**, 331-333 (2003).
114. Igor V. Ciapurin, Leonid B. Glebov, Larissa N. Glebova, Vadim I. Smirnov, and Eugeniu V. Rotari, "Incoherent combining of 100-W Yb-fiber laser beams by PTR Bragg grating," *Proc. SPIE*, Vol. **4974**, 209 (2003).
115. K. Regelskis, K. Hou, G. Raciukaitis, and A. Galvanauskas, "Spatial-Dispersion-Free Spectral Beam Combining of High Power Pulsed Yb-Doped Fiber Lasers," in *Conference on Lasers and Electro-Optics/Quantum Electronics and Laser Science Conference and Photonic Applications Systems Technologies*, OSA Technical Digest (CD) (Optical Society of America, 2008), paper CMA4.
116. Armen Seviaan, Oleksiy Andrusyak, Igor Ciapurin, Vadim Smirnov, George Venus, and Leonid Glebov, "Efficient power scaling of laser radiation by spectral beam combining," *Opt. Lett.* **33**, 384-386 (2008).
117. C. Wirth, O. Schmidt, I. Tsybin, T. Schreiber, T. Peschel, F. Brückner, T. Clausnitzer, J. Limpert, R. Eberhardt, A. Tünnermann, M. Gowin, E. ten Have, K. Ludewigt, and M. Jung, "2 kW incoherent beam combining of four narrow-linewidth photonic crystal fiber amplifiers," *Opt. Express* **17**, 1178-1183 (2009).
118. G. Mourou, private communication.
119. L. Siiman, T. Zhou, W.Z. Chang and A. Galvanauskas, "Femtosecond pulses from coherently combined parallel chirped pulse fiber amplifiers," CLEO 2011 (2011).
120. L. Daniault, M. Hanna, L. Lombard, Y. Zaouter, E. Motlay, D. Goular, P. Bourdon, F. Druon and P. Georges, "Coherent beam combining of two femtosecond fiber chirped-pulse amplifiers," *Optics Letters*, vol. **36**, pp. 621-623 (2011).

121. E. Seise, A. Klenke, S. Breikopf, J. Limpert and A. Tünnermann, "88 W, 0.5 mJ femtosecond laser pulses from two coherently combined fiber amplifiers," *Optics Letters*, vol. **36**, pp. 3858-3860 (2011).
122. L. Daniault, M. Hanna, D.N. Papadopoulos, Y. Zaouter, E. Mottay, F. Druon and P. Georges, "Passive coherent beam combining of two femtosecond fiber chirped-pulse amplifiers," *Optics Letters*, vol. **36**, pp. 4023-4025 (2011).
123. A. Klene, S. Demmler, J. Rothardt, E. Seise, S. Breikopf, J. Limpert and A. Tünnermann, "Coherently-combined two channel femtosecond fiber CPA system producing 3mJ pulse energy," accepted by *Optics Express* (ID: 153561).
124. A. Dubietis et al., "Powerful femtosecond pulse generation by chirped and stretched pulse parametric amplification in BBO crystal", *Opt. Commun.* **88**, 433 (1992).
125. I. N. Ross et al., "The prospects for ultrashort pulse duration and ultrahigh intensity using optical parametric chirped pulse amplifiers", *Opt. Commun.* **144**, 125 (1997).
126. James R. Leger, Gary J. Swanson, and Wilfrid B. Veldkamp, "Coherent laser addition using binary phase gratings," *Appl. Opt.* **26**, 4391-4399 (1987).
127. Shu-Wei Huang, Giovanni Cirmi, Jeffrey Moses, Kyung-Han Hong, Siddharth Bhardwaj, Jonathan R. Birge, Li-Jin Chen, Enbang Li, Benjamin J. Eggleton, Giulio Cerullo, and Franz X. Kärtner, "High-energy pulse synthesis with sub-cycle waveform control for strong-field physics", *Nature Photonics* **5**, 475-479 (2011).
128. Wei-Zung Chang, Tong Zhou, Leo A. Siiman, and Almantas Galvanauskas, "Femtosecond pulse coherent combining and spectral synthesis using four parallel chirped pulse fiber amplifiers", *Advanced Solid State Photonics*, San Diego, Jan 29 – Feb 1, 2012.
129. I. N. Ross et al., "The prospects for ultrashort pulse duration and ultrahigh intensity using optical parametric chirped pulse amplifiers", *Opt. Commun.* **144**, 125 (1997).
130. X. Yang et al., "Multiterawatt laser system based on optical parametric chirped pulse amplification", *Opt. Lett.* **27** (13), 1135 (2002).
131. Y. Kitagawa et al., "Prepulse-free petawatt laser for a fast ignitor", *IEEE J. Quantum Electron.* **40** (3), 281 (2004).
132. C. N. Danson et al., "Vulcan petawatt: design, operation, and interactions at  $5 \times 10^{20}$  Wcm<sup>-2</sup>", *Laser Part. Beams* **23**, 87 (2005).
133. L. J. Waxer et al., "High-energy petawatt capability for the Omega laser", *Opt. Photon. News* **16** (7), 30 (2005).
134. V. V. Lozhkarev et al., "200 TW 45 fs laser based on optical parametric chirped pulse amplification", *Opt. Express* **14** (1), 446 (2006).
135. A. Dubietis, R. Butkus, and A. P. Piskarskas, "Trends in chirped pulse optical parametric amplification", *IEEE J. Sel. Top. Quantum Electron.* **12** (2), 163 (2006).
136. F. Tavella et al., "Dispersion management for a sub-10-fs, 10 TW optical parametric chirped-pulse amplifier", *Opt. Lett.* **32** (15), 2227 (2007).
137. S. Adachi et al., "5-fs, multi-mJ, CEP-locked parametric chirped-pulse amplifier pumped by a 450-nm source at 1 kHz", *Opt. Express* **16** (19), 14341 (2008).
138. S. Witte et al., "Generation of few-cycle terawatt light pulses using optical parametric chirped pulse amplification", *Opt. Express* **13** (13), 4903 (2005).
139. V. Bagnoud et al., "High-dynamic-range temporal measurements of short pulses amplified by OPCPA", *Opt. Express* **15** (9), 5504 (2007).
140. H. Kiriyama et al., "Prepulse-free, multi-terawatt, sub-30-fs laser system", *Opt. Express* **14** (1), 438 (2005).
141. L. J. Waxer et al., "High-conversion-efficiency optical parametric chirped-pulse amplification system using spatiotemporally shaped pump pulses", *Opt. Lett.* **28** (14), 1245 (2003).
142. D. Kezys et al., "Multibeam pumping of OPA by radiation of fibre amplifiers", *Lithuanian Journal of Physics*, Vol. **51**, No. 2, pp. 137-142 (2011).

143. A. Dubietis et al., "Combining effect in a multiple-beam pumped optical parametric amplifier", *J. Opt. Soc. Am. B* **15** (3), 1135–1139 (1998).
144. G. Tamošauskas et al., "Optical parametric amplifier pumped by two mutually incoherent laser beams", *Appl. Phys. B* **91** (2), 305–307 (2008).
145. S. Ališauskas et al., "Prospects for increasing average power of optical parametric chirped pulse amplifiers via multi-beam pumping", *Opt. Commun.* **283** (3), 469–473 (2010).
146. T. Kurita et al., "Experimental demonstration of spatially coherent beam combining using optical parametric amplification", *Opt. Express* **18**(14), 14541–14546 (2010).
147. Z.M. Liao et al., "Energy and average power scalable optical parametric chirped-pulse amplification in yttrium calcium oxyborate," *Optics Letters* **31**, 1277 (2006).
148. R. Danielius et al., "Self-diffraction through cascaded second-order frequency-mixing effects in Beta-barium borate", *Opt. Lett.* **18**(8), 574–576 (1993).
149. <http://www.icuil.org/events-a-activities/facilities.html>
150. A. Bayramian et al., "Compact, Efficient Laser Systems Required For Laser Inertial Fusion Energy," *Fus. Sci. & Tech.* **60**, 28-48 (2011).
151. A.J. Bayramian et al., "High Average Power Petawatt Laser Pumped by The Mercury Laser for Fusion Materials Engineering," *Fus. Sci. & Tech.* **56**, 295-300 (2009).
152. A. Bayramian et al., "The Mercury Project: A High Average Power, Gas-Cooled Laser For Inertial Fusion Energy Development," *Fus. Sci. & Tech.* **52**, 383-387 (2007).
153. R. Deri et al., "Semiconductor Laser Diode Pumps for Inertial Fusion Energy Lasers," LLNL White Paper LLNL-TR-465931 (2011).